論文 / 著書情報
Article / Book Information

題目(和文)	コンピュータ支援診断システムの普及効果の評価およびセキュアな医療画像共有システムの開発
Title(English)	Assessment of dissemination effect of computer-aided detection/diagnosis and development of secure medical image sharing system
著者(和文)	高橋遼平
Author(English)	Ryohei Takahashi
出典(和文)	学位:博士(工学), 学位授与機関:東京工業大学, 報告番号:甲第10887号, 授与年月日:2018年3月26日, 学位の種別:課程博士, 審査員:梶川 裕矢,仙石 慎太郎,日髙 一義,橋本　正洋,後藤 美香
Citation(English)	Degree:Doctor (Engineering), Conferring organization: Tokyo Institute of Technology, Report number:甲第10887号, Conferred date:2018/3/26, Degree Type:Course doctor, Examiner:,,,,
学位種別(和文)	博士論文
Type(English)	Doctoral Thesis

Doctoral Dissertation

Assessment of dissemination effect of computer-aided detection/diagnosis and development of secure medical image sharing system

School of Environment and Society

Tokyo Institute of Technology

March 2018

RYOHEI TAKAHASHI

Table of Contents

List of Figures

List of Tables

ABSTRACT

The last two decades have seen a rapid increase in government healthcare expenditures. A previous study estimated that global spending on healthcare is expected to increase from 7.83 trillion US$ in 2013 to 18.28 trillion US$ in 2040. One of the most commonly expressed reasons for this phenomenon could be a significant progress in health technologies. In particular, radiology is now threatened by its own success. The cost of modality development has been increasing, the workload of radiologists has dramatically increased owing to overly large volumes and high-resolution images, and the number of radiologists may remain limited. As a result, health care costs have been rising in spite of a limited benefit. Therefore, some approaches to handling the data explosion are needed. In this context, a computerized analysis of medical images, known as computer-aided detection/diagnosis (CAD), has been highly expected to reduce costs and burden, and improve the quality of healthcare services. However, some technical and societal challenges still remain. The research described in this dissertation is therefore related to one of these challenges, namely, “the problem of datasets,” and was conducted to improve the cost effectiveness.

In chapter 1, a literature survey on a CAD system is provided based on a bibliometric analysis. This analysis determined that CAD research has been classified and categorized according to the disease type and imaging modality. This classification began with the CAD of mammograms, and eventually progressed to that of brain disease. Furthermore, based on the results, some challenges were discussed, including “the problem of datasets,” particularly their insufficiency. Several studies concluded that the accuracy of a CAD system not only depends on the algorithm used, but also on the quality of the training datasets. Therefore, a way to resolve this problem is proposed herein: the accumulation of medical images though their sharing among healthcare establishments to increase cost-effectiveness under a central assumption: First, medical images are shared between healthcare establishments and CAD system developers. Second, medical images can be accumulated in greater amounts than ever before, and such image data are applied to the training dataset. Third, training dataset accumulation can improve the CAD system performance. Fourth, doctors using the system will be able to detect many more diseases such as neoplastic lesions. As a result, more patient’s lives can be saved, and a favorable effect on our society can be achieved.

In chapter 2, the effect on the accumulation of medical images from a societal perspective is evaluated. The Markov model is applied to three types of CAD systems: breast cancer (BC), colorectal cancer (CRC), and Alzheimer’s disease (AD). Furthermore, the following comparisons were made: 1) costs versus effectiveness, 2)

life years gained versus quality-adjusted life years (QALYs) associated with strategies involving a standard clinical work-up, 3) the standard clinical work-up using each type of CAD system, and 4) the standard clinical work-up using each type of CAD system considering an improvement through the accumulation of datasets. Furthermore, a one-way sensitivity analysis and a scenario analysis were carried out to assess the robustness of the results. For the BC and CRC diagnosis models, the accumulation of medical images can drastically improve the cost-effectiveness; on the other hand, it can adversely deteriorate the cost-effectiveness of AD CAD, as dependent on certain social factors. Although several social changes might be required, the effect could have significant social value to CAD systems.

In chapter 3, a method is proposed that applies blockchain technology to a cloud-based environment to share medical images between healthcare and research establishments. At present, there are several ways to share medical images, such as encrypted communication from physician to physician, and the use of a private network; in addition, cloud computing has been expected to be highly applicable owing to its scalability. However, image sharing through a cloud-based environment has raised certain security and privacy concerns. The proposal described herein divides medical images into metadata and pixel data. The former is managed using blockchain technology in a secure manner, and the latter is managed in a cloud-based environment for scalability. In addition, a multi-use key is created from the metadata. When physicians use medical images, the original information can be reconstructed using this key. Furthermore, this methodology was implemented in a test environment, and the results regarding the scalability and security are discussed. Although certain technical challenges remain, this technology can be used to resolve various challenges to security and privacy without impairing the effectiveness of IT resources on a practical level. In addition to this proposal, a meeting with stake-holders was conducted for a deeper understanding of what each stake-holder wants and needs, and a system architecture was designed for social implementation.

Finally, some concluding remarks are provided in chapter 4. First, it can be concluded that the sharing of medical image data is valuable for our society and could resolve the issue about dataset from a CAD diagnostic perspective. Second, the proposed method could not only improve the CAD system’s performance, but also decrease long-term management costs for healthcare establishments, improve the healthcare quality and increase patient satisfaction. Third, designing a system architecture could reveal the feasibility of my proposal. Overall, my doctoral research has potential to improve cost-effectiveness on our society with social implementation.

1 INTRODUCTIONS

1.1 Background

The last two decades have seen a rapid increase of government expenditures on public welfare arrangements. Increasing healthcare expenditures form a significant part of these outlays, and its share of total government expenditure has risen rapidly. Previous study estimated that global spending on healthcare is expected to increase from US$7.83 trillion in 2013 to $18.28 trillion in 2040 [1]. On the other hand, public sources fund 83% of health spending, health expenditures have great implications for health care sustainability in Japan [2]. The most commonly expressed reasons for this phenomenon could be considered as a population explosion, an aging population, and a significant progress in technology [3]–[5]. For technological progress example, three-dimensional printing can rapidly and inexpensively create human organs and these can support doctor to make decision earlier [6], “Proton therapy offers an opportunity to continue to improve the therapeutic ratio for breast cancer patients by targeting tissue at risk and optimizing tumor control, while simultaneously maximally sparing non-target tissue and reducing treatment morbidity.”[7], an immunotherapy medication for advanced melanoma, Nivolumab was developed [8], and the high-technology operation room SCOT (Smart Cyber Operating Theater) which combines cyber space and physical space has been developing in Japan [9]. This technological advancement can help patients get well, avoid disease and delay death, however, they also drive up spending because prices for newer treatments or medical equipment are often higher than for the products they replace. Especially, advanced diagnostic imaging technologies, such as computed tomography (CT), magnetic resonance imaging (MRI), single photon emission computerized tomography (SPECT) and positron emission tomography (PET), have been more expensive day by day, and also medical imaging is an indispensable tool of patients' healthcare in modern medicine [10]. On the other hand, these equipment output; medical images recently have been too high-resolution and too large-volume images are presented for medical doctor to use in daily practice. Then, doctor could not make best use of modality’s potential, therefore, its effectiveness could be limited comparing its cost rising [11], [12]. It is said that radiology is now threatened by its own success. The workload of radiologists has dramatically increased, the number of radiologists still could be limited, and health care costs related to imaging have been rising. Therefore, some approaches to handle the data explosion are needed [13].

In such a situation, computerized analysis of medical images, known as computer-aided detection/diagnosis (CAD), has been highly expected to reduce cost and improve healthcare service quality. CAD was originally developed for breast cancer

using mammography in the 1960s, and has since been extended to the diagnosis of lung cancer, colorectal cancer, and so on [14]–[16]. Using CAD, doctors can use computer support as a "second opinion" and make a final decision more quickly and with greater confidence. In other word, to be used CAD system, the radiologist or medical doctor first reviews the examination without the system, then refers the CAD system's result and re-evaluates the CAD-marked areas of concern before making the final decision. Furthermore, some CAD systems were US Food and Drug Administration (FDA) and Conformité Européenne (CE) approved for use with both film and digital mammography, for both screening and diagnostic exams; for chest CT; and, for chest radiographs [17], while digital mammography was also approved by Pharmaceuticals and Medical Devices Agency (PMDA) in Japan. Global industry analysis Inc. showed the estimation that the CAD market in the US is $376 million and sold out over 4,000 units by 2020, driven by rising cancer incidence, focus on early diagnosis, and proven efficiency in breast cancer detection [18].

There are two types of CAD research—"Detection" and "Diagnosis"—and it consists of two phases—a "propose phase" and an "evaluation phase" [19] (Fig. 1). In CAD research, "Detection" implies a technology designed to reduce observational oversight in general by marking the regions of an image that have potential for specific abnormalities. "Diagnosis" implies a technology designed to assess a disease using image-based information. In this framework, receiver evaluation is quiet critical factor for practical use, because the system with satisfactory performance on unit test could not necessarily show the same performance on practice.

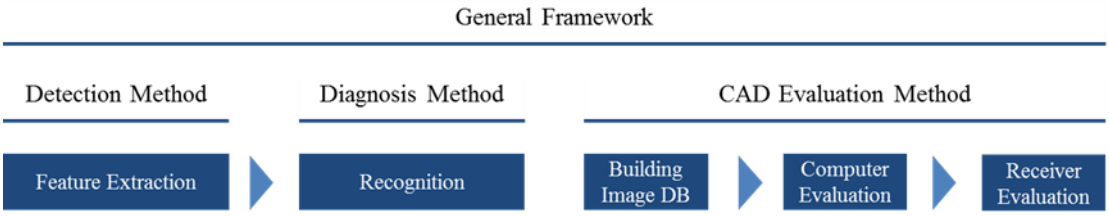

Figure 1. General CAD framework

Thus, CAD is considered as an important and practical technology to reduce the burden on doctors and medical staff, and shorten the time required for the interpretation of medical images. Furthermore, CAD systems have increased the accuracy of diagnosis, which has led to their increased use over the years, such that CAD technology is now a major research subject in medicine [14], [20]–[23]. I conducted systematic CAD research review for comprehensive understanding in next Section.

1.2 Systematic Review for CAD

1.2.1 Overview

I conducted systematic review by using bibliometric analysis (Appendix 1). CAD research was divided into clusters that depended upon on their direct citation topology. I focused on seven clusters with over 100 papers; an overview of these clusters is provided in Fig. 2 and Table 1. These seven clusters featuring 4,705 papers occupied more than 90% of the largest component of the network.

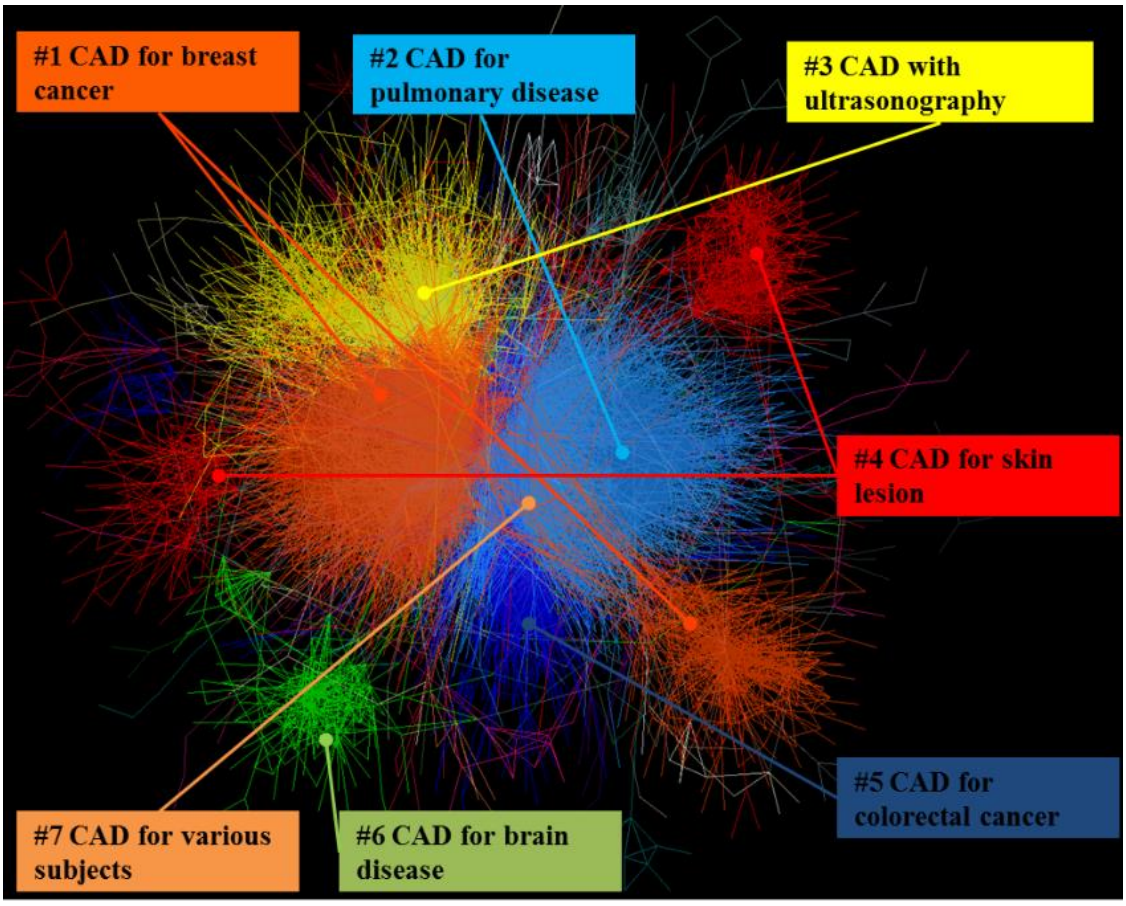

Figure 2. CAD academic research overview

Table 1. Cluster information summary

ID	Cluster Info					
	Name	Average Publication year	# Papers	# Citation	Citation/Paper ratio	Tf-idf
1	CAD for breast cancer	2004.2	1,628	10,082	6.2	mammogram breast mass mammography breast cancer
2	CAD for pulmonary disease	2007.0	1,345	7,805	5.8	nodule lung lung nodule pulmonary pulmonary nodule
3	CAD with ultrasonography	2010.1	652	2,275	3.5	breast lesion tumor ultrasound prostate
4	CAD for skin lesion	2009.8	429	1,062	2.5	dermoscopy melanoma retinal skin skin lesion
5	CAD for colorectal cancer	2007.7	402	1,498	3.7	polyp colonography colonic ctc colonoscopy
6	CAD for brain disease	2011.0	142	400	2.8	alzheimer spect brain pet spect image
7	CAD for various subjects	2009.0	107	132	1.2	osteoporosis bmd liver kidney aih

By briefly reviewing the clusters, I determined that CAD-related papers were from the departments of medicine and imaging modalities. I examined the history and progress of CAD by rearranging the clusters according to average publication year (Fig. 3).

Figure 3. CAD development history

Cluster #6 (CAD for brain disease) was the latest, and can be regarded as the popular subject of research in the area in the past few years. On the other hand, cluster #1 (CAD

for breast cancer) and cluster #2 (CAD for pulmonary disease) had the highest citation per paper in the seven clusters, which implied significant scientific work in the area and good knowledge sharing in these fields. Cluster #7 (CAD for tooth and internal organs), cluster #4 (CAD for skin lesion), and cluster #6 had lower citations per ratio, and can be regarded as areas with less advanced knowledge sharing where topics of research are quite specific. Moreover, in Figure 3, cluster #6 has is at a considerable distance from the other clusters, which indicates low inter-citation between it and them.

After reviewing the academic landscape of CAD research, I extracted the top four highest-frequency journals in each cluster (Table 2). The results showed us distinctive features of the major journals (e.g., Society of Photo-optical Instrumentation, Medical Physics, and so on) that were highly cited in each cluster. For example, in cluster #6, journals in computer science (e.g., Lecture Notes in Computer Science, Expert Systems with Applications, and Neurocomputing) were preferred. This may indicate that CAD for brain diseases requires advanced computation methods to process images.

Table 2. Journal analysis

Cluster#	Journal name	Frequency Rate
ALL	P SOC PHOTO-OPT INS	7.62%
	PROC SPIE	6.79%
	MED PHYS	5.70%
	ACAD RADIOL	4.21%
#1	P SOC PHOTO-OPT INS	8.60%
	MED PHYS	7.19%
	PROC SPIE	5.96%
	ACAD RADIOL	4.79%
#2	P SOC PHOTO-OPT INS	10.41%
	PROC SPIE	7.58%
	MED PHYS	7.29%
	ACAD RADIOL	6.10%
#3	PROC SPIE	8.59%
	ULTRASOUND MED BIOL	6.13%
	MED PHYS	5.83%
	P SOC PHOTO-OPT INS	4.75%
#4	PROC SPIE	5.83%
	IEEE ENG MED BIO	4.90%
	LECT NOTES COMPUT SC	4.43%
	SKIN RES TECHNOL	4.43%
#5	PROC SPIE	11.44%
	P SOC PHOTO-OPT INS	8.71%
	MED PHYS	6.22%
	ACAD RADIOL	5.72%
#6	LECT NOTES COMPUT SC	12.68%
	EXPERT SYST APPL	7.75%
	NEUROSCI LETT	6.34%
	NEUROCOMPUTING	4.93%
#7	PROC SPIE	7.48%
	MED PHYS	6.54%
	P SOC PHOTO-OPT INS	5.61%
	COMPUT MED IMAG GRAP	4.67%

Finally, a heat map analysis was conducted to obtain semantic linkages among the CAD research fields in Fig. 4. Each cell gradient represents relatedness between a pair of clusters; dark blue indicates high relatedness (over 0.1 cosine similarity), light blue indicates low relatedness (under 0.1 cosine similarity), and white implies no relation between the given clusters (cosine similarity is 0). The highest average similarity between clusters was in #1 (0.096) and lowest in #6 (0.014). There was high relatedness between clusters #1 and #3. It is no wonder that #1 had was highly related to #3 because the latter focused on ultrasonography, which modality is mainly intended to diagnose breast tissue and the prostate gland. Hence, it is highly likely that the word “breast” may be regarded as its similarity and relatedness. There was no relatedness between clusters #4 and #6, clusters #5 and #6, and clusters #1 and #7. This implies that cluster #6

contained methods that were not regarded as standard in clusters #4 and #5, or that there may be opportunities for improvement in cluster #6 by adapting the other clusters' concepts. Further, I concluded that cluster #6, CAD for brain disease, is a highly applied research domain that uses a different technological system from CAD to focus on other regions of the body.

	#1	#2	#3	#4	#5	#6	#7	Ave
#1	1.000	0.049	0.385	0.021	0.048	0.012	0.000	0.086
#2	0.049	1.000	0.032	0.025	0.031	0.011	0.032	0.030
#3	0.385	0.032	1.000	0.064	0.038	0.042	0.017	0.096
#4	0.021	0.025	0.064	1.000	0.016	0.000	0.012	0.023
#5	0.048	0.031	0.038	0.016	1.000	0.000	0.018	0.025
#6	0.012	0.011	0.042	0.000	0.000	1.000	0.017	0.014
#7	0.000	0.032	0.017	0.012	0.018	0.017	1.000	0.016

Figure 4. Heat map analysis

Following an examination of the overall structure of CAD research, I conducted a survey of each cluster. I selected the top 10 most-cited papers through all years, and also the top 10 most-cited papers published in 2015 from each cluster (thus, a total 20 papers were selected), and summarize them in the Appendix 2.

In cluster #1, all 20 papers [14], [24]–[42] were concerned with research on the detection or diagnosis of breast cancer, and all adopted mammography as the imaging modality. Breast cancer starts when cells in the breast begin to grow out of control. These cells usually form a tumor that can often be seen on an x-ray or felt as a lump. The tumor is malignant if the cells can grow into surrounding tissues or spread to distant areas of the body. Breast cancer occurs almost entirely in women; however, a small percentage of men are also inflicted with breast cancer. Breast cancer observations can be divided into three topics based on the purposes of detection: "microcalcifications," "mass," and "architectural distortion." Furthermore, a mammography is one of the most preferred screening examination types for breast cancer, and is widely available, well tolerated, and inexpensive. A large amount of research into breast cancer CAD during the diagnosis phase has been attained [25], [27], [29], [30], [34], [35], [39]–[42]. For

this reason, a commercial CAD product, ImageChecker (R2 Technology), was produced early on, and research into this area has thoroughly advanced. Previous research interpreting 12,860 screening mammograms was conducted over a 12 month period with the assistance of a CAD system [14]. This report concluded that the use of CAD in the interpretation of screening mammograms can increase the detection of early-stage malignancies without an undue effect on the recall rate. On the other hand, 107 radiologist-related studies mentioned that the screening performance is not improved through the use of CAD [36]. Therefore, its efficacy seems to remain controversial, however, mammography CAD is the most popular CAD system, and has the support of a large number of doctors.

In cluster #2, pulmonary disease CAD, lung nodule detection for pulmonary disease was the main topic, and all 20 papers [15], [19], [20], [43]–[59] adopted CT as imaging modality. Lung cancer, also known as lung carcinoma, is a malignant lung tumor characteristic of uncontrolled cell growth in tissues of the lung. This growth could be distributed beyond the lung through the process of metastasis into nearby tissue or other portions of the body. Almost all cancers that start in the lung, known as primary lung cancers, are carcinomas. The two main types are small-cell lung carcinoma and non-small-cell lung carcinoma. Small cell carcinoma generally has a shorter doubling time, higher growth fraction, and earlier development of metastases; on the other hand, non-small-cell lung carcinoma accounts for about 85% of all lung cancers and is relatively insensitive to chemotherapy, compared to small cell carcinoma. The most common symptoms are coughing, weight loss, shortness of breath, and chest pain. To detect lung nodules, two- and three-dimensional analyses are effective [15], [47], [49]. In contrast to cluster #1, pulmonary disease CAD research can be considered a transition between the development and diagnosis phases. Some papers have shown tremendous results with detection rates of over 0.95 [45], [53], [58]. On the other hand, a previous study indicated that the reported performances of the radiologist-CAD team seemed to be lower than what might be expected based on the performance of a radiologist and a CAD system in isolation, which might indicate that the interaction between radiologists and a CAD system is not optimal [43]. Therefore, lung cancer CAD has a large room for improvement in terms of its performance by constructing trust between the radiologist and the system itself.

In cluster #3, ultrasonography CAD, treatment pertaining to breast and prostate cancer CAD was expected from a keyword analysis (the top-five frequently used words were “breast,” “lesion,” “tumor,” “ultrasound,” and “prostate”) [16], [21], [60]–[77]. However, all 20 papers focused on breast cancer. Therefore, a recursive clustering was

attempted using the same bibliometric analysis method to extract the sub-clusters, and the top-ten cited papers [78]–[87] were reviewed. For cluster #3 and its sub-clusters, the main modalities were ultrasonography and magnetic resonance (MR) imaging apparatuses; in addition, breast and prostate cancers were studied. Prostate cancer begins when cells in the prostate gland start to grow out of control. The prostate is a body part existing only in males, and is responsible for making some of the fluid in semen and is located below the bladder and in front of the rectum. Its size changes with age. In early stages, it is about the size of a walnut, but can grow much larger with age. The urethra, which is the tube that carries urine and semen out of the body through the penis, goes through the center of the prostate. Almost all prostate cancers are adenocarcinomas and these cancers develop from the gland cells. While only slight, other types of prostate cancer include sarcomas, small cell carcinomas, neuroendocrine tumors, and transitional cell carcinomas. As with cluster #1, CAD for breast cancer [16] [21], [61]–[64], [66]–[71], [73], [75] and prostate cancer [78], [79], [81]–[86] has developed to the diagnosis phase. In general, ultrasonography detection for breast cancer has not been equivalent to mammography in terms of performance, particularly for microcalcifications, which are tiny dots of calcification seen in early breast cancer. However, some ultrasonography equipment is less expensive, and the procedure is less painful than a mammogram. Therefore, widespread use of ultrasonography could popularize screening for breast cancer, and may consequently detect more potential breast cancers and thereby save lives. On the other hand, to diagnose prostate cancer, an ultrasound-guided biopsy is the most popular standard procedure.

For cluster #4, a dermoscope has been the most verified modality, and skin lesions (especially skin cancer) have been the primary focus [22], [88]–[106]. Skin cancer is commonly started as a locally destructive cancerous growth on the skin. It originates from the cells that line up along the membrane that separates the superficial layer of the skin from the deeper layers. Unlike cutaneous malignant melanoma, the vast majority of these sorts of skin cancers has limited potential to spread to other parts of the body, and could become life threatening. Furthermore, there are three major types of skin cancer: basal cell carcinoma, which is the most common skin cancer; squamous cell carcinoma, which is the second most common skin cancer and originates from skin cells; and melanoma, which originates from the pigment-producing skin cells (melanocytes); however, this type of skin cancer is less common, though more dangerous, than the first two varieties. Skin CAD has been used for detection, and some researchers have used it for diagnosis [91], [97], [98], [102]. At present, computer-aided diagnosis systems based on an individual pigmented skin lesion (PSL) image analysis have been

developed for skin cancer recognition. However, it cannot yet be used to provide the best diagnostic results. Furthermore, the absence of benchmark datasets for a standardized algorithm evaluation could be considered a barrier to a more dynamic development of this research area [107].

In cluster #5, colorectal cancer CAD, colonic polyp detection with CT colonography (CTC), was the focus [23], [108]–[126]. Colorectal cancer normally starts in the colon or rectum. Both tissues are a part of the large intestine, which is the lower part of the digestive system in the human body. During digestion, food moves through the stomach and small intestine into the colon. The colon absorbs a variety of nutrients and water from food, and stores waste matter (i.e., stool). The stool moves from the colon into the rectum before it leaves the body. Most colorectal cancers are adenocarcinomas. This type of cancer begins in cells that make and release mucus and other fluids. Colorectal cancer often begins as a growth called a polyp, which may form on the inner wall of the colon or rectum. Some polyps become cancerous over time. Finding and removing polyps can be regarded as the most expected way to prevent colorectal cancer. Furthermore, colorectal cancer is the fourth most common type of cancer diagnosed in the United States. Deaths from colorectal cancer have decreased with the use of colonoscopies and fecal occult blood tests, which check for blood in the stool. In our analysis, colorectal cancer CAD has not been used for diagnosis (detection only), and there were no papers focusing on computer-aided "diagnosis" of the selected bibliometric data. Thus, it seems to be in a nascent stage of development, and furthermore, colorectal cancer CAD has been facing a large problem in terms of the detection of small polyps [113]. The system can detect large polyps with high accuracy (i.e., over 90% sensitivity) [114]; however, it can only detect small polyps with an unacceptable level of accuracy [110].

In cluster # 6, brain disease CAD, three modalities were discussed [127]–[146]: single-photon emission computed tomography (SPECT) [127]–[130], [132], [134], [136], [145], positron emission tomography (PET) [130]–[132], [135], and MR [133], [137]–[144], [146]. MR has been a focus of recent research; however, SPECT and PET have been more widely spread owing to these specific functions. A SPECT scan is a type of nuclear imaging test that shows how blood flows through the tissues and organs. This modality is composed of two technologies, namely, CT and a radioactive material, which we call a tracer. SPECT tests have shown that it might be more sensitive to brain injury than conventional scanning because it can visualize the amount of blood flow to injured sites. On the other hand, PET is also a technique for measuring the physiological function by visualizing the blood flow, metabolism, neurotransmitters, and radiolabeled

drugs [147]. PET can supply doctors with quantitative analyses and allow relative changes over time to be monitored as a disease progresses, or in response to a specific stimulus. PET is often more suitable for cancer detection; however, a steady drug supply may be expensive. Alzheimer's disease was the most-cited subject, and is the most widespread type of dementia, affecting an estimated 850,000 people in the UK. Dementia is usually considered a progressive neurological disease that affects multiple brain functions, such as memory, the sense of judgement, and cognition. However, the exact cause of Alzheimer's disease is unknown. Therefore, early detection has been a promising method of prevention, and the use of CAD in this capacity has been an expected screening tool. On the other hand, machine-learning methods, particularly a support vector machine, are preferred for analysis. The necessity for advanced computing might be the cause of its weak relatedness with the other clusters, as shown in Fig. 4. Some systems used to detect Alzheimer's disease have recently attained a performance equivalent to that of a radiologist [127], [130], [139]; however, much earlier detection (in research conducted on detection seven years prior to conversion into dementia) has still been difficult to achieve, and the detection rate has also remained quite low [148].

In cluster #7, the use of various modalities and a large number of subject diseases were observed in 18 papers (this cluster had fewer than ten papers published in 2015) [149]–[166]. For instance, the cluster included osteoporosis on dental panoramic radiographs [150], [153], [159], [162], liver disease [154], [157], [158], [163], [164], [166], kidney disease [152], and so on. Liver cancer begins in the cells of the liver. The liver is a football-sized organ that sits in the upper right portion of the abdomen, beneath the diaphragm and above the stomach. The most common type of liver cancer is hepatocellular carcinoma, which begins in the main type of liver cells, such as the hepatocyte. Other types of liver cancer, such as intrahepatic cholangiocarcinoma and hepatoblastoma, are much less common. On the other hand, kidney cancer, also called renal cancer, is one of the most common types of cancer around the world. It usually affects adults in their 60s or 70s and is rarely developed in people under 50. It can often be cured if caught early; however, a cure is likely to be impossible if not diagnosed until after it has spread beyond the kidneys. There are several types of kidney cancer, and renal cell carcinoma is the most widespread. Furthermore, osteoporosis causes bones to become weak and brittle. Thus, a fall or even mild stress such as bending over or coughing can cause a fracture. Osteoporosis-related fractures most commonly occur in the hip, wrist, spine, and jawbone. Bone is living tissue that is constantly being broken down and replaced, and therefore, osteoporosis occurs when the creation of new bone is

unable to keep up with the removal of old bone. With regard to methodology, auto-segmentation for the liver and kidneys is a popular research domain [152], [154], [158]. The diversity of modalities and subject diseases might be the cause of a weak relatedness with other clusters, however, as shown in Fig. 4.

1.2.2 Findings

I'll discuss above results. First, as shown in the above results, current CAD research covers a wide range of diseases. In the US, the top 10 causes of death are heart disease (23.53%), cancer (22.52%), respiratory disease (5.74%), accidents (5.02%), stroke (4.97%), Alzheimer's disease (3.26%), diabetes (2.91%), influenza and pneumonia (2.19%), kidney disease (1.81%), and suicide (1.58%) [167]. Within cancer, lung and bronchi, prostate, breast, colon and rectum, and pancreas were the top fatal diseases. To exclude non-disease factors, easy-to-diagnose diseases, and pancreatic cancer, almost all causes of deaths were covered within the major research domain of CAD. Therefore, it can be said that CAD research has developed to meet medical demands. Therefore, pancreas cancer could be more promising in the near future.

Second, as shown in Table. 1, clusters #1 and #2 are mature research fields comparing other clusters. The research trend has shifted from clusters #1 and #2 to #3-7, whereas research in clusters #1 and #2 is still active, as shown in Fig. 5. In the figure, the solid line shows the sum of the number of papers in each year in clusters #1 (breast cancer CAD) and #2 (pulmonary disease CAD). These two clusters, which are the largest and oldest clusters in my research, contained 2,973 papers. On the other hand, the dotted line expresses the same information for clusters #3 (ultrasonography CAD), #4 (skin lesion CAD), #5 (colorectal cancer CAD), #6 (brain disease CAD), and #7 (various subjects). These five clusters contained 1,732 papers. The results shown in this figure help us conclude that research relating to typical CAD technology, i.e., breast cancer and pulmonary cancer CAD, peaked early in the first decade of the 21st century; on the other hand, research in other CAD domains has been progressing steadily since.

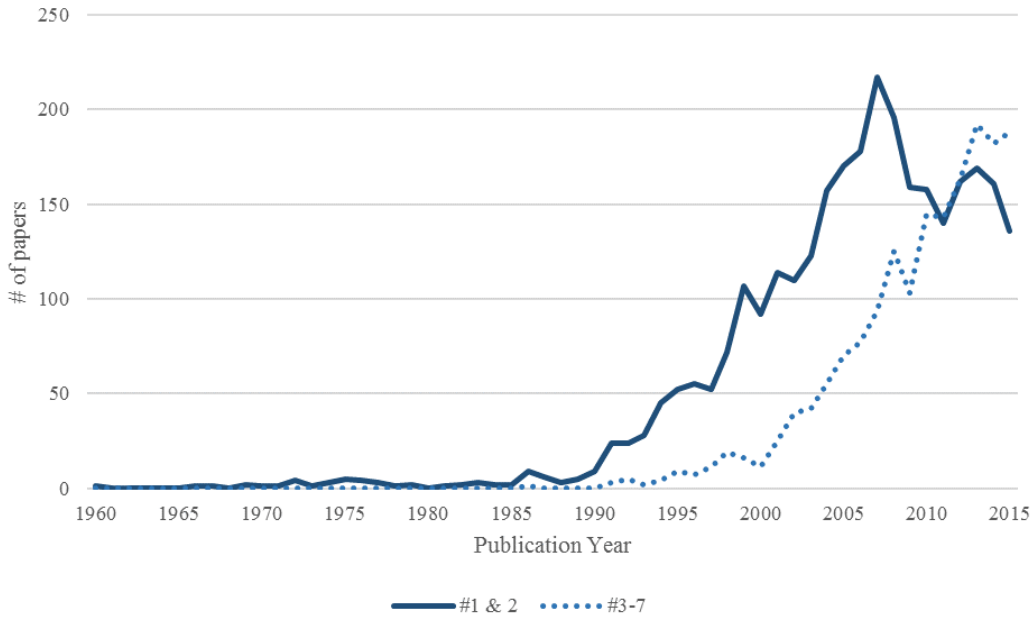

Figure 5. CAD research trends

Third, in addition to academic research review, bibliographic data of patents were briefly reviewed on the same way as a research paper analysis (Appendix 1). An overview of these clusters is provided in Fig. 6 and Table 3. By reviewing the clusters, it was determined that patents related to CAD involve departments of medicine and their function. Moreover, among the five clusters shown, cluster #3 (post-processing) and cluster #4 (pre-processing) have a lower number of citations per patent, which could imply that knowledge sharing has not progressed. Furthermore, cluster #4 (pre-processing) is the youngest and has been regarded as an important topic during the past few years.

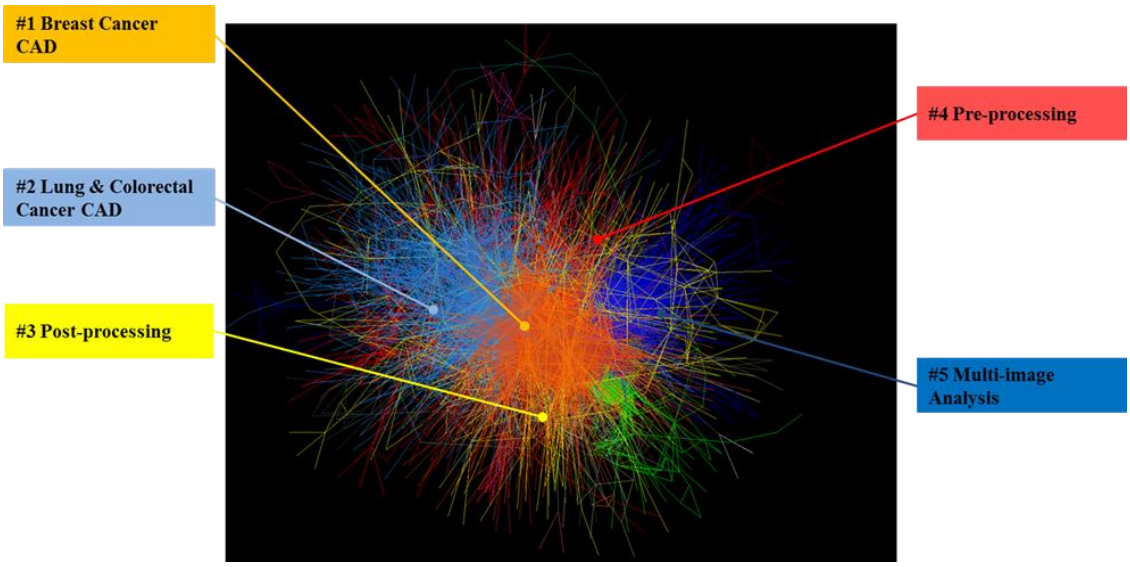

Figure 6 Patent citation overview

Table 3 Patent cluster information summary

ID	Cluster Info					
	Name	Average Publication year	# Patents	# Citation	Citation/Paper ratio	Tf-idf
1	Breast Cancer CAD	2006.6	649	4,868	7.5	breast digital mammogram abnormality lesion
2	Lung & Colorectal Cancer CAD	2008.9	633	2,626	4.1	polyp candidate nodule lung vessel
3	Post-processing	2007.9	399	697	1.7	shadow unit abnormal apparatus detector
4	Pre-processing	2011.0	334	595	1.8	mri boundary classification embedding prostate
5	Multi-image Analysis	2010.2	332	1,857	5.6	tomosynthesis breast ray tomosynthesis image biopsy

The cluster most worthy of special mention is #3 (post-processing), and patents in this cluster have proposed a way to improve the CAD system performance based on its usability, namely, how to display the CAD output [168]–[170], how to access the diagnostic data quality [171], [172], or how to store the processed data. The background of this type of invention may be related to the trust between the human user and the system. A previous study reported that the performance of radiologists using CAD is

much lower than what might be expected based on the performance of radiologists and CAD systems in isolation [43]. It was concluded that optimization of the interaction between radiologists and a CAD system may be critical for practical use; therefore, it can be concluded that the development of an interface is a more important challenge for practical use than academic research.

Fourth, I showed that papers on Alzheimer's disease were highly cited in the brain disease cluster #6, and had used such statistical methods as principal component analysis (PCA) [128], [131], [132], [141], [143], [144] and machine learning. For the gold standard of developing a CAD algorithm, engineers conduct feature selection for computer diagnosis with the consultation of doctors, whereas PCA and machine learning, which involve latent variables, can skip this process and deal directly with the medical images. Thus, I can develop a model for CAD using medical image data, even without annotation by doctors. Can I regard this situation as indicating a transition from a hypothetical-testing approach to a data-driven approach? The latter approach may have the potential to show relevant features that even a doctor might not be able to perceive. However, it is difficult to evaluate the quality of a system depending on the data-driven approach. At least, there is little research to evaluate false-negative cases through a medical check and cases where diagnosis by doctor and prediction by machine did not match. Therefore, I need to consider ways to guarantee the outcome in approaches that use latent variables and machine learning. I raise this issue as a common problem to be addressed and resolved in CAD research

Fifth, based on the summary and comparison of the research results, it is difficult to evaluate the system or algorithm that delivers high performance, or is more effective for diagnosis, because the test datasets and evaluation methods are not standardized. The accuracy of a CAD system not only depends on the algorithm, but also on the quality of the training datasets [173]. The standardization and normalization of datasets and evaluation methods is expected to be quite difficult; however, I need to implement standardization from the perspective of evidence-based medicine. In addition to the necessity of research and evaluation schema for guaranteeing the reliability of methods, a scheme for data collection is necessary to improve performance.

Sixth, I point out the importance of the co-evolution of CAD research and imaging instruments. For the development of CAD research, I need a salient algorithm for modeling as well as medical imaging instruments for measurement. An example is the improvement in MRI accuracy, which will contribute to progress in bone CAD and pancreatic cancer CAD. Bone CAD was not featured in the major research domains that I described. This can be attributed to the fact that computed tomographic scanning is not

favored because of radiation exposure; moreover, the bone is not identified clearly with other imaging modalities, such as MRI. Hence, research and development in MRI will improve research in bone CAD. Furthermore, there are cases where early detection is critical for prevention, but they are difficult to diagnose early on, such as pancreatic cancer. Pancreatic cancer CAD can be considered a developing research domain in spite of the demand for it [174]–[178]. This is mainly why it has encountered difficulties in image classification in areas occupied by the pancreatic tumor [175], [179]. In developing CAD systems for such cases, it is challenging to collect datasets for early stage detection, let alone from the viewpoint of quality and quantity. Therefore, progress is needed in research on diagnostic imaging instruments for better imaging for some diseases, such as pancreatic cancer CAD.

Sixth, previous studies referred that a large amount of diagnosed data is required to improve the performance of the system [180], and this might be why some type of CAD system could not attain a competent performance[105], [159], [181], [182]. However, it is often quite difficult to procure sufficient data which were already diagnosed in the laboratory [180], [183]. Furthermore, existing systems are poorly suited for data sharing between establishments [180]. Therefore, it could be quite useful to construct environment for sharing medical images.

Finally, in this systematic review, I only focused on CAD, analyzed its trend, and discussed opportunities through bibliometric analysis in the above. To improve CAD and further develop its contribution to medical treatment, however, I need to expand my research scope from CAD to decision support systems (DSS) [184]–[186]. DSS can be regarded as “active knowledge systems which use two or more items of patient data to generate case-specific advice”[187]. For example, in case of the diagnosis of the severity of asthma, it makes use of the patient’s symptoms, exacerbations, and spirometry (lung function) as parameters [188]. I illustrate the relationship between CAD and DSS for diagnosis in Fig.7.

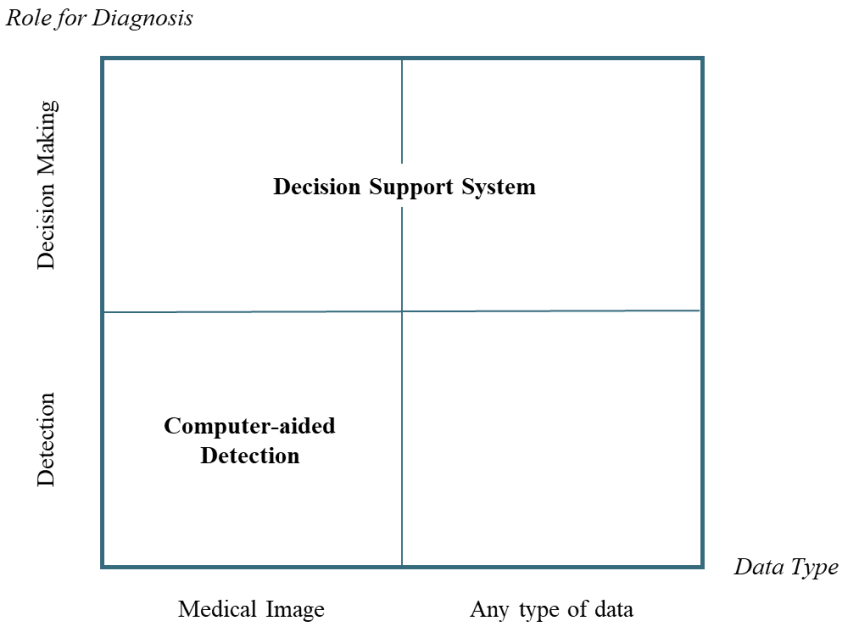

Figure 7 Relationship between CAD and decision support systems for diagnosis

Furthermore, I am exactly sure that CAD systems become much more useful through connectivity with DSS, especially for the diagnosis of diseases where the determining factors are various (e.g., Alzheimer's disease (AD) diagnosis). I propose some keys to generate a synergy effect between both technologies in the example of AD diagnosis as follows; First, I need to weigh each determination factor. In the case of AD, diagnosis is conducted according to the information provided by clinical examination, a thorough interview of the patient and relatives, and medical imaging. The first set of information can be analyzed in DSS and the last in CAD systems. Therefore, it is necessary to evaluate each output and integrate all of them. This can make diagnosis more accurate, even in early AD, which is extremely difficult to diagnose at present. Second, I should suppose a comprehensive judgment. There can be a large number of factors to consider for doctors, in addition to medical observation (e.g., patient's quality of life, preference and economic condition, and cost-effectiveness from a social perspective). Ideally, all factors should be analyzed by the DSS and CAD should act as a go-between. Third, I need to manage regulations. For practical use of systems, some criteria need to be met to ensure system quality based on the regulations. Therefore, I need to clarify the effects of system output, how each function works with regard to the quality of the system, and why diagnosis results differ in each case. It might be challenging to synchronize CAD with DSS.

1.3 Research Object

As described above, CAD still has significant potential for practical use; however, some technical and societal challenges still remain. Research related to “the problem of datasets” (nonstandard datasets and dataset insufficiency) was conducted in this study to improve the cost-effectiveness of CAD, with the eventual aim to help resolve rising social healthcare costs. Constructing a medical image sharing system could be considered a promising way to resolve the difficulties in finding datasets because medical practice can provide a variety of datasets of ailments that have already been diagnosed (i.e., a large number of diagnosed datasets can be created). However, two main challenges remain. First, “does a data-sharing environment really contribute to an improvement in societal cost-effectiveness?” In other words, the effect of data sharing on the cost-effectiveness of CAD remains unclear. Insight is required to consider the value of technology from a social perspective. Second, a secure and scalable environment is required to share image data in wide use; however, existing technologies cannot be considered sufficient in the healthcare industry. Therefore, this paper mainly argues that cost-effectiveness with regard to data sharing through a CAD system, proposes a new method for sharing image data in a secure and scalable manner, and describes the design of the proposed social implementation.

The rest of the paper is organized as following. In Chapter 2, an analysis of the cost-effectiveness is provided to evaluate the effect of image data sharing in a quantitative manner. In Chapter 3, a methodology to securely and scalably share medical images is proposed, and matters related to the social implementation of the paper’s proposal, including the system architecture, are discussed. Finally, some concluding remarks are provided in Chapter 4.

1.4 Appendixes

1.4.1 Appendix 1

Bibliometrics is a field of research in library and information science (LIS) that features various methods to quantitatively analyze the bibliographic information of papers, patents, and so on. Bibliometric methodologies generally use Information Technology to process and analyze quantitative as well as qualitative data from bibliographic information and provide meaningful implications. In this research, I selected citation network analysis, which is an effective bibliometrics methodology to identify an overview of an academic field. This technique analyzes the characteristics of a field with little chance of missing important research in each domain [189]–[192].

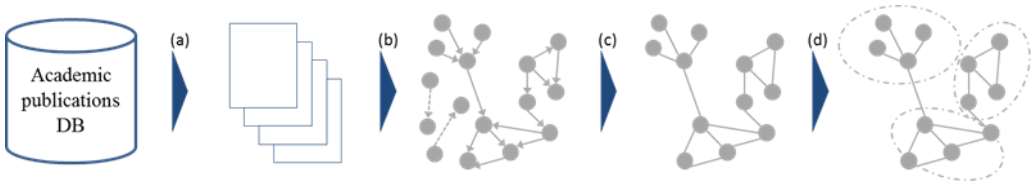

Fig A. Methodology overview

Fig. A shows an overview of my research methodology [189]. I first acquired relevant CAD research papers from each academic domain of interest using an academic publication database by using selected queries (Fig. Aa). I then constructed a citation network by regarding papers as nodes and direct citations as links (Fig. Ab). I did this because a previous study had indicated that direct citation is the best approach to detect emerging trends [193]. Following this, I eliminated irrelevant papers that were not linked to other papers in the largest graph component of the citation network to focus on the mainstream of research (Fig. Ac). Finally, I organized the network into clusters (Fig. Ad) using a topological clustering method known as Newman's algorithm [194]. In Newman's algorithm, clusters are divided into subsets in accordance with a rule that maximize modularity: Q. Then, Q is defined as follows;

$$Q = \sum_{s=1}^{M} \left[\frac{l_s}{l} - \left(\frac{d_s}{2l} \right)^2 \right] \quad , \qquad (1)$$

where Q is the independence of a cluster, M is the number of clusters, s is the cluster ID, l is the number of links in the entire network, l_s is the number of links inside module S, and d_s is the total number of links of nodes in S. Newman's algorithm has been noted to build well-separated clusters in terms of research domains [189]–[192], [195]. The network is visualized using a large graph layout (LGL) [196]. The LGL can help

visualize large-scale networks containing thousands of nodes and millions of links within a reasonable computational time. For ease of recognition, intra-cluster links in the same network are expressed in the same color. Following clustering, I analyzed the characteristics of each cluster, including the average publication year of papers, the number of citations, journal name, and the term frequency-inverse document frequency (tf-idf). Tf-idf is the best approach for discovering corresponding relationships between papers [191], and is defined as follows;

$$\text{Tf-idf} = \frac{n_{i,j}}{\sum_k n_{k,j}} \cdot \log \frac{D}{\{d : d \ni t_i\}} \quad , \tag{2}$$

where t_i is the given term, $n_{i,j}$ is the number of occurrences of term t_i, D is the total number of documents, and d is the number of documents containing term t_i.

In addition to simple keyword analysis, semantic similarities between clusters were measured to investigate semantic linkages of topics [197]. Semantic similarity was measured by cosine similarity [195], defined as follows;

$$\text{CosineSimilarity}(t, s) = \frac{\overline{j_t} \cdot \overline{j_s}}{\sqrt{\sum_i j_t^{(i)} \cdot j_s^{(i)}}} \quad , \tag{3}$$

where t and s are clusters in each domain, and j_t and j_s are term vectors of clusters t and s, respectively. Cosine similarity increases when each cluster tends to share the same words more frequently, which implies the existence of common research topics among clusters.

I collected bibliographic data from academic publications related to CAD. My data, including title, author, publication year, abstract, address, and references, were retrieved from the Science Citation Index Expanded (SCI-Expanded), the Social Sciences Citation Index (SSCI), the Conference Proceedings Citation Index (CPCI), and the Book Citation Index (BKCI). The information was compiled by Thomson Reuters. I used the Web of Science, a Web-based interface that enables users to access database services. I used the queries “computer-aided diagnosis” and “computer-aided detection,” and retrieved 7,834 papers published through 2015. The largest graph component contained 5,197 papers.

On the other hand, the bibliographic data of patents were collected from Derwent enhanced database, Derwent World Patents Index (DWPI), through Thomson Innovation by Thomson Reuters. All patents in the DWPI were collected. We used the

query, ““Computer aided detection” OR “Computer-aided detection” OR Computer aided diagnosis” OR “Computer-aided diagnosis”” to collect data from patents and retrieved 4,478 patents published through July in 2016. The largest graph component includes 2,779 patents.

1.4.2 Appendix 2

Table A. Cluster #1-1

Author	Publication Year	Journal	# of citation in Cluster	Modality is Mammogram	Main Subject	Method Keyword	Summary of results
Freer, TW et al	2001	Radiology	178	✔	Mass Detection	Performance evaluation	Comparing the radiologist's performance without and with CAD. ・Recall rate from 6.5% to 7.7% ・No change in the positive predictive value ・19.5% increase in the number of cancers detected ・Early-stage (0 and 1) malignancies detected from 73% to 78%
Chan, HP et al	1990	Investigative Radiology	169	✔	Microcalcifications Detection	Performance evaluation	Significantly improve radiologists' accuracy in detecting clustered microcalcifications
Jiang, YL et al	1999	Academic Radiology	137	✔	Microcalcifications Diagnosis	Performance evaluation	A(z) increased 0.61 without aid to 0.75 with the computer aid
Burhenne, LJW et al	2000	Radiology	136	✔	Microcalcifications /Mass /Architectural Distortion Detection	Performance evaluation	Sensitivity of ・75% in the detection of masses and architectural distortion ・99% in the detection of microcalcifications
Chan, HP et al	1999	Radiology	133	✔	Mass Diagnosis	Performance evaluation	・A(z) value for the computer classifier was 0.92 ・Radiologists' A(z) values ranged from 0.79 to 0.92 without CAD ・Radiologists' A(z) values ranged from 0.88 to 0.95 with CAD
Kegelmeyer, WP et al	1994	Radiology	125	✔	Mass Detection	Decision Trees, Performance evaluation	・The algorithm alone achieved 100% sensitivity, with a specificity of 82% ・Radiologist sensitivity increased from 80.6% to 90.3%, with no decrease in average specificity
Elter, M et al	2009	Medical Physics	124	✔	-	Review	-
WU, YZ et al	1993	Radiology	116	✔	Mass Diagnosis	Artificial neural networks, Back-propagation algorithm	A(z) value is 0.95
Jiang, YL et al	1996	Radiology	114	✔	Microcalcifications Diagnosis	Artificial neural networks	・Computer analysis allowed identification of 100% of the patients with breast cancer and 82% of the patients with benign conditions ・The accuracy of computer analysis was statistically significantly better than that of five radiologists
Giger, ML et al	2008	Medical Physics	112	✔	-	Review	-

Table B. Cluster #1-2

Author	Publication Year	Journal	# of citation in Cluster	Modality is Mammogram	Main Subject	Method Keyword	Summary of results
Nithya, R et al	2015	Journal of Medical Imaging and Health Informatics	58	✔	–	Review	-
Arikidis, N et al	2015	Medical Physics	20	✔	Microcalcifications Detection	Semiautomated segmentation , Level set method, Active contour model	A(z) value is 0.80/Standard Error is 0.04
Liu, XM et al	2015	Neurocomputing	18	✔	Mass Detection	Level set, Local binary pattern, Support vector machine	Achieved a sensitivity 75.6% at 1.38 false positives per image
Dheeba, J et al	2015	Computational Intelligence Applications in Modeling and Control	18	✔	Microcalcifications /Mass /Architectural Distortion Detection	Machine learning, Differential evolution optimized wavelet neural network	-
Sharma, S et al	2015	Journal of Digital Imaging	16	✔	–	Segmentation , Zernike moments , Support vector machine	・On IRMA reference dataset, it attains 99 % sensitivity and 99 % specificity ・On DDSM mammogram database, it obtained 97 % sensitivity and 96 % specificity
Liu, B	2015	Artificial Neural Networks	15	✔	Mass Detection	Artificial neural network	-
Lehman, CD et al	2015	JAMA Internal Medicine	14	✔	Mass Detection	Logistic regression , Performance evaluation	・Screening performance was not improved with CAD ・There was no difference in cancer detection rate
Pak, F et al	2015	Comput Methods Programs Biomed	14	✔	Microcalcifications /Mass /Architectural Distortion Detection	Non-Subsampled contourlet Transform, Super resolution	91.43% and 6.42% as a mean accuracy and FPR
Liu, XM et al	2015	EURASIP Journal on Advances in Signal Processing	14	✔	Microcalcifications Detection	Possibilistic fuzzy c-means , Support vector machine	・A(z) value is 0.8676 ・Sensitivity of 92 % with a false-positive rate of 2.3 clusters/image
Celaya-Padilla, J et al	2015	BioMed Research International	13	✔	Microcalcifications /Mass Diagnosis	Morphological high frequency enhancement filter, Laplacian of Gaussian filter	A(z) value is 0.882

Table C. Cluster #2-1

Author	Publication Year	Journal	# of citation in Cluster	Main Subject	Method Keyword	Summary of results
Armato, SG et al	1999	Radiographics	144	Lung Nodule Detection	2D&3D analyses, A rolling ball algorithm	A(z) value is 0.93
Lee, Y et al	2001	IEEE Transactions on Medical Imaging	143	Lung Nodule Detection	Genetic algorithm template matching	・Detection rate of about 72% ・Number of false positives at approximately 1.1/sectional image
Doi, K	2007	Computerized Medical Imaging and Graphics	133	-	Review of CADx	-
Giger, ML et al	1994	Investigative Radiology	136	Lung Nodule Detection	Features arising at different threshold levels	Sensitivity of 94% for nodule detection and an average of 1.25 false-positive results per case
Kanazawa, K et al	1998	Computerized Medical Imaging and Graphics	133	Lung Nodule Detection	Fuzzy clustering algorithm	The sensitivity for 230 nodules was 90%
Gurcan, MN et al	2002	Medical Physics	125	Lung Nodule Detection	2D&3D analyses, K-means clustering technique, Linear discriminant analysis	Sensitivity was 84% (53/63) with 5.48 (7961/1454) false positive objects per slice
Giger, ML et al	1988	Medical Physics	124	Lung Nodule Detection	Tests for circularity, size, and their variation with threshold level	-
Armato, SG et al	2001	Medical Physics	116	Lung Nodule Detection	2D&3D analyses	・A(z) value is 0.93 ・Overall nodule detection sensitivity of 70% with 1.5 false-positive detections ・A corresponding nodule, detection sensitivity of 89% with
Kobayashi, T et al	1996	Radiology	114	Lung Nodule Detection	Performanc e evaluation	A(z) values are 0.940 / 0.894(with / without CAD)
Awai, K et al	2004	Radiology	112	Lung Nodule Detection	Performance evaluation	A(z) values are 0.67 / 0.64(with / without CAD)

Table D. Cluster #2-2

Author	Publication Year	Journal	# of citation in Cluster	Main Subject	Method Keyword	Summary of results
Rubin, GD	2015	Journal of Thoracic Imaging	20	–	Review of lung nodule detection	-
Mansoor, A et al	2015	RadioGraphics	19	–	Review of Segmentatio n of Lungs	-
Tasci, E et al	2015	Journal of Medical Systems	18	Lung Nodule Diagnosis	Automated juxtapleural nodule detection	A(z) value is 0.9679
Bartholmai, BJ et al	2015	Journal Of Thoracic Imaging	18	Lung Nodule Detection	Review of lung nodles diagnosis	-
Duggan, N et al	2015	Lecture Notes in Computer Science	16	Lung Nodule Detection	Application of global segmentation, Mean curvature minimization, Simple rule-based filtering	-
Wang, B et al	2015	Medical Physics	15	Lung Nodule Detection	Shape constraint Chan-Vese model	Detect 88% of all the nodules in the data set with 4 FPs per case
Jorritsma, W et al	2015	Clinical Radiology	15	-	Review of CADx	-
Han, H et al	2015	Journal of Biomedical and Health Informatics	14	Lung Nodule Detection	Hierarchical vector quantization scheme	Sensitivity of 82.7% at a specificity of 4 FPs/scan
Shen, SW et al	2015	Computers in Biology and Medicine	14	Lung Nodule Detection	Parameter-free lung segmentation algorithm, Bidirectional chain codes	92.6% re-inclusion rate
Kao, EF et al	2015	Acta Radiologica	13	Lung Nodule Detection	Performance evaluation	・Sensitivity is 0.790 ・Specificity is 0.697

Table E. Cluster #3-1

Author	Publication Year	Journal	# of citation in Cluster	Modality is Ultrasonograph	MR	Main Subject	Method Keyword	Summary of results
Chen, CM et al	2003	Radiology	75	✔		Breast Cancer Diagnosis	Multilayer feed-forward neural network	・A(z) value is 0.952 for the first set ・A(z) value is 0.982 for the first set as the training set ・A(z) value is 0.982 for the second set as the training set
Chen, DR et al	1999	Radiology	71	✔		Breast Cancer Diagnosis	Neural network classifier	・The accuracy of classifying malignancies is 95.0% ・The sensitivity is 98% ・The specificity is 93%
Cheng, HD et al	2010	Pattern Recognition	60	✔		-	Review	-
Chen, DR et al	2002	Ultrasound in Medicine & Biology	52	✔		Breast Cancer Diagnosis	Multilayered perceptron neural network, Error back-propagation algorithm	・A(z) value is 0.9396 ・The sensitivity is 98.77% ・The specificity is 81.37%
Joo, S et al	2004	IEEE Transactions on Medical Imaging	50	✔		Breast Cancer Diagnosis	Artificial neural network	・A(z) value is 0.95 with 99.3% sensitivity
Chang, RF et al	2005	Breast Cancer Research and Treatment	49	✔		Breast Cancer Diagnosis	Support vector machine	-
Drukker, K et al	2002	Medical Physics	46	✔		Breast Cancer Detection	Radial gradient index filtering technique, Maximizing an average radial gradient index	94% sensitivity at 0.48 false-positives per image
Prabusankarl, KM et al	2014	Journal of Medical Imaging and Health Informatics	46	✔		-	Review	-
Meinel, LA et al	2007	Journal of Magnetic Resonance Imaging	46		✔	Breast Cancer Diagnosis	Backpropagation neural network	A(z) values are 0.792 / 0.912 (without / with CAD)
Chen, WJ et al	2004	Medical Physics	43		✔	Breast Cancer Diagnosis	Automatic volume-growing algorithm, Linear discriminant analysis	A(z) value of 0.80 for the LDA in leave-one-out cross-validation testin

Table F. Cluster #3-2

Author	Publication Year	Journal	# of citation in Cluster	Modality is Ultrasonograph	MR	Main Subject	Method Keyword	Summary of results
Flores, WG et al	2015	Pattern Recognition	16	✔		Breast Cancer Diagnosis	Mutual information and statistical tests	A(z) value is 0.942
Moon, WK et al	2015	Medical Physics	14	✔		Breast Cancer Diagnosis	Linear support vector machine, Leave-one-out cross-validation schema	・The A(z) values of the morphology is 0.8470 ・The A(z) values of conventional texture is 0.8542 ・The A(z) values of multiresolution gray-scale invariant texture feature sets is 0.9695
Uniyal, N et al	2015	IEEE Transactions on Medical Imaging	13	✔		Breast Cancer Diagnosis	Radio frequency time	・The A(z) values is 0.86 using support vector machines ・The A(z) values is 0.81 using Random Forests classification algorithms
Shimauchi, A et al	2015	European Radiology	12		✔	Breast Cancer Detection /Diagnosis	Kinetic entropy	The A(z) values are IU, SER, and KE were 0.479, 0.615, and 0.662
Rodrigues, R et al	2015	Ultrasound in Medicine & Biology	12	✔		Breast Cancer Detection	Support vector machine, Discriminant analysis pixel classification, AdaBoost algorithm	・Recall rates were 79.6% for AdaBoost and 77.8% for active contours ・The precision rate was 89.3% for both methods
Cai, LY et al	2015	BioMedical Engineering OnLine	12	✔		Breast Cancer Diagnosis	Support vector machine, Phased congruency-based binary pattern	PCBP texture descriptor achieves the highest values (i.e. A(z) values is 0.894)
Gubern-Merida, A et al	2015	Medical Image Analysis	11		✔	Breast Cancer Detection	Dynamic contrast-enhanced MRI, Segmentation	89% of the breast cancers were correctly detected
Lo, CM et al	2015	Ultrasound in Medicine & Biology	10	✔		Breast Cancer Diagnosis	Intensity-invariant ranklet coefficients	The A(z) values are 0.83 / 0.80(with / without ranklet transformation)
Wang, J et al	2015	PLOS ONE	10		✔	Breast Cancer Detection	Background Parenchymal Enhancement Heterogeneity	The A(z) value is 0.878(0.782 with previous method)
Xian, M et al	2015	Pattern Recognition	9	✔		Breast Cancer Detection	Segmentation, Reference point generation algorithm	The A(z) value is 0.9843(0.9664 with previous method)

Table G. Cluster #4-1

Author	Publication Year	Journal	# of citation in Cluster	Modality is Dermoscope	other	Main Subject	Method Keyword	Summary of results
Korotkov, K et al	2012	Artificial Intelligence in Medicine	64	✔		-	Review	-
Iyatomi, H et al	2008	Computerized Medical Imaging and Graphics	45	✔		Skin Lesions Detection	Internet-based melanoma screening system	・Sensitivity of 85.9% ・Specificity of 86.0%
Muller, H et al	2004	International Journal of Medical Informatics	38			-	Content-based visual information retrieval, Review	-
Schmid-Saugeon, P et al	2003	Computerized Medical Imaging and Graphics	35	✔		Skin Lesions Detection / Diagnosis	Principal component decomposition	-
Celebi, ME et al	2009	Computerized Medical Imaging and Graphics	34	✔		-	Review	-
Celebi, ME et al	2008	Skin Research and Technology	28	✔		Skin Lesions Detection	Automated Segmentaiton, Statistical region merging algorithm, Meanshift clustering	Lowest error rate is 4.186% (melanoma) and 8.290% (benign)
Burroni, M et al	2004	Clinical Cancer Research	26	✔		Skin Lesions Detection	K-nearest-neighbor classifier	・The linear classifier produced a mean sensitivity of 95%, and specificity of 78% ・The K-nearest-neighbor classifier produced a mean sensitivity of 98% and specificity of 79%
Celebi, ME et al	2007	Skin Research and Technology	25	✔		Skin Lesions Detection	Automated Segmentaiton, JSEG algorithm	The error rate is 14.91% (melanoma) and 10.78% (benign)
Niemeijer, M et al	2005	IEEE Transactions on Medical Imaging	24		✔	Skin Lesions Detection	Pixel classification, K-nearest neighbor classifie	The system achieves a sensitivity of 100% at a specificity of 87%
Hoffmann, K et al	2003	British Journal of Dermatology	24	✔		Skin Lesions Detection	Evaluation Studies, Artificial neural networks	-

Table H. Cluster #4-2

Author	Publication Year	Journal	# of citation in Cluster	Modality is Dermoscope	other	Main Subject	Method Keyword	Summary of results
Chang, WY et al	2015	BMJ Open	10	✔		Skin Lesions Diagnosis	Performance evaluation ,Dermatologists ,general practitioners and system	・A(z) value is 0.893 by the gold standard ・A(z) value is 0.886 by the dermatologists ・A(z) value is 0.883 by the general practitioners ・A(z) value is 0.856 by the JSEG ・Sensitivity and specificity were 80.07% and 81.47% for dermatologists and 79.90% and 80.20% for general practitioners.
Mollersen, K et al	2015	BioMed Research International	10	✔		Skin Lesions Detection / Diagnosis	Nevus Doctor system	・ For ND at 95% melanoma sensitivity, the NMSC sensitivity was 100%, and the specificity was 12%. ・The melanomas misclassified by ND at 95% sensitivity were correctly classified by ME, and vice versa
Shimizu, K et al	2015	IEEE Transactions on Biomedical Engineering	10	✔		Skin Lesions Detection	Layered models, Flat models	・Detection rates of 90.48% for melanomas ・Detection rates of 82.51% for nevi, ・Detection rates of 82.61% for BCCs ・Detection rates of 80.61% for SKs
Ng, KH et al	2015	Journal of Medical Imaging and Health Informatics	8		✔	-	Data Management	-
Mookiah, MRK et al	2015	Journal of Mechanics in Medicine and Biology	8		✔	-	Support vector machine	-
Guo, LY et al	2015	Computers in Industry	8		✔	Fundus Image Analysis	Real-world usage scenario	・The correct classification rates of two-class classification and cataract grading are 90.9% and 77.1% for the wavelet transform based method ・The correct classification rates of two-class classification and cataract grading are 86.1% and 74.0% for the sketch based method
MRK et al	2015	Computers in Biology and Medicine	8		✔	-	Review	-
Lee, TK et al	2015	Frontiers of Medical Imaging	7	✔		Melanoma Detection	Tree-based framework	・Achieved sensitivity and specificity of 0.89 and 0.90 ・Achived 0.86 and 0.85 for precision and recall
Oloumi, F et al	2015	Computers in Biology and Medicine	6		✔	Skin Lesions Detection	Gabor filters , Morphological image processing methods	A(z) value is 0.76
Sudarshan, VK et al	2015	Computers in Biology and Medicine	6		✔	Skin Lesions Detection	Discrete wavelet transform, Support vector machine	Obtained an accuracy of 99.5%, sensitivity of 99.75% and specificity of 99.25%

Table G. Cluster #5-1

Author	Publication Year	Journal	# of citation in Cluster	Modality is CTC	Others	Main Subject	Method Keyword	Summary of results
Yoshida, H et al	2001	IEEE Transactions on Medical Imaging	102	✔		Polyps Detection	Fuzzy clustering	A(z) value is 0.95
Kiss, G et al	2002	European Radiology	58	✔		Polyps Detection	Surface normal and sphere fitting methods	・Detection rate for polyps of 10 mm or larger was 100%, comparable to that of human readers ・Eight false-positive findings per case
Yoshida, H et al	2002	Radiology	58	✔		Polyps Detection	Means of hysteresis thresholding, Fuzzy clustering	・89% (16 of 18) of true polyps were detected, with a false-positive rate of 2.0 per data set
Summers, RM et al	2005	Gastroenterology	58	✔		Polyps Detection	Comparison to optical colonoscopy	・Per-polyp and per-patient sensitivities for CAD were both 89.3%
Gokturk, SB et al	2001	IEEE Transactions on Medical Imaging	50	✔		Polyps Detection	Support vector machine, Random orthogonal shape sections method	The system increases the specificity from 0.19 (0.35) to 0.69 (0.74) at a sensitivity level of 1.0 (0.95)
Yoshida, H et al	2005	Abdominal Imaging	50	✔		-	Review	-
Yoshida, H et al	2002	RadioGraphics	46	✔		Polyps Detection	Hysteresis thresholding, Fuzzy clustering	・At by-patient analysis, sensitivity was 100%, with an average false-positive rate of 2.0 per patient ・At by-polyp analysis, the scheme detected 90% of the polyps at the same false-positive rate
Summers, RM et al	2002	Radiology	45	✔		Polyps Detection	Performance evaluation	・By radiologist, large polyps sensitivity for detection is 48% ・By the CAD, large polyps sensitivity for detection is 48% too
Yoshida, H et al	2007	Computerized Medical Imaging and Graphics	44	✔		-	Review	-
Wang, ZA et al	2005	Medical Physics	44	✔		Polyps Detection	Surface-based measures	100% detection sensitivity (on polyps)

Table H. Cluster #5-2

Author	Publication Year	Journal	# of citation in Cluster	Modality is CTC	Others	Main Subject	Method Keyword	Summary of results
Motai, Y et al	2015	ACM Transactions on Intelligent Systems	9	✔		Polyps Detection	Multiple institution-wide databases, Group Kernel Feature Analysis	-
Wang, HF et al	2015	Physics in Medicine and Biology	8	✔		Polyps Detection	Ridge-shaped haustral folds, Initial polyp candidates	-
Thilo, C et al	2015	European Radiology	6	✔		Polyps Detection	Performance evaluation	・The sensitivity of the CAD system alone is 71 % per-vessel and 100 % per-patient ・With CAD, one inexperienced reader's per-patient sensitivity and negative predictive value significantly improved from 79 % to 100 %
Nasirudin, RA et al	2015	Proceedings of SPIE	5	✔		Polyps Detection	Image-based decomposition, Projection-based method	The highest A(z) value is 0.66 with projection-based method
Helbren, E et al	2015	European Radiology	5	✔		Polyps Detection	Performance evaluation, Inexperienced and experienced readers	・Median 'time to first pursuit' is 0.48 s with CAD, versus 0.58 s without ・Number of correct polyp identifications is 74 % / 87 % (without / with)
Liu, JF et al	2015	Medical Image Analysis	5	✔		Renal Lesions Detection	Renal lesions, Machine learning	95% sensitivity with 15 false positives per patient for detecting exophytic renal lesions
Suzuki, K et al	2015	IEEE International Conference on Systems	4	✔		Polyps Diagnosis	Shape-index-based coarse segmentation, Wilks' lambda-based stepwise feature selection	A(z) value is 0.82
Plumb, AA et al	2015	American Journal of Roentgenol	3	✔		Polyps Detection	Performance evaluation, Eye movements tracking	・97% of false-negative polyp diagnoses were nonetheless preceded by the reader observing the polyp
Koizumi, M et al	2015	Annals of Nuclear Medicine	3		✔	Bone Lesions Detection	Performance evaluation , BONEVAVI version 2	・The sensitivity of patient ANN values was 85 % for all cancers, 86 % for prostate cancer, 88 % for lung cancer,82 % for breast cancer, and 86 % for other cancers ・The specificity of ANN values was 82 % for normal bone scans, 81 % for consecutive patients with several days of no skeletal metastasis, and 54 % for patients with abnormal bone scans but no skeletal metastasis
Lee, ES et al	2015	European Journal of Radiology	3	✔		Polyps Detection	Statistical iterative reconstruction, Model-based iterative reconstruction	・With MBIR per-polyp sensitivity is 45.9 % ・With ASIR80 per-polyp sensitivity is 44.3 % ・With FBP per-polyp sensitivity is 35.2 %

Table I. Cluster #6-1

Author	Publication Year	Journal	# of citation in Cluster	Modality is SPECT	PET	MRI	Main Subject	Method Keyword	Summary of results
Chaves, R et al	2009	Neuroscience Letters	37	✔			Alzheimer's disease	Linear kernel support vector machine, T-test feature selection	·NMSE features of cubic blocks located in the temporoparietal brain region yields peak accuracy values of 98.3%
Lopez, MM et al	2009	Neuroscience Letters	25	✔			Alzheimer's disease	Kernel principal component analysis, Linear discriminant analysis, Support vector machine	Distinguish AD from normal subjects with 92.31% accuracy rate
Saxena, P et al	1998	Lecture Notes in Computer Science	23	✔			Alzheimer's disease	Statistical parametric mapping	–
Lopez, M et al	2011	Neurocomputing	23	✔	✔		Alzheimer's disease	Neural networks, Support vector machine	Achieved accuracy results of up to 96.7% and 89.52% for SPEDT and PET images
Illan, IA et al	2011	Information Sciences	21		✔		Alzheimer's disease	Principal component analysis , Independent component analysis, Support vector machine	88.24% accuracy in identifying mild AD, with 88.64% specificity, and 87.70% sensitivity is obtained
Martinez-Murcia, FJ et al	2012	Expert Systems with Applications	16	✔	✔		Alzheimer's disease	Mann–whitney–wilcoxon u-test, Factor analysis, Support vector machine	Achieves accuracy results of up to 93.7% and 92.9% for SPECT and PET images
Grana, M et al	2011	Neuroscience Letters	16			✔	Alzheimer's disease	Support vector machine	Achieving Accuracy = 100%, Sensitivity = 100% and Specificity = 100% in a leave-one-out cross-validation
Ramirez, J et al	2010	Neuroscience Letters	16	✔			Alzheimer's disease	Partial least squares regression model, Random forest predictor	PLS feature extraction yield sensitivity, specificity and accuracy values of 100%, 92.7%, and 96.9%
Segovia, F et al	2012	Neurocomputing	15		✔		Alzheimer's disease	Gaussian mixture model, Partial least squares algorithm, Support vector machine	-
Illan, IA et al	2011	Applied Soft Computing	15	✔			Alzheimer's disease	Support vector machine, Pasting votes technique	-

Table J. Cluster #6-2

Author	Publication Year	Journal	# of citation in Cluster	Modality is SPECT	PET	MRI	Main Subject	Method Keyword	Summary of results
Zhang, YD et al	2015	Frontiers in Computational Neuroscience	12			✔	Alzheimer's disease	Eigenbrain, Machine learning	Accuracy of the polynomial kernel (92.36 +/- 0.94) was better than the linear kernel of 91.47 +/- 1.02 and the radial basis function (RBF) kernel of 86.71 +/- 1.93
Zhang, YD et al	2015	PeerJ	10			✔	Alzheimer's disease	Displacement field estimation, Eigenvalue proximal support vector machine	Accuracy of 92.75 +/- 1.77, sensitivity of 90.56 +/- 1.15, specificity of 93.37 +/- 2.05, and precision of 79.61 +/- 2.21
Zhang, YD et al	2015	Entropy	9			✔	Alzheimer's disease	Eigenvalue proximate support vector machine	Accuracy of 100%, 100%, and 99.53% on Dataset-66, Dataset-160, and Dataset-255
Wang, SH et al	2015	Entropy	8			✔	Pathological Brain Detection	Fractional fourier entropy, Fractional fourier transform, Shannon entropy, Support vector machine	Accuracy of 100.00%, 100.00%, and 99.57% on datasets that contained 66, 160, and 255 brain images,
Khedher, L et al	2015	Neurocomputing	8			✔	Alzheimer's disease	Tissue-segmented brain images, Partial least squares, Principal component analysis	Sensitivity, specificity and accuracy values of 85.11%, 91.27% and 88.49%
Zhang, YD et al	2015	Progress In Electromagnetics Research	7			✔	Pathological Brain Detection	Wavelet entropy, Feed-forward neural network	Accuracy of 100%, 100%, and 99.49% over Dataset-66, Dataset-160, and Dataset-255
Zhang, YD et al	2015	International Journal of Imaging Systems and Technology	7			✔	Pathological Brain Detection	Support vector machine, Weighted-type fractional Fourier transform, Principal component analysis	Sensitivity of 99.53%, specificity of 92.00%, precision of 99.53%, and accuracy of 99.11%
Khedher, L et al	2015	Lecture Notes in Computer Science	5			✔	Alzheimer's disease	Independent component analysis	87.5% accuracy in identifying AD from NC, with 90.4% specificity and 84.6% sensitivity
Brahim, A et al	2015	Applied Soft Computing	5	✔			Intensity normalization of DaTSCAN SPECT imaging	Gaussian mixture models, Intensity normalization	-
Beheshti, I et al	2015	Computers in Biology and Medicine	5			✔	Alzheimer's disease	Voxel-based morphometry, Probability distribution function	With SVM by linear Kernel, 89.65% accuracy, 87.73% sensitivity, 91.57% specificity, and 95.33% AUC

Table K. Cluster #7-1

Author	Publication Year	Journal	# of citation in Cluster	Main Subject	Method Keyword	Summary of results
Giger, ML et al	2001	IEEE Transactions on Medical Imaging	14	-	CAD&Medicacl Imaging Review	-
Kavitha, MS et al	2012	BMC Medical Imaging	10	Mandibular Cortical Bone Osteoporosis	Dental osteoporosis, Kernel-based support vector machin	·The sensitivity and specificity using RBF kernel-SVM method were 90.9% and 83.8% ·The sensitivity and specificity at either the lumbar spine or femoral neck were 90.6% and 80.9%
Qi, X et al	2006	Journal of Biomedical Optics	10	Dysplasia in Barrett's esophagus	Barrett‘s esophagus,Standard texture analysis method	·Sensitivity of 82% ·Specificity of 74% ·Accuracy of 83%
Lin, DT et al	2006	IEEE Transactions on Information Technology in Biomedicine	9	Kidney Disease	Kidney, Automatic segmentation , Second-order neighborhood edge detection	·Sensitivity and specificity with low spinal BMD were 88.0% and 58.7% ·Sensitivity and specificity with low femoral neck BMD were 87.5% and 56.3%
Arifin, AZ et al	2006	Osteoporosis International	9	Mandibular Cortical Bone Osteoporosis	Dental osteoporosis, Performance evaluation	-
Lim, SJ et al	2006	Journal of Visual Communication and Image Representation	8	Liver Disease	Automatic segmentation, Volume measurement, Morphological filtering, Deformable contouring	-
Chan, T	2007	Computerized Medical Imaging and Graphics	7	Small Acute Intracranial Hemorrhage	Acute intracranial hemorrhage, Knowledge-based classification	·Sensitivity of 95% and specificity of 88.8% in the training dataset ·The sensitivity and specificity were 100% and 84.1% in the validation cases ·False positive rates were 0. 19 and 0.29 false positive lesion per case for the training and validation datasets
Chen, Y et al	2008	Optics Express	6	-	Barrett‘s esophagus, Principal component analysis, Linear discrimination analysis	Enhanced discrimination of normal and Barrett's esophagus with UHR-OCT
Lim, SJ et al	2004	The International Society for Optics and Photonics	5	Liver Disease	Automatic segmentation, Morphological filters, Priori knowledge	Acquire a more accurate liver region
Kumar, SS et al	2013	Signal, Image and Video Processing	5	Liver Disease	Automatic segmentation, Alternative fuzzy C-means clustering	·Volume measurement error is 1.52% for liver segmentation and 1.93% for lesion segmentation ·The mean FPE for liver segmentation is 0.4360% and for lesion it is 1.1230%

Table L. Cluster #7-2

Author	Publication Year	Journal	# of citation in Cluster	Main Subject	Method Keyword	Summary of results
Horiba, K et al	2015	Proceedings of SPIE	3	Mandibular Cortical Bone Osteoporosis	Dental osteoporosis, Support vector machine	Sensitivities for the classes I, II, and III were 94.6%, 57.7% and 94.1%
Sethi, G et al	2015	Australasian physical & engineering sciences in medicine	3	Abdomen Disease Diagnosis	Feature extraction , Genetic algorithm	Flexi-scale curvelet transform were more discriminative than conventional methods
Wrosch, JK et al	2015	Frontiers in Neurology	3	Ischemic Stroke Territory Recognition	Artery territory recognition, Segmentation, Geoprojected two-dimensional maps	Sensitivity was 81% with a specificity of 87%
Kavitha, MS et al	2015	Oral Surgery, Oral Medicine, Oral Pathology, Oral Radiology	2	Mandibular Cortical Bone Osteoporosis	K-nearest neighbor algorithm, Support vector machine	Accuracy with the use of the naive Bayes, k-NN, and support vector machine classifiers ・FD plus MCW (95.3%, 92.1%, 96.8%) ・GLCM plus MCW (93.7%, 89.5%,
Acharya, UR et al	2015	Knowledge-Based Systems	2	Liver Disease	Fatty Liver Disease, Review	-
Sun, JJ et al	2015	Journal of Medical Imaging and Health Informatics	1	Liver Disease	Multi-cascade & multi-featured classifier	Accuracy rate of normal patient or abnormal patient reaches 99.49 percent
Bonanno, L et al	2015	Ultrasound in Medicine & Biology	1	Carotid Atherosclerosis	Watershed segmentation	・A(z) value is 0.89 ・Diagnostic accuracy was 89%,sensitivity was 83% and specificity reached a value of 85%
Hori, M et al	2015	Academic Radiology	1	Liver Disease	Segmentation, Statistical shape model, Linear support vector regression	In SSM/SVR models, the A(z) values were 0.96 (F0 vs. F1-4), 0.95 (F0-1 vs. F2-4), 0.96 (F0-2 vs. F3-4), and 0.95 (F0-3 vs. F4)

2 EVALUATION OF MEDICAL IMAGE DATA SHARING

2.1 Introduction

Previous studies have argued that sufficient medical images can lead to a performance improvement of CAD systems [107], [198]. However, whether this performance improvement can really have a positive societal effect, and how large, remains unclear. Fig. 8 shows how data sharing effects our society. First, medical images are shared between healthcare establishments and CAD system developers. Second, more medical images can be accumulated than ever before, and such image data are applied to the training dataset. Third, training dataset accumulation could improve the CAD system performance, and fourth, doctors using the system are able to detect many more diseases, including neoplastic lesions. As a result, more patient lives can be saved, and a favorable effect on our society can be achieved. Furthermore, a health technology assessment (HTA) was conducted for this study, and its effect based on a cost-effectiveness analysis (CEA) and a cost-utility analysis (CUA) was evaluated [199]. With finite financial resources, global health expenditures—particularly in developed economies—have been experiencing a dramatic increase. This growth in health expenditure has required the adoption of new technologies, as well as the management of its impact on long-term health care spending. HTA or CEA methodologies assess efficiency in resource allocation and support decision-making on the use of new technologies [200]. CEA usually presents a cost–effect ratio (i.e., incremental cost-effectiveness ratio (ICER)) as an indicator for decision-making. The effects should then be varied depending on various purposes (e.g., life years gained, or quality-adjusted life year (QALY)). QALY may be thought of as a year of life that is lived in perfect health. To calculate the costs and effects, it is important to estimate the probabilities of all events that occur as a result of intervention, which is assumed herein. These probabilities can be expressed as a decision tree model. A decision tree model, however, was not adopted to simulate multiple outcome events that recur over time. On the other hand, state-transition models, particularly Markov models [201], are more suitable for calculating recurring events. These models allocate members of a population, which are considered as “states” in the present analysis (i.e., disease stage, treatment status, or their combination). Populations proceed from one state to another at defined time intervals. In the Markov model, transition probabilities depend on the current state. Therefore, Markov models are useful when a decision problem involves risk that is continuous over time, when the timing of events is important, and when important events may occur more than once. The purpose of this chapter is to assess the effect of medical image data sharing on the cost-effectiveness through a comparative

case study of breast cancer, colorectal cancer (CRC), and Alzheimer's disease CAD systems.

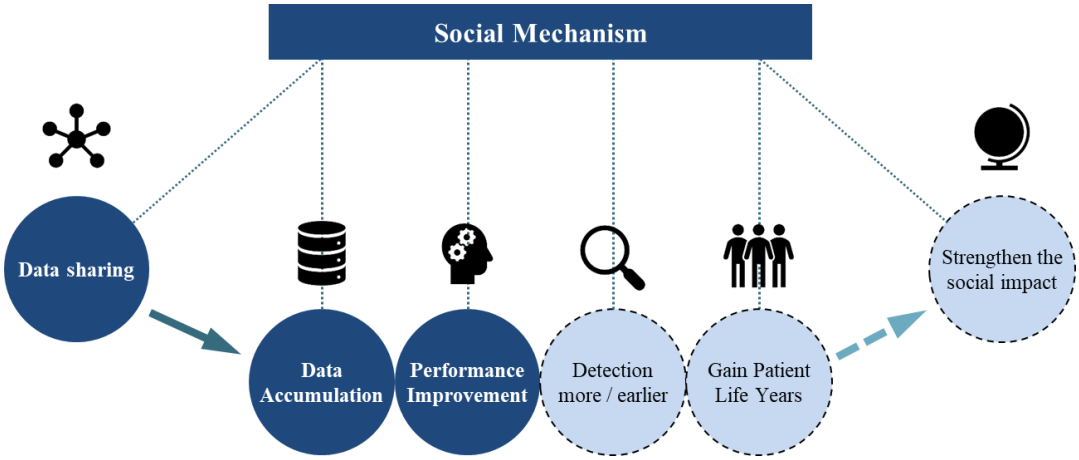

Figure 8. Social mechanism of data sharing effect

2.2 Related Work

There have been some studies which adopts CEA and Markov models to assess BC and CRC CAD system's cost-effectiveness [202]–[205]. The first research, as far as I know, to analyze the cost-effectiveness of adding CAD was published in 2007 [202]. This study compared three hypothetical groups of women aged 40–79 years; women undergoing mammographic screening without CAD, women undergoing mammographic screening with CAD, and women undergoing observation without screening. The study also concluded that marginal cost per year of life saved is 19% greater for CAD added to screening versus screening mammography alone, however CAD addition is still within the accepted range for cost-effectiveness. Furthermore, two studies was to investigate whether use of a single reader with CAD is more cost-effective than double reading in UK and Japan [203], [204]. On the UK research, CAD was unlikely to be more cost effective alternative than double reading for mammography screening. One of the main factor not to improve introduction of CAD's cost-effectiveness might be the cost of CAD equipment. The cost of CAD equipment, staff training, and the higher assessment cost associated with CAD were higher than the cost to be saved in reading. With concrete figures, the introduction of single reading with CAD, in place of double reading, would produce an additional cost of £227 and £253 per 1,000 women. On the other hand, research in Japan concluded that single reading using CAD in mammography screening was more cost-effective than double reading, although the sensitivity and specificity of CAD and the number of breast cancer screening examinees greatly affected the results. In addition to breast cancer

modeling, research for colorectal cancer CAD cost-effectiveness was also conducted [206]. In the model, a hypothetical population of 100,000 persons aged 50 years underwent colorectal screening every 10 years, and the research mainly compared diagnosis by experienced reader without CAD and inexperienced reader with CAD. The conclusion was that the addition of CAD improved the CRC prevention rate, and also improved cost-effectiveness in societal perspective.

2.3 Method

2.3.1 Cost, Effectiveness and Utility

In our cost-effectiveness and cost-utility analysis, I use the best point estimates for all inputs (e.g., parameters and event probabilities). Benefits are expressed as gain in life years or quality adjusted life years (QALYs), where 0 represents the patient's death and 1.0 the patient being in perfect health; these weights are assigned to each year of life. Costs are expressed in 2016 US dollars adjusted for inflation by using the medical care component of the consumer price index. Future costs and QALYs are discounted at 5% annually. The main outcome measure for each strategy or intervention is the incremental cost-effectiveness ratio, ICER, where changes in resource use compared to other strategies are divided by QALYs gained compared to other strategies. ICER is expressed in Δ Costs /Δ Life or QALYs. The study is conducted from a societal perspective, and incorporates all costs and effectiveness and utility factors regardless of who incurred them.

2.3.2 Cases and Models

I modeled a breast cancer screening process and principally referred to previous research data [204]. Mammography is acknowledged as the most effective screening intervention for breast cancer. It is credited for reducing breast cancer mortality [207], [208]. Additionally, mammography CAD is expected—as an adjunct to screening mammography—to increase breast cancer detection rates [14]. However, the cost-effectiveness of mammography CAD remains controversial [202]–[204]. The model in this study is established by extending the concept of the Markov model to compare readings between two physicians using mammography and between a physician using mammography and CAD; the latter comparison was conducted by and without considering the learning model. The baseline assumptions (probabilities [204], [209], [210] and costs [204], [211]) and ranges used in the model are provided in Table 4 and 5. Health state is divided into six states; women with non-breast cancer (BC) history, early stage by screening (SC) follow-up, advanced stage by SC follow-up, early stage by outpatient visit (OP) follow-up, advanced stage by OP follow-up, and death

(Fig.9). In this simulation model, every population starts with women with non-BC history. Initially, the population is divided into breast cancer positive (BC+) or breast cancer negative (BC-), and a transition rule is followed. Every case is subject to the same flow, probabilities, and cost, except for assumptions related to screening (Fig.10). Considering standard mammography screening frequency, one cycle of simulation comprises two years.

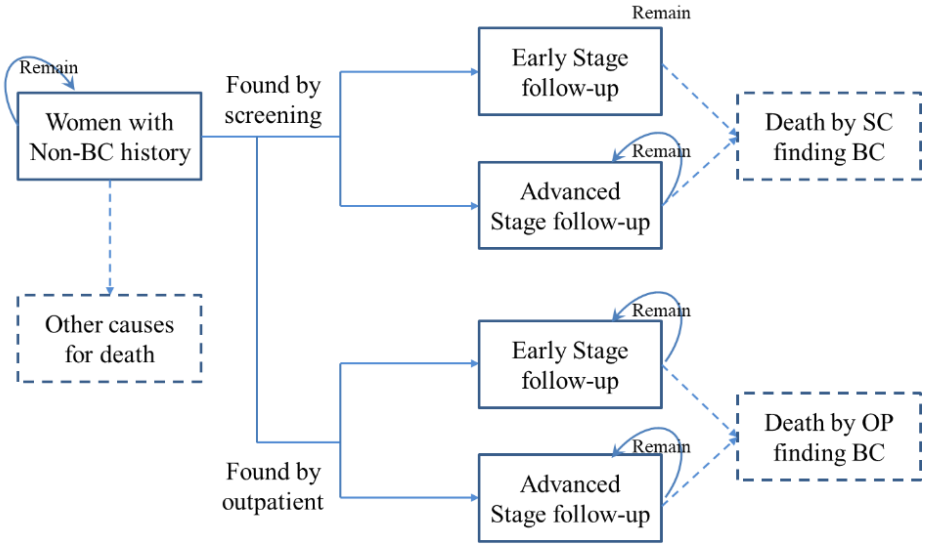

Figure 9. Breast cancer state transition

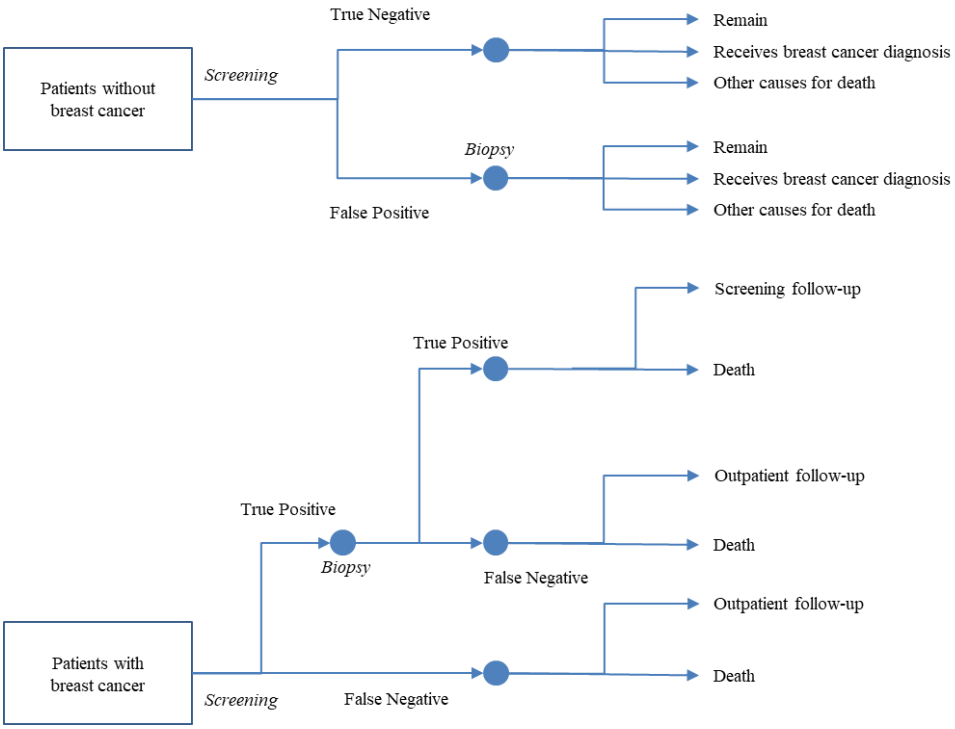

Figure 10. Breast cancer model structure

Table 4. Mammography model probabilities

Probabilities Data		
	Probabilities	References
Epidemic Data		
Breast cancer prevalence	0.003	A. Suzuki et al (2008)
Screening found breast cancer		M. Sato et al (2014)
Early stage	0.830	
Advanced stage	#	
Interval breast cancer		M. Sato et al (2014)
Early stage	0.560	
Advanced stage	#	
Sensitivity and Specificity		
Mammography double reading		A. Suzuki et al (2008)
Sensitivity	0.858	
Specificity	0.907	
Mammography CAD		L. H. Eadie et al (2012)
Sensitivity	0.908	
Specificity	0.927	
Biopsy		M. Sato et al (2014)
Sensitivity	0.956	
Specificity	1.000	
Mortality Rates		
Women with non-BC history	0.002	M. Sato et al (2014)
Screening found breast cancer		M. Sato et al (2014)
Early stage	0.011	
Advanced stage	0.111	
Interval breast cancer		M. Sato et al (2014)
Early stage	0.028	
Advanced stage	0.281	

Table 5. Mammography model costs

Costs Data			
		Costs	References
Diagnosis Fee	US$ / 1 diagnosis		M. Sato et al (2014)
Screening Fee			
Mammography + 1 doctor		75	
Second Reading		1	
CAD		3	
Biopsy		84	
Outpatient		385	
Treatment costs	US$ / first 2 years		J. Ferlay (2012)
Early stage		22,115	
Advanced stage		39,016	
Follow-up costs	US$ / 1 year		M. Sato et al (2014)
Early stage		3,562	
Advanced stage		14,401	

I also modeled a colorectal cancer (CRC) screening process based on previous research [205]. CRC is one of the leading causes of cancer death in the world [212]. Screening for CRC has been identified as a factor in reducing mortality [213], [214], and recent studies have demonstrated the clinical and cost-effectiveness of computed tomographic colonography (CTC) for CRC [215], [216]. Moreover, CRC CAD is expected to take over the role of a second reader [217]. This model is established with a Markov model to compare the cost-effectiveness of CTCs performed by inexperienced readers without CAD, with CAD, and with CAD considering a learning model. Health state is divided into eight states; no colorectal neoplasia; diminutive (≤5 mm), medium (6–9 mm), or large (≥10 mm) adenomatous polyp; localized, regional, or distant CRC; and CRC-related death (Fig.11). As with the first mammography CAD assumption, every case is subject to the same flow, probabilities, and cost, except for assumptions related to screening (Fig.12). In each case, screening is assumed to be repeated every five years due to popular screening frequency, and one cycle of simulation comprises one year. Probabilities [218]–[240] and costs [240]–[245] are shown in Table 6 and 7, respectively.

To our knowledge, cost-effectiveness related to AD CAD has not yet been discussed. AD is a progressive type of dementia that, in its early stage, affects memory functions.

As the disease progresses, its symptoms gradually develop, affecting all cognitive functions [246]. In 2015, 46.8 million people experienced this disease all over the world, and AD is predicted to affect 1 in 85 people globally by 2050 [247]. Furthermore, it is widely assumed that a cure for AD is not feasible as it would account for an annual economic cost exceeding $600 million [248], [249]. However, early and accurate detection of AD is beneficial to control the disease's progression [250]. An AD diagnosis is reliant on data from clinical examinations, a thorough interview of the patient and relatives, and medical imaging. Non-invasive tests like Positron Emission Tomography (PET), Single Photon Emission Computed Tomography (SPECT), and Magnetic Resonance Imaging (MRI) are mainly used for AD imaging diagnosis. While these testing modalities are highly efficient, early detection of AD still remains a difficult task [251]. Firstly, the clinical diagnosis of AD comes relatively late into the disease's progression. Secondly, it is difficult to distinguish the initial stages of AD from natural cognitive impairment due to aging processes. Thirdly, conventional evaluation of imaging scans often relies on manual reorientation, visual reading, and subjective medical analysis, as there is no standardized diagnostic process. Hence, CAD is highly expected to be developed as a tool for early detection of AD, and to help patients gain more patients' a higher Quality of Life (QoL). Presently, the AD CAD research domain can be divided into three groups as per imaging modality; PET [130]–[132], SPECT [127], [128], [130], [132], and MRI [133], [137], [141], [252], [253].

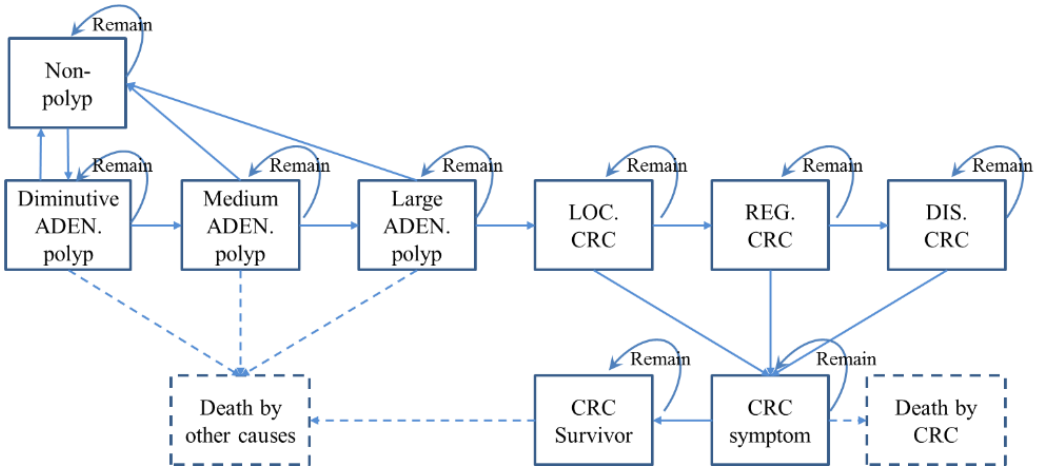

Figure 11. CRC state transition

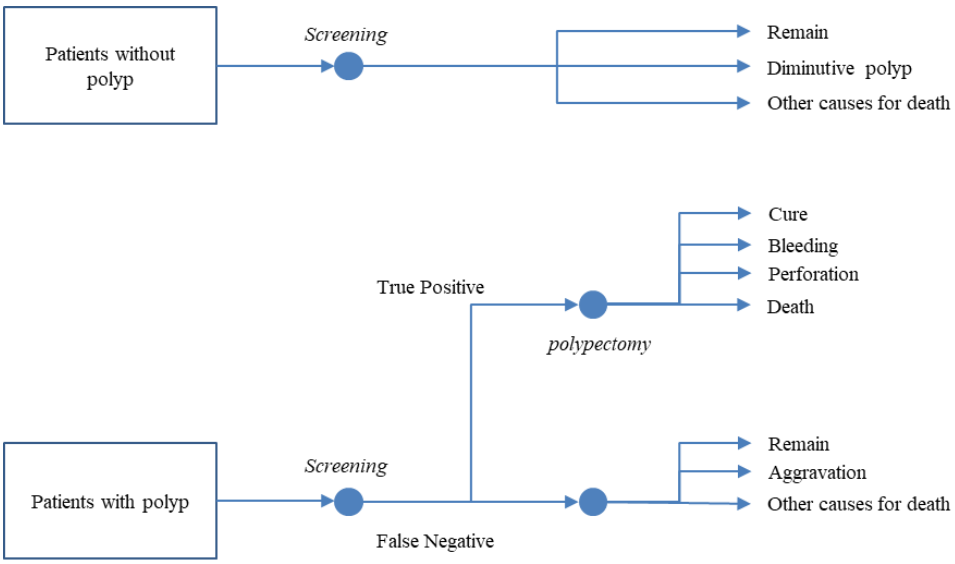

Figure 12. CRC model structure

Table 6. CTC model probabilities

Probabilities Data	Probabilities	References
Epidemic Data		
Adenoma prevalence at age 50	0.150	*1
Polyp<10 mm	0.950	
Polyp>=10 mm	0.050	
New adenomatous polyp rate	0.019-0.033	F. Loeve et al (2004)
Annual transition rate		*2
From small to medium	0.0002-0.078	
From medium to large	0.0002-0.078	
From large to LOC CRC	0.01-0.1	
From LOC to REG CRC	0.330	
From REG to DIS CRC	0.400	
Symptomatic presentation		SEER Cancer Statistics Review
LOC CRC	0.200	
REG CRC	0.650	
DIS CRC	1.000	
Moratality Rates		Fast Stats
LOC CRC in first 5y (per year)	0.017	
REG CRC in first 5y (per year)	0.086	
Mean survival from DIS CRC	0.019	
Screening		B. Levin et al (2008)
Adherence	0.700	
Sensitivity and Specificity		*3
Inexperienced Reader without CAD		
Sensitivity		
Medium ADEN	0.495	
Large ADEN	0.648	
CRC	0.950	
Specificity	0.887	
Inexperienced Reader with CAD		
Sensitivity		
Medium ADEN	0.608	
Large ADEN	0.861	
CRC	0.950	
Specificity	0.819	
After Detection Follow-Up		C. Hassan et al (2008)
Colonoscopy Perforation	0.00060	
Polypectomy Bleeding	0.00480	
Polypectomy Perforation	0.00110	
Colonoscopy-related death	0.00006	

*1: J. Disario et al (1991), M. Vatn et al (1982), R. R. Rickert (1979), T. C. Arminski et al (1964), G. N. Stemmermann (1986), T. J. Eide et al (1986), D. Johnson et al (1990), J. Yee, G et al (2001), A. R. Williams et al (1982), J. Clark et al (1985), R. Koretz (1993)

*2: B. Hofstad et al (1996), G. Hoff et al (1986), S. J. Stryker (1987), S. Welin et al (1963), U. Ladabaum et al (2001)

*3: N. Petrick et al (2008), S. Halligan et al (2006), A. H. Dachman et al (2010)

Table 7. CTC model costs

Costs Data			
		Costs	References
Diagnosis			*4
Start-up CRC screening program	US$	50,000	
CT Colonography	US$	665	
CAD	US$	50	
Indirect cost, CT colonography	US$	75	
After Detection Follow-Up			*4
Optical colonoscopy with polypectomy	US$	877	
Optical colonoscopy	US$	1,265	
Bleeding care	US$	5,494	
Perforation care	US$	16,380	
Treatment			*5
LCO CRC	US$	51,800	
REG CRC	US$	76,500	
DIS CRC	US$	80,000	

*4: C. Hassan et al (2008), F. K. L. Tangka et al (2008), Edgar-Online-Web-site, U.S. Bureau of Labor Statistics, T. R. Levin et al (2006)
*5: S. H. Taplin et al (1995), B. H. Fireman et al (1997), M. L. Brown et al (1999)

I applied the Markov model [254], [255] wherein AD and potential AD patients receive a standard diagnosis, including acquisition of detailed medical history, assessment of cognition and functional status, laboratory testing, structural brain imaging with dynamic susceptibility-weighted contrast-enhanced MR imaging [256], and CAD and standard diagnosis with and without considering the learning model. As patients transition between disease stages following diagnosis and treatment, they accrue costs and benefits over each cycle. Disease stages are classified into five states: mild, moderate, and severe, according to the categories in the Clinical Dementia Rating (CDR) scale [257], in addition to the states of no AD and death. The structure of the model with all five health states can be seen in Fig. 13. Previous studies observed how AD progresses in a month [258], and according to the research, I constructed a model wherein patients are re-classified as per each disease stage for a four-week cycle. The diagnosis flow chart is shown in Fig. 14. The model assumes that all patients who receive a diagnosis of probable AD receive treatment with donepezil. Once a patient

progresses to severe AD, no further drug treatment is given, because exiting trial data does not support the efficacy of the drug in patients with severe AD [259]. I also assume that treatment would not be discontinued unless the patient progresses to severe AD or dies.

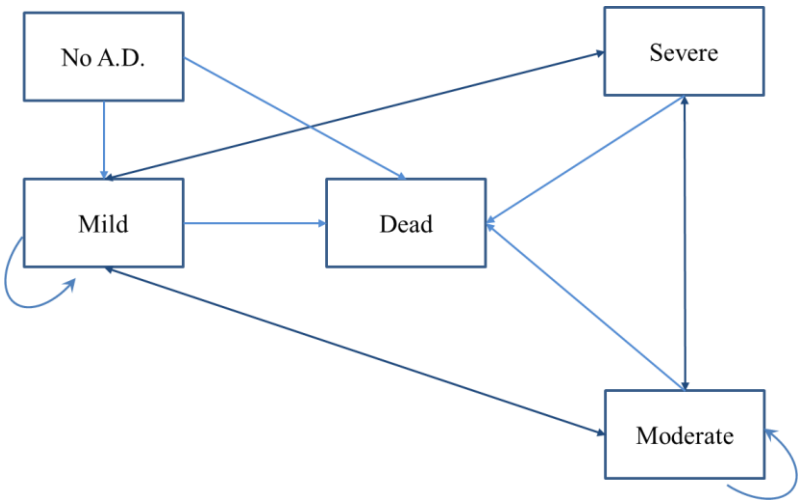

Figure 13. Alzheimer Disease states

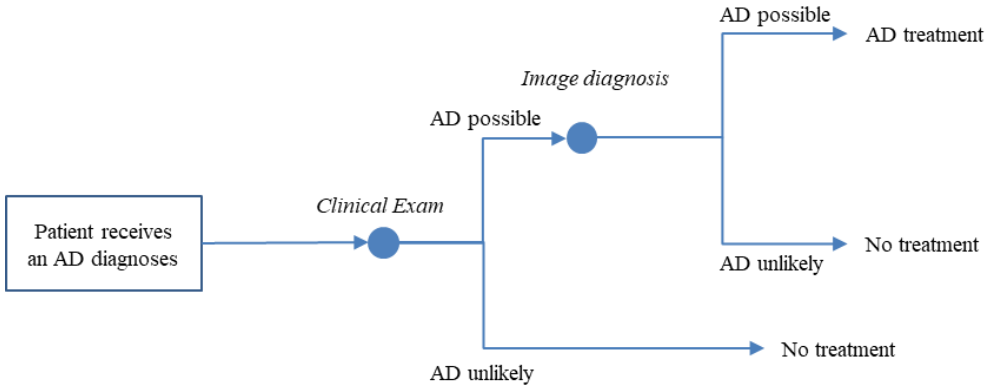

Figure 14. Alzheimer Disease diagnosis flow chart

Considering previous studies [259], [260], donepezil treatment has been shown to reduce the annual decline in cognition of AD patients. Therefore, I adopt these studies' estimations [258] for state transition probabilities with or without donepezil (Table 8). These effects are assumed to be constant throughout the duration of the treatment with no residual effect at drug discontinuation. For the base-case analysis, I estimate the initial ratio of no AD, and mild and moderate to severe AD cases to be 1.5:1.5:1:0 [261]. The general diagnostic work-up consists of two physician consultations, a series of laboratory tests, and a structural imaging examination. Furthermore, for the diagnosis,

the patient's travel cost and the time cost for the caretaker and patient are also required. The total cost has been already estimated in a previous study [261]. Subsequently, I estimate the costs to be approximately US$500 per diagnosis, US$350 per clinical exam, and US$150 per imaging diagnosis based on it. Furthermore, since AD CAD systems' cost is not available to the public, our estimation uses the average cost of other types of CAD systems [202]–[205]; US$22. With respect to routine life, direct medical costs (donepezil, medical visits, hospital admissions, emergency visits, orthopedic devices, and others), and direct non-medical costs (costs of cares) are also incurred, and I estimate monthly costs at each state [262] (Table 9).

Table 8. AD transaction probabilities

■Monthly transition probabilities
K. Mirsaeedi-Farahani et al (2015)

	Next state without donepezil				
Initial states	No AD	Mild	Moderate	Severe	Dead
No AD	0.995	0.003	0.000	0.000	0.002
Mild	0.000	0.962	0.032	0.004	0.002
Moderate	0.000	0.003	0.958	0.034	0.005
Severe	0.000	0.000	0.000	0.986	0.014

	Next state with donepezil				
Initial states	No AD	Mild	Moderate	Severe	Dead
No AD	0.995	0.003	0.000	0.000	0.002
Mild	0.000	0.980	0.014	0.004	0.002
Moderate	0.000	0.009	0.952	0.034	0.005
Severe	0.000	0.000	0.000	0.986	0.014

Table 9. AD monthly treatment cost

■Monthly cost
J. López-Bastida et al (2009)

Costs($)	Mild	Moderate	Severe
Direct health care cost	85.93	160.00	268.19
Direct non-health care cost	1,196.28	2,202.93	3,791.54
Total Cost	1,282.21	2,362.93	4,059.73

For the test characteristics of the standard clinical examination, I estimate sensitivities of 0.70 and 0.80 for the detection of mild and moderate AD, respectively, and a specificity of 0.73 for the detection of AD. These estimates are based on the

results of published studies wherein sensitivity values were estimated according to the stage of the disease [260], [263], [264]. Furthermore, MR imaging sensitivity for mild AD and moderate AD and specificity are estimated at 0.88, 0.95, and 096, respectively [265]. In our assumption, CAD system only affects mild AD sensitivity, and its value is estimated to be 0.91 [133], [137], [141], [252], [253]. Quality-of-life weights for patients without AD are estimated at 0.826 on a scale of 0 (dead) to 1 (perfect health) at 65-84 years of age [266]. Quality-of-life weights for patients with AD at each disease stage are based on [258]; mild is 0.651, moderate is 0.428, and severe is 0.307.

2.3.3 Data Sharing Effects

Several studies have used computer-generated databases to predict the effect, if any, of database selection on the CAD performance, and reported a substantially possible bias if CAD is trained using a small dataset or a large number of features [267], [268]. Furthermore, a study investigated the dependence of CAD performance on the "difficulty" of the testing datasets, where at a false-positive rate of 1 per image, the sensitivity levels of a pre-optimized CAD scheme were 26%, 74%, and 100% on three testing datasets with different difficulty levels [269]. Another study reported that the CAD system performance increased from a AUC of 0.724 to 0.836 as the size of training dataset increased from 50 to 500 [270], and yet another study reported that the CAD performance increased from a AUC of 0.715 to 0.874 as the training database size increased from 630 to approximately 2,000, and then reached a plateau as the training database size increased to 3,150 [271].

A model was constructed herein in which the CAD performance gradually improves with each diagnosis, which is applied mainly depending on a latest study evaluating the effect on a training dataset [198]. In this study, a full-field digital mammographic image database including 525 cases depicting malignant masses was randomly partitioned into three subsets. A mammography CAD scheme was applied to detect all initially suspected mass regions, and compute the region conspicuity. Training samples were iteratively selected from two of the subsets. Four types of training datasets were applied, as described below. The first included all available true-positive mass regions in the two subsets. The second included 350 randomly selected mass regions. The third contained 350 high-conspicuity mass regions, and the fourth included 350 low-conspicuity mass regions. Furthermore, the same number of randomly selected false-positive regions as true-positives was also included in each subset. Two classifiers, an artificial neural network (ANN) and a k-nearest neighbor (KNN) algorithm, were trained using each of the four training datasets and tested on all suspected regions in the remaining dataset.

Using a threefold cross-validation method, the performance changes of the CAD schemes trained using one of the four training datasets were computed and compared. Using all training datasets, CAD achieved the highest overall performance on the entire testing database. In particular, the detection of low-conspicuity masses increased by 7.1% and 15.1% for the ANN and KNN algorithms, respectively.

Based on the above, I assume that an improvement in data accumulation attains a 10% enhancement in accuracy to the maximum degree. Additionally, I assume that this enhancement forms a sigmoid curve, and reaches the highest point in five years based on the standard durable life of software. Moreover, I assume that sensitivity and specificity cannot yet attain 100% accuracy; therefore, when sensitivity and specificity are over 99% accuracy, I adopt 99% as the performance.

2.3.4 Sensitivity Analysis

Most of the probability and cost data described herein are from published research papers; however, a large amount of the data includes certain assumption. Therefore, a one-way sensitivity analysis was carried out to assess the robustness of ICERs according to the variation in each variable, and the top-ten high-impact variables were selected based on the results. Through an analysis, each parameter was increased and decreased by 20%, and the BC simulation model was adopted.

2.3.5 Scenario Analysis

Furthermore, a scenario analysis was conducted for four cases using the CTC simulation model. The above model is based on best-estimate assumptions, and therefore was validated to increase the accuracy of the results. First, it was assumed that the improvement in data accumulation attained a 5% enhancement in accuracy to the maximum degree, forming a sigmoid curve, and reaching the highest point in five years. This scenario can be possible if the systems have a more sufficient training dataset at the release point than expected. Herein, this scenario is called “scenario A.” Second, it was assumed the case accrued medical images faster than expected, and therefore, improvement in data accumulation reached the highest point within two-and-a-half years, all other conditions being equal. Third, this scenario refers to a case in which the CTC CAD system has much more room to be refined; therefore, it is assumed that the improvement in data accumulation attains a 15% enhancement in accuracy to the maximum degree. The other conditions are also equal, and this scenario is called “scenario C-i.” Moreover, this “scenario C-i” model was expanded to reflect the fact that it is more difficult to accrue diagnosed image data for a small polyp than a large one [272]; therefore, it was assumed a large amount of large polyp image data is

accumulated than small polyp image data when the simulation begins. This model is called “scenario C-ii,” and it estimated that a 12% enhancement has already been achieved for large polyp detection. In addition to the CTC model scenario analysis, a scenario analysis for an AD model was also conducted. It was assumed that medical doctors do not make a diagnostic decision based on a clinical examination, but only an image diagnosis. This scenario is called “scenario D” herein.

2.4 Result

2.4.1 Base Case Analysis

The results of our base case analysis are as follows. According to BC diagnosis, the strategy of introducing CAD, compared to standard diagnosis, yields an ICER of US$2,438. The learning model shows an ICER of US$1,415 per life year gained. According to CRC diagnosis, the strategy of introducing CAD, compared to standard diagnosis, gives an ICER of US$42,277, while the learning model yields US$35,477 per life year gained. Finally, in AD diagnosis, introducing CAD, compared to standard diagnosis, yields an ICER of US$797,378 or US$1,017,911 per QALY.

2.4.2 Sensitivity Analysis

The results of the sensitivity analysis are as follows. The parameter that had the largest impact on ICER was the double-reading specificity of the mammography CAD, and the second was the specificity. The third and fourth influential parameters were related to follow-up medical costs. On the other hand, diagnostic costs did not have as large an impact on the results. A tornado diagram is shown in Fig. 15, and details are shown in the Appendix.

Figure 15 Tornado diagram for sensitivity analysis

2.4.3 Scenario Analysis

In the scenario analysis of the CTC model (scenarios A, B, C-i, and C-ii), the difference in ICER between the no-improvement model and improvement model is 5,518, 6,943, 7,804, and 7,795 US$. A summary of the results and conditions is shown in Fig. 16. On the other hand, in the scenario D analysis, the improvement model, compared to the no-improvement model, shows a decrease in the ICER of 1,938,868 to 1,900,012 US$ per QALY.

		Enhancement Maximum Degree	Required Years for Highest Point	Considering Polyp Size	ICER Ratio
No Improvement Model		-	-	-	100%
Base Improve Model		10%	5year	-	84.11%
Scenario A		5%	5year	-	86.91%
Scenario B		10%	2.5year	-	83.53%
Scenario C	Case-i	15%	5year	-	81.50%
	Case-ii	15%	5year	○	81.52%

Figure 16 Scenario analysis result

2.5 Discussion

2.5.1 Base Case

In the hypothetical population of our study, training data accumulation or medical image sharing drastically improved the cost-effectiveness of BC and CRC CAD, while AD CAD did not improve. Therefore, I considered that data sharing effect improved social cost-effectiveness of some type of CAD; however, this tendency does not apply to the AD CAD case. I surmised that, firstly, BC and CRC are curable or likely to improve with timely and appropriate treatment. However, AD is a progressive type of dementia, incurable, and patients seldom recover from it. With AD CAD observations, the progression of the disease can only be delayed, hence, CAD performance improvement could not largely impact obtainable effectiveness. Secondly, BC and CRC are life-threatening diseases, while AD only deteriorates QoL. Therefore, the detection of AD could not improve obtainable effectiveness, and the greater life expectancy involved implied additional costs for society. Thirdly, doctors consider medical imaging central to BC and CRC diagnoses; hence, CAD accuracy directly links to diagnosis accuracy. On the other hand, in AD diagnosis, doctors prioritize clinical examination, while medical imaging is used to confirm observations (Fig. 17).

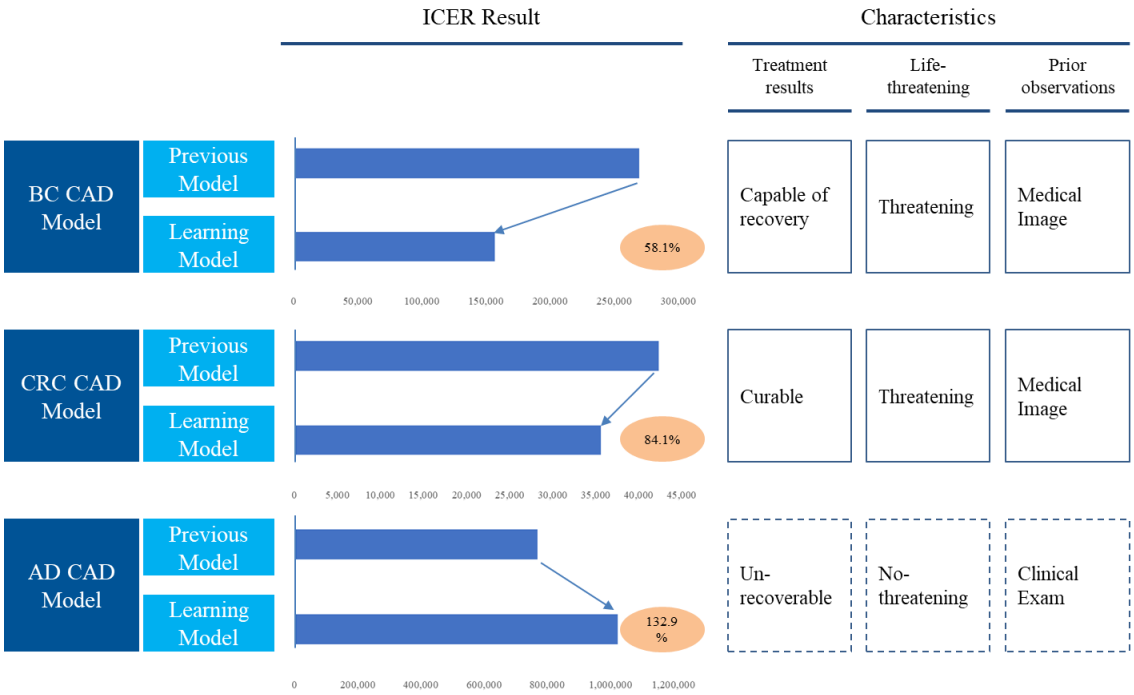

Figure 17 Comparison of each model result

However, AD CAD improvements do enhance patients' QALYs; therefore, social change may increase the system's cost-effectiveness. For example, the best reliable AD treatment, donepezil, only eases the patient's condition, but does not suppress it. Developing high-efficacy medication to improve or cure the patient's condition could improve AD CAD's cost-effectiveness. Moreover, in the AD diagnosis model, cost also includes a high standard of follow-up care required, involving caregiver burden. The social cost of AD could be reduced by increasing AD facilities where patients could lead normal lives. Additionally, a change in the diagnosis flow might also improve cost-effectiveness. Current standard diagnosis does not prioritize observations made through medical imaging; therefore, CAD accuracy improvement does not directly impact diagnosis accuracy. With further advancement and reliability of CAD accuracy, doctors could prioritize CAD-based diagnoses, thereby improving patients' QALYs.

2.5.2 Sensitivity Analysis and Scenario Analysis

First, the above sensitivity analysis is discussed. In the base case analysis, the parameters applied to the model are based on best estimate assumptions, and the appropriateness of the parameters could vary. However, the results of the sensitivity analysis showed that the most influential parameters of a CAD are the specificity of a double reading and the follow-up medical costs, which may be more valid because these parameters have been the grounds of certain empirical studies. On the other hand,

certain parameters such as the cost of installation of the CAD system were on the ground some assumptions; however, the parameters did not have a large effect on the proposed model. Furthermore, the scenario analysis results are discussed. First, to make a comparison between the “base case model” and “scenario A,” it was concluded that data-sharing effects have a certain impact on the social cost-effectiveness if the improvement is more limited. This result can increase the reliability of the base case results. Second, based on the “scenario B” analysis results, it was considered that a high-performance detection at a later stage has less effect on cost-effectiveness than at earlier stages. Hence, introducing an image-sharing environment should be conducted during an earlier phase. Third, from the “scenario C-” and “scenario C-ii” results, it was found that a quicker training dataset accumulation has only a limited effect, whereas the best point estimation model result is adverse (i.e., social cost-effectiveness decreased through data accumulation). Therefore, image data accumulation may affect the cost-effectiveness more if doctors prioritize their medical image observations.

2.5.3 Threshold Assessment

In addition to a scenario analysis, a threshold assessment on the cost-effectiveness of the data-sharing environment was conducted in the present study. This assessment was subject to breast cancer and CRC. In the United States, the cost-effectiveness threshold of ICER can conventionally be considered between 50,000 and 100,000 US$ [273]. Therefore, the effects of the cost per diagnosis on the total cost-effectiveness, and how much additional diagnosis cost may be acceptable from a social perspective, were both evaluated. As shown in Table 10 and Fig. 18, it was concluded that 40 US$ per diagnosis is considered to exceed the ICER threshold. Therefore, a medical-image sharing environment below this cost index should be established for greater cost-effectiveness.

Table 10. Relationship diagnosis cost and societal ICER

Data Sharing Cost per diagnosis ($)	ICER for breast cancer model ($)	ICER for CTC model ($)	Average ($)
0	892.9	16,122.0	8,507.5
10	14,818.9	39,286.7	27,052.8
20	28,744.8	62,451.5	45,598.1
30	42,670.8	85,616.2	64,143.5
40	56,596.7	108,780.9	82,688.8
50	70,522.7	131,945.7	101,234.2
60	84,448.7	155,110.4	119,779.5
70	98,374.6	178,275.1	138,324.9
80	112,300.6	201,439.9	156,870.2
90	126,226.5	224,604.6	175,415.6
100	140,152.5	247,769.4	193,960.9
110	154,078.5	270,934.1	212,506.3

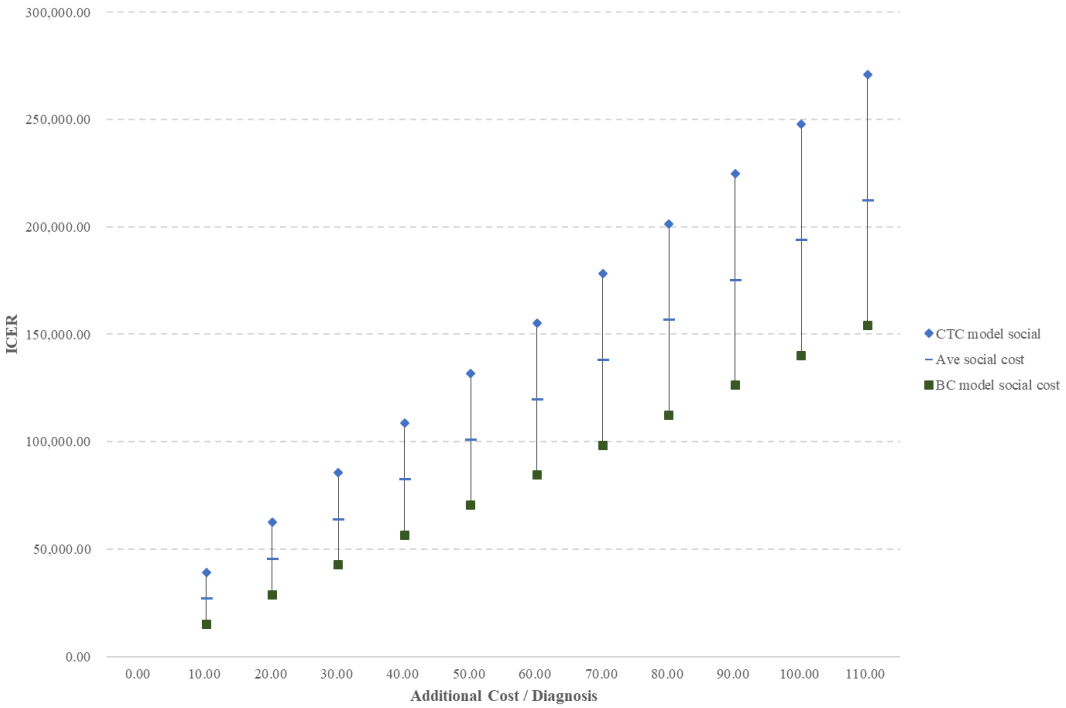

Figure 18. Threshold assessment

2.5.4 Additional Discussion

Considering the above discussion, two additional possibilities are suggested. First, should an applied training dataset be selected for developing a CAD system? Some previous researches have stated that for certain distributions and learning algorithms, increasing the size of the training set might cause a worse performance, whereas an

infinite increase in the size could also result in the worst performance owing to the occurrence of random noises [274]. Some images taken using an older modality often are unable to be used for the training dataset owing to its low resolution and different specifications. Furthermore, it was concluded herein that an improvement in the large polyp detection rate may not have as great an effect on the cost-effectiveness. A previous study revealed that the diagnostic findings differ at each stage, and that the feature values applied to the CAD system should also differ. As an example, the size of a colonic polyp is a biomarker for colonic cancer diagnosis, and correlates with its risk of malignancy and thereby guides its clinical management [275]; in addition, there are two important polyp characteristics that vary with the polyp size: the presence of high-grade dysplasia and villous features [276]. Therefore, specific data such as early stage diagnosis data might need to be fed into a CAD system.

Second, image accumulation can reduce a patient's exposure to radiation and save more lives. It is widely known that most imaging quality, including that of CT images, is described in terms of contrast, spatial resolution, image noise, and artifacts, and its strength is the ability to visualize structures of low contrast in a subject, and hence medical image quality is closely related to radiation dose [277], [278]. On the other hand, the question of risk from radiation exposure has been a much-debated topic of discussion [279], [280]. The predominant risks from typical medical radiation exposure could increase one's chances of acquiring cancer or leukaemia. A previous study concluded that long-term low-dose radiation exposure increases leukemia risk [281], whereas another research pointed that a patient's fear of medical radiation exposure could result in inappropriate treatment [282]. Furthermore, medical image accumulation can improve the accuracy of segmentation, which is part of a CAD system's functionality, and radiologists can make diagnoses using low-quality images but at a low level of radiation. Furthermore, radiologists can substitute an MRI for CT imaging in certain cases. In general, a CT scan is considered one of the best suited means for viewing bone injuries, diagnosing lung and chest problems, and detecting cancers, with radiation exposure, whereas an MRI is best suited for examining soft tissue in ligament and tendon injuries, spinal cord injuries, and brain tumors, without exposure dose. If the CAD segmentation function can be clearly extracted, it can be applied to an MRI for viewing diseases of the lung and chest. For this reason, medical image accumulation, improvements in the CAD system (particularly the segmentation performance), and low-radiation exposure diagnosis can save more patients' lives.

Third, it is likely that the improvement in performance will depend on the algorithm applied to the CAD development and target diseases. However, a previous

study did not reveal the relation between training dataset accumulation and each particular condition. Therefore, in this study a sensitivity analysis and a scenario analysis classified based on lesion progression for the result validation were conducted, which can be a way to report health technology assessments. In addition to sensitivity analysis and scenario analysis, I'll discuss the disease features separately. The first one is breast cancer. As I referred, I applied learning curve depending on the research related to breast cancer [198]. Hence, performance improvement and result on breast cancer model are most solid and could not so fluctuate. Second, I'll consider colorectal cancer. Colorectal cancer stage is classified by depth of tumor progress. In general, tumor originate from mucosa (M) and progress to submucosa (SM), muscularis propria (MP), subserosa (SS) and serosa (SE). Tumor under SM is considered as early stage cancer and it is widely known that early stage cancer is more curable. Although I concluded that early stage detection is critical for better cost-effectiveness, the most applied feature value (i.e., roughness) is faint in phase M and SM [113]. Therefore CAD system for early detection has to depend on other type of feature value (e.g., tone of color and boundary) and performance improvement could not be improved as I assumed. Lastly, I'll discuss Alzheimer's disease model. In the disease, focal atrophy in the medial temporal lobe region is the focus of recent study. It reflects the general feature of progression of neuropathology, spreading from the entorhinal cortex and hippocampus to the association cortices [283]. Algorisms applied this CAD system usually focus on the volume of neuroimaging, therefore, segmentation could be one of the most valuable factor for CAD performance improvement. Furthermore, previous study pointed out that accuracy of neuroimage segmentation is highly depend on the size of training dataset [284]. Therefore, learning model could properly work for AD CAD, and there could be high possibility to have larger effect on performance improvement.

Last, I concluded that early stage diagnosis and accumulation of medical image of early stage disease especially could improve social cost-effectiveness, therefore, I'll discuss some potential way to accumulate much them. First of all, number of accumulated medical images depends on two factors, chances of image diagnosis and detection rate. Furthermore, chances of image diagnosis could be divided into three parts, screening or periodic health checkup, outpatient without symptoms, and outpatient with symptoms. Among those, outpatient with symptoms could not make a contribution to accumulation of early stage images, because when patient gets symptoms is generally middle or later stage. Hence, I'll discuss how to increase the number of chance for periodic health checkup and outpatient without symptoms. First, the former chances could be easily increased by encouraging more frequently checkup.

Latter improvement might be more difficult, however, repurposing images could be solution for out challenge. For example, previous study proposed that dental panoramic radiographs should be reused for osteoporosis detection [285]. There could be other similar cases where medical images could be repurposed, and we should make use of these cased for better societal cost-effectiveness.

2.6 Conclusion

In this chapter, a cost-effectiveness analysis to assess the medical image data sharing effect was described. The cost-effectiveness of BC and CRC CAD can be drastically improved, whereas that of AD CAD cannot. This result probably depends on certain pathologic features and a standard diagnosis flow. However, if medical doctors give priority to image diagnosis results, the cost-effectiveness of AD CAD may be improved. Overall, the sharing of medical image data is valuable for our society from a CAD diagnostic perspective. In chapter 3, the difficulties in sharing medical images between healthcare establishments are discussed from a technical perspective, along with how to solve this challenge, including the proposed method and system design.

2.7 Appendix

Table A. Sensitivity analysis results

Variable	Result			Variable	
	Low	High	Spread	Low	High
Double reading specificity	-11,890	8,999	20,889	0.726	0.99
Specificity of mammography CAD	-2,554	17,228	19,781	0.74	0.99
Follow-up medical costs of advanced stage in two years	2,213	21,661	19,447	2,534,414	38,016,216
Follow-up medical costs of early stage in two years	2,091	13,879	11,788	626,899	940,349
The first outpatient visit + biopsy fee	-175	3,218	3,392	7,432	11,148
Probability of screening found breast cancer in early stage	1,770	3,683	1,912	0.66	0.99
Specificity of biospy	987	2,431	1,445	0.8	1
Mortality rates of IBC (Advanced)	1,923	2,763	840	0.225	0.337
Mortality rates of Screening found BC (Advanced)	2,180	2,753	573	0.089	0.133
Sensityvity of biopsy	2,026	2,485	459	0.76	0.99

3 PROPOSAL OF MEDICAL IMAGE DATA SHARING SYSTEM

3.1 Introduction

I propose a method to manage medical images and for accelerating sharing image in this Chapter. Sharing medical images have some benefit except for CAD system effects. Previous studies have argued that sharing images can not only reduce unnecessary redundancy but also provide diverse benefits. For example, access to outside medical images reduces time and labor for diagnosis [286]. Without access, trauma transfers, for example, can lead to significant delays in treatment [287]. However, medical image sharing is not widely spread due to security/privacy and scalability challenge. As shown in Fig. 19, there have been several ways to construct an environment for sharing medical images, such as encrypted communication from physician to physician and a private network. Although it could spend a lot of time and require for approval procedure, hard copy or portable storage medium is one of the most widely accepted way to send medical images especially in Japan. On the other hand, encrypted communication via public communication network is very easy way. However, both communication way is not scalable. Private network including physical and virtual is more secure and could be expand to other establishments with tremendous development cost. In the past decade, cloud computing has been regarded to have a great deal of promise because of its scalability [288]–[290].

Classification			Overview	Security	Scalability	Cost
1:1	Hard Copy		• To rewrite medical image to hard memory device.	• High	• Very Low	• Very Low
	Encrypted Communication		• To send encryption medical image data via network with password.	• High	• Very Low	• Very Low
N:N	Private Network	Physical	• To build physical private network.	• High	• Low	• High
		Virtual	• To build virtual private network(VRN) including via the Internet and IP-VPN.	• Middle	• Middle	• Middle
	Cloud Computing		• To store medical image in external server.	• Low	• High	• Low

Figure 19. Typical methods of sharing medical images

However, image sharing via a cloud-based environment has raised some security and privacy concerns. Medical images usually have to include patient information such as height, weight, and also contain sensitive information [291]. Therefore, patient information protection is a sensitive issue, and national, international, and institutional regulations are in place to limit how and where such sensitive data are acquired and stored [292]–[294]. Furthermore, cloud computing technology has several immanent security challenges [289], [295], and many healthcare establishments are still reluctant to store medical images in a cloud database. Therefore, constructing a reliable environment for physicians to share medical images that is secure, effective, low-cost, and scalable is a challenge for medical practice. In this Chapter 3, I propose a method that applies blockchain technology to cloud-based environment to resolve above challenges. Furthermore, I conducted hearing to some stakeholders, and designed system architecture for implementation.

The rest of this Chapter is organized as follows. Section 3.2 introduces related work on electronic health records (EHR) including Digital Imaging and Communications in Medicine (DICOM), picture archiving and communication systems (PACSs), cloud computing, and blockchains. In addition, I'll present previously identified security challenges and technical limitations of both technologies. I conducted hearing to some stakeholders to design my proposal and system architecture in Section 3.3. Section 3.4 describes my methodology and test implementation scheme, and Section 3.5 presents this result. System architecture based on my hearing is shown in Section 3.6. Section 3.7 discuss the advantages, limitations, and practical application of my methodology and summarize the main points in Section 3.8.

3.2 Related Work

3.2.1 EHR

The EHR can be defined as a repository of patient data in digital form, stored and exchanged securely, and accessible by multiple authorized users. It contains retrospective, concurrent, and prospective information and its primary purpose is to support continuing, efficient and quality integrated health care [296]. Furthermore, the need to manage EHR is becoming a worldwide priority [294]. Several countries have been trying to develop an infrastructure for national health information; examples include Canada [297], England [298], the United States [299] and also Japan [300], [301]. EHR has always had security and privacy concerns, and healthcare providers must meet legal obligations, such as the Health Insurance Portability and Accountability Act of 1996 (HIPAA) in the United States of America (USA) [292], [302]. For example,

the security rule specifies a series of administrative, physical, and technical safeguards. On the other hand, to gain access to high-quality health data is an essential requirement to make decision for healthcare practitioners and pharmaceutical researchers. Driven by mutual benefits and regulations, there has been a strong demand for healthcare establishments to share patient data with various parties for research and education purposes. However, health data in its original form often contains sensitive data related to personality, and diffusing this type of data could violate their privacy. Medical practice in data sharing mainly relies on country's policies and guidelines on the types of data that could be shared and agreements on the use of shared data. This approach might cause an excessive data distortion or insufficient protection [303].

Furthermore, a more secure and cost-effective system is strongly required for sharing EHR because present local or enterprise-wide information systems are generally not intended for cross-organizational secure access of EHR [304]. In our situation, EHR involves medical images. I assumed the most popular standard in healthcare literature; DICOM [305]. DICOM specifies a data interchange protocol, digital image format, and file structure for biomedical images and image-related information. The DICOM standard also directs how to format and exchange medical images and associated information, both within and outside the hospital [306]. A DICOM file stores the digital image along with a series of tags that contain not only general personal information such as the name, sex, height, weight, and blood pressure but also highly sensitive data such as fertility, abortion data, and sexually transmitted diseases [291]. Therefore, healthcare providers have to carefully control DICOM files. Widely known technical challenges are anonymization and image defacing for images that include facial features [307]. DICOM images have to be anonymized before being transmitted for sharing, which means that a subject's confidential data must be replaced with random strings. One of the HIPAA-defined identifiers that must be removed is "full face photographic images and any comparable images." Although DICOM brain images with facial features (e.g., mouth, nose, and eyes) are usually presented in 2D slices, a 3D image that explicitly shows a subject's facial features can easily be rendered from 2D slices. This is why a subject's DICOM brain images need to be defaced. Furthermore, there are several cases that need to be considered; ophthalmology images, specific modalities, and special patient devices. First, retinal and iris images may be inherently identifiable because they are used in biometric identification systems [308]. Second, some modalities, such as ultrasonic diagnostic equipment, output medical images that include patient information in the pixel data. Finally, prostheses or other patient devices sometimes have unique ID numbers that can be read in high-resolution scans and again

allow for reidentification [309].

3.2.2 PACS

A PACS refers to an infrastructure that links modalities, workstations, an image archive, and a medical record information system into an integrated system. It allows for efficient electronic distribution and storage of medical images and access to medical record data [310]. Usually, a PACS needs to be manufactured by the same vendor if data are to be shared. However, with the introduction of standards and vendor conformance, modalities of different vendors can communicate with each other within a department. Seamless integration enables more efficient workflow. Although this multivendor setup seems quite functional, a serious problem can arise if there is a need to change the PACS vendor. The new vendor may experience difficulty in reading the data stored in the server because the format can only be read by the earlier vendor. Another problem may involve integrating a PACS installed in the radiology department with a PACS installed in the cardiology department. Even if both are DICOM-compliant, making them communicate with each other and share data is never a simple "plug and play" situation. Interoperability has emerged as a hugely contentious issue. The concept of a vendor neutral archive (VNA) has increasingly become accepted as a method to address the practical problems of interoperability [311]. A VNA simply decouples the PACS and workstations at the archival layer. This is achieved by developing an application engine that receives, integrates, and transmits the data by using the different syntax of the DICOM format. The data belonging to an old PACS is transferred to a new one by a process called migration of data. For a VNA, a number of different data migration techniques are available to facilitate transfer from the old PACS to the new one. The choice depends on the speed of the migration and importance of the data [312]. On the other hand, to improve operation efficiency and to realize a cost-effective healthcare, a lot of large-scale or wide-area PACS pilot studies and implementation are proposed [313], [314]. These types of proposal for large-scale PACS could be mainly divide into two schemes; distributed or centralized [315]. Distributed architecture could be defined as "The hospital archive distributes images through intra-hospital and inter-hospital networks. Clinical units in the hospital can also query/retrieve images from the database of other hospitals". On the other hand, centralized is the concept that "Archived images in the hospital are sent continuously to the enterprise data center for long term archive," and this concept is quite close to cloud computing. Both schemes might not have sufficient scalability for widespread use because they only consider applying hospitals which have the close relationship such as affiliations or in the same region, and require a tremendous cost of constructing this environment. My proposal could incorporate

these types of PACS and be part of a VNA.

3.2.3 Cloud Computing

In the last two decades, cloud computing has been growing as one of the most promising domains of the information technology (IT) industry. Cloud computing consists of a set of resources and services offered through the Internet; it allows capacity to be added without large investments in new infrastructure [288]. The word “cloud” is a part of a network, and now is widely used as a metaphor for Web. Operating systems (OS), applications, storage, data, and processing capacity can all exist on the Web. The main purpose of cloud computing is to make more effective use of distributed resources. In my situation, cloud services enable the storage, archiving, sharing, and access of images so that healthcare organizations can manage data more efficiently and cost-effectively. This model is called “Infrastructure as a Service” (IaaS) or “Hardware as a Service” (HaaS). However, cloud computing has some challenges regarding security and privacy [316]. It is widely accepted that security has mainly four elements; integrity, confidentiality, accountability, and availability. First, the physical security of the infrastructure and management for disaster recovery are some of the most important issues that have to be considered. Cloud service providers have taken measures to solve these challenges, such as physical gateway control [317], load balancing [318], [319] and virtual machine rollback [320], [321]. This physical security is related to integrity, confidentiality and availability. Second, the possibility of data leakage increases in a cloud; depending on the number of parties, devices, and applications involved, this can increase the number of transactions and level of access [322]. Possibility data leakage could lead confidentiality challenge. Third, cloud data centers tend to become the targets of attacks and intrusions, which challenge cloud data security, which is a challenge to availability [323]. Fourth, risks in the provision and verification of accounts are related to accountability [324]. Last, many organizations are still resistant to storing their data in the cloud because people who manage cloud services can access user data, which depend on privacy concern [325], [326]. Many solutions have been proposed [327], [328]. Especially, cryptography has been widely applied to ensure data security, privacy, and trust in cloud computing [329]. However, existing cryptography solutions are still impractical because of the high computational complexity and inefficiency [323], [330]. Overall, the cloud data security, privacy, and trust level have become crucial issues that impede the development of a large-scale medical image sharing system.

3.2.4 Blockchains

The blockchain is a technology developed first in the financial service industry (e.g., bitcoins). This technology is considered a public ledger system or distributed database solution for maintaining the integrity of transaction data records, which is confirmed by participating nodes [331], [332]. At present, blockchains are still regarded as management technology for bitcoins and also have all bitcoin transactions which have ever been executed [333]. Bitcoins are a digital currency transaction system where each user has a public transaction ledger, or a blockchain [334]. The reason why the blockchain is applied and apprised is so that the public ledger cannot be modified or deleted after the data have been approved by all nodes. Therefore, the data integrity and security, especially integrity and availability, are assured. Furthermore, no third party is required to control the transaction in the Bitcoins literature. Anyone can join and participate in the Bitcoins network, therefore, this type of blockchain is called public blockchain.

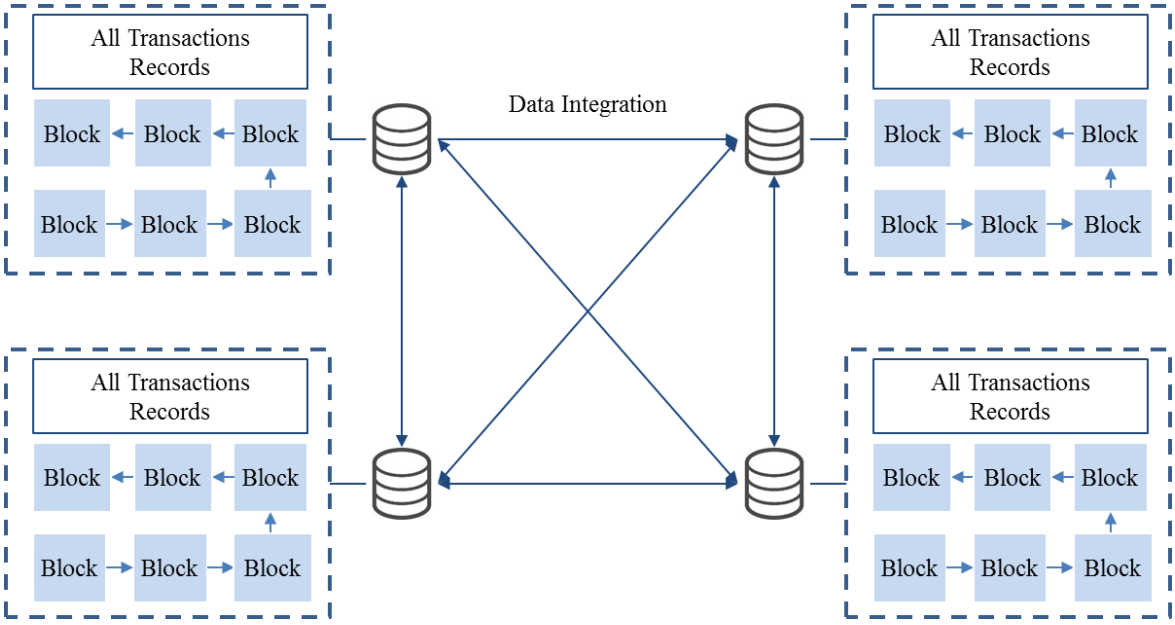

Figure 20. Data integration with blockchains

In the following, I describe how a blockchain works in detail below based on a review of the literature on bitcoins. In the bitcoin system, all transactions that change the distributed bitcoin ledger are bundled into blocks. For a block to be validated, it has to fulfill a consensus condition, especially proof-of-work for bitcoins. Proof-of-work describes a system that requires a not insignificant but feasible amount of effort in order to deter frivolous or malicious uses of computing power, such as sending spam emails or launching denial-of-service attacks. A particular cryptographic hash involving the

block's content is formed and must be below a threshold value. In other words, nodes that wish to publish new blocks have to perform a brute-force search for a partial hash collision. This ensures that a block cannot be changed without all of the work to find hash values being redone. In addition to information on current transactions, each block also includes some information related to a previous block information. Fig. 20 shows an overview of data integration with blockchain technology.

It is true that blockchain technology may be hard to decode (Fig. 21). Currently, many researchers and practitioners have insisted that blockchains can be applied to other uses, including the healthcare industry [335], [336]. A previous study proposed a methodology that uses a public blockchain as an access control manager for health records [337]. However, a number of technical challenge related to the blockchain such as the throughput, latency, size and bandwidth, security, usability, and wasted resources [332] have been identified.

- ✓ Throughput: In studies on bitcoin, network throughput has been a potential issue in that only one transaction is processed per second (tps), with a theoretical current maximum of 7 tps (comparison metrics with other transaction processing networks include VISA, at between 2,000 to 10,000 tps, and Twitter, at between 5,000 to 15,000 tps). A potential solution allowing bitcoin to handle higher throughput is to increase the block size, which leads to other issues with regard to size and blockchain bloating.
- ✓ Latency: Each bitcoin transaction block takes 10 min to process for sufficient security because the blockchain must assure data integrity through computational complexity. Therefore, this would pertain organically to the blockchain security level.
- ✓ Size and bandwidth: An entire blockchain is 125 GB (as of August 3, 2017) and has increased by about 120 MB in a day. If the throughput problem is solved, the rate of increase in size could also rise. Furthermore, to go back to the principle of a blockchain, it aims at decentralization, and full data should be able to be confirmed by each peer. Therefore, it could be difficult to divide and store a blockchain.
- ✓ Security; There are several potential security challenges with the use of a blockchain. One of the most critical issues may be the possibility of a 51-percent attack. If a peer, or some part of a peer, gains power over the remaining blocks,

they could control the entire blockchain. In addition, double-transaction might also be possible challenge owing to the existence of spoofing users.

- ✓ Usability: A number of blockchain APIs and platforms are far less user-friendly than the current typical services, which are easy to use. Therefore, difficulty in diffusing future services may occur.
- ✓ Wasted resources: Creating a block requires a certain amount of energy, all of which is wasted. An earlier estimate cited was $15 million per day, although other estimates have been higher [332]. In one aspect, it is the very wastefulness of creating blocks that makes it trustable; however, such spent resources have no benefit other than the block creation.

In particular, the "size and bandwidth problem" is critical for the potential application of blockchains in medical image transactions because medical images typically have a large data size, and many images are required for medical practice. Therefore, a hurdle for many establishments is the need for a tremendous amount of storage to contain all medical image data created. However, throughput, latency, and wasted resources would not make a significant difference because, if we construct a medical image platform, every peer will be reliable, which is typical for a healthcare establishment, and therefore assurances through huge amounts of mathematical computations will not be required. Furthermore, medical examinations and medical images will not be required for every patient, and thus the throughput and latency are not as critical.

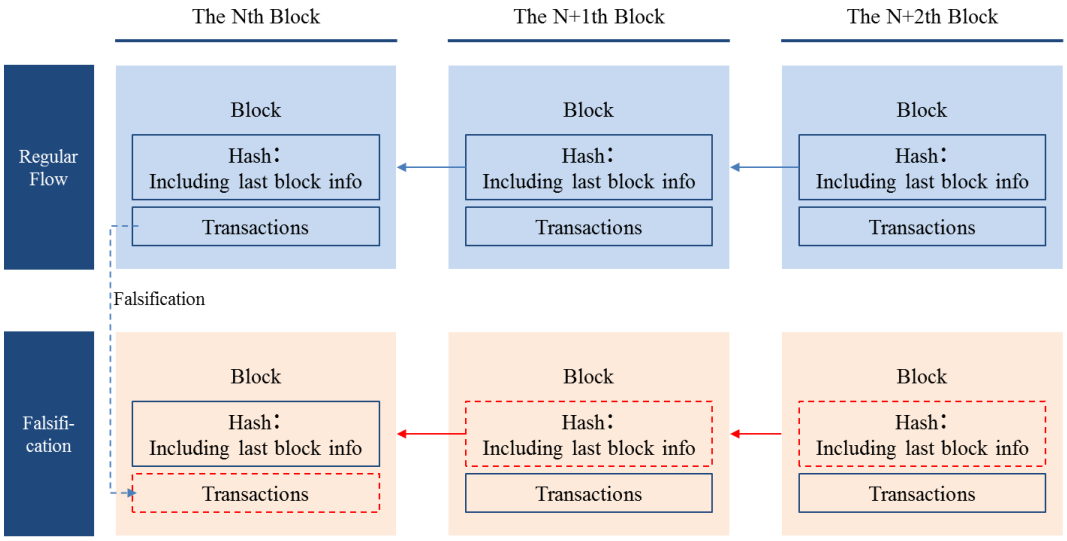

Figure 21. Falsification case

*block info: Hash value in previous block

3.3 Actual Survey

For this study, multi-stakeholder meetings were conducted for a deep understand of the stakeholder needs and wants, and how regulations and business operations can be fulfilled in practice. The multi-stakeholders included two medical doctors, a radiological technologist, a Japanese medical regulatory authority representative, an internal management system vendor, and the developer of image-based systems (e.g., computer-aided diagnosis, treatment planning, and image-guided surgery).

Based on these meetings, the requirements with regard to archiving medical image data in a cloud environment, and sharing medical images for healthcare establishments and system developers in Japan were ascertained. From the perspective of healthcare establishments, the growing long-term costs of managing a medical image archive has been a subject of struggle, and it has been estimated that over 1 billion diagnostic imaging procedures are performed in a single year in the US, generating about 100 petabytes of data [338], and it was also estimated that about 33% of the world's storage demands could have a relation to medical imaging storage [339]. Furthermore, medical image sharing through the cloud has had a certain contribution in practice. First, healthcare practitioners can save time in contacting other establishments and conducting internal authorizations. Being able to access past medical images could allow radiologists to make a decision whether to take additional imaging through another type of modality (e.g., if CT and MR images have been taken, radiologists could add PET or SPECT imaging). However, many hospitals are unwilling to introduce cloud archiving services because medical images include personal information. This depends on the hospital policy and affective logic, not on the law or regulations matters. However, healthcare system developers (e.g., CAD developers) require large amounts of medical image data to build their systems. At present, they can only access data through a partnership with different hospitals, and a number of restrictions and procedural requirements exist, and a sufficient volume of data is often not provided. In addition, permission usually allows the developer to apply image data to only one system. Therefore, there seems to be a high demand for access to medical image data by system developers.

Next, some subjects were confirmed as related to business and system requirements. First, 5 years' worth of archives for medical images has been defined through two regulations: the "Japanese Medical Practitioners' Act" and "Rules for Health Insurance-covered Medical Facilities and Medical Practitioners." However, radiological

technologists have mentioned that medical images are stored for more than 5 years (for about 20 years at most). Some healthcare establishments compress their images for long-term storage; however, the total volume of data is tremendous and is still growing rapidly. A number of hospitals have system servers that consist partly of a PACS and a so-called “image server” dedicated to storing medical images. On the other hand, medical doctors often require a response time to view patient DICOM data within a 5 s period. This seems to be a strict limitation to apply to cloud storage because some DICOM series data are over 1 GB, and the time to download such data takes a few minutes depending on the network bandwidth. Therefore, many cloud service vendors have taken measures to deal with the response time problem by storing frequently used image data in cache memory; however, the cost to build this type of hardware device is very high. As a result, a number of hospitals may store only old image data (e.g., from more than 5 years earlier) in a cloud environment.

Regulations and hospital policies demand data integrity, and therefore cloud vendors duplicate their storage (usually called “database mirroring”) to prepare for an unintentional disaster or misuse of data. They typically apply double mirroring, not triple or quadruple mirroring. On the other hand, image-based system developers need to utilize DICOM data tags with pixel data for development, namely, “sex,” “age,” and “modality code.” Sex and age are necessary to classify the training dataset, and a modality code is also important to view the data because a number of latest DICOM viewers can be optimized to view DICOM according to the modality, and a modality code is used for such optimization. From an access control perspective, four categories can be seen in a general internal hospital: “inaccessible,” “available for viewing,” “update authority,” and “administrative privilege.” If healthcare establishments grant other hospitals permission to access their medical image database, they generally have to exchange a pledge, and medical images from different establishments seem to be managed differently. All processes can be conducted using a VPN.

Finally, a meeting with a regulatory authority was conducted during this study with regard to the control of DICOM data using the proposed method, as well as on how to deal with AI technology for the healthcare system. First, the authority mentioned that privacy and personal information issues seem to have been resolved from a regulation perspective. However, if DICOM data are divided into certain parts, we must be assured of data integrity for compliance. On the other hand, the Japanese Ministry of Health, Labor, and Welfare has been developing rules and guidelines necessary for the implementation of AI technology to medical equipment [340]. The regulatory authority mentioned that, although a specific requirement is still undecided, prompt feedback

from the training dataset might not be allowed, and if the system developer applies an improvement using data, it will be necessary for the developer to gain approval again if the system is sold along with a different type of medical equipment A summary of this meeting is provided in the Appendix.

3.4 Methodology

3.4.1 Overview

In this Section, I propose a methodology that combines cloud computing and blockchain technology to securely share, decrease privacy risk and manage medical images especially DICOM. My methodology divides medical images into metadata and pixel data. The former is managed by blockchain technology, and the latter is managed by cloud computing. Furthermore, keys identifying patients and images can be used to reconstruct the original image information with metadata and to encrypt metadata and pixel data.

Below, I describe the methodology in detail. First, I introduce certain terms defined as follows. “Processing server” is the hospital internal server that has functions to divide medical images and to transmit information to other systems. “BlockChain server” and “BC-server” are also hospital internal servers, which have functions to create a multi-use key and maintain encrypted metadata. “Hospital system” is an integrated system including processing server, BlockChain server, and imaging modality in the hospital. “External server” is a hospital external server, which is also the Cloud environment. Furthermore, this server has functions to maintain encrypted pixel data with the multi-use key, which can specify medical image and response BlockChain server. This methodology overview is shown in Fig. 22.

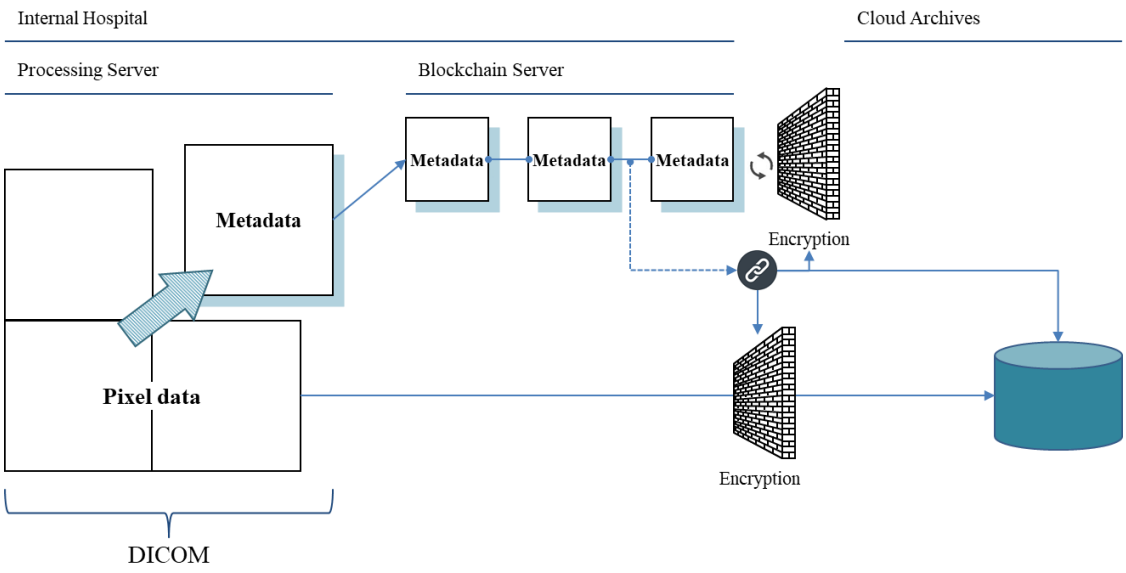

Figure 22. Proposal overview

3.4.2 Patient Registration

First, a unique patient identification (ID), I call Patient ID is issued. Information about patients are managed in an external managing server. Patients can request to issue patient ID with their own devices, such as smart device or personal computer (PC), to external managing server. This server receives the patient request and issues a unique patient ID, which it sends to the patient. For the practical use, patient explicit approval could be given at the same time as patient registration. In most of cases, health care professionals have right to use images without patient's permission in the case of direct care and consultations. However, there are two issues relating to regulation and privacy. First, the system could allow the usage to secondary purposes including even private system developer use under patient's permission. Using patient information for private sector is usually illegal without patient permission. Therefore, the system use has to be started form patient user agreement for application of CAD development. It will enable to utilize images for the patient outside the focal hospital. Second, this system could diffuse patient information more widely than now and can contribute to improve the accuracy of image-based system (e.g. computer-aided diagnosis, treatment planning and image-guided surgery), while the use of images should be explicitly declared. This is related to privacy, moral and user emotion matters, not regulation. Fig. 23 shows the registration process.

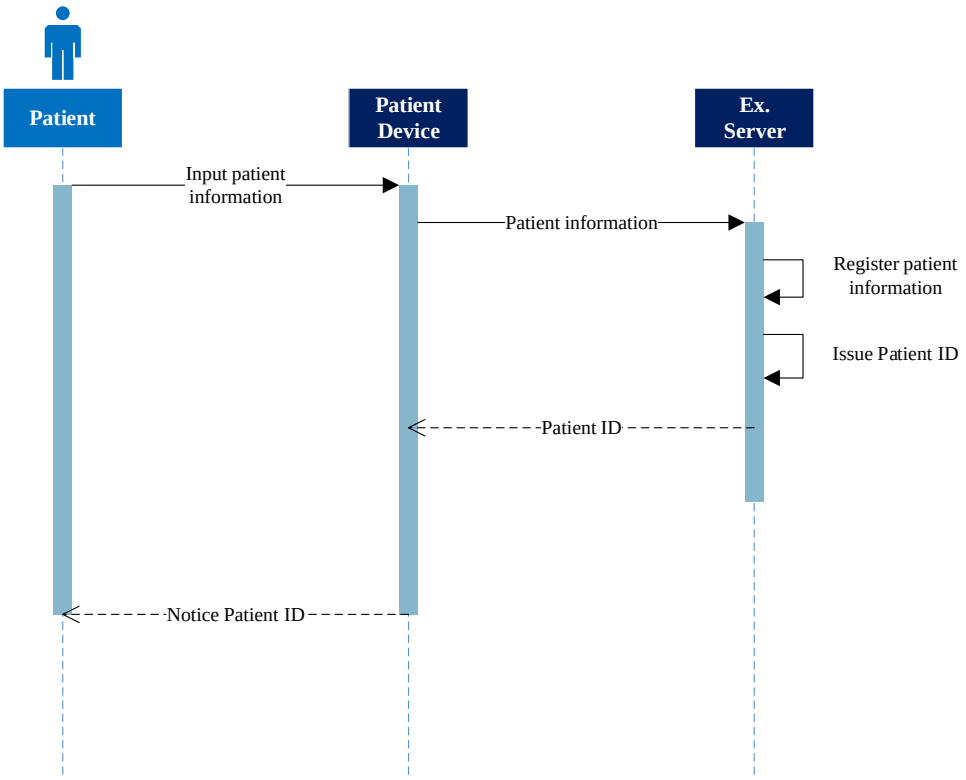

Figure 23. Sequence diagram: Registering patient information

3.4.3 Creating a Blockchain

After patient ID are registered, he or she could make use of this service. When patients have medical image taken, they could notice their Patient ID to hospital. The medical image data is processed for division into metadata and pixel data. Most healthcare establishments sored medical image into PACS and this convention could not probably be changed. Therefore, processing server should be able to get medical images from internal PACS. Multi-use key is created from the metadata and previous block information. Furthermore, to make security firmer, multi-use key is used for encryption of metadata and pixel data. Fig. 24 illustrates the process to create a block from taking medical image, and Fig. 25 shows the structure of system configuration sample.

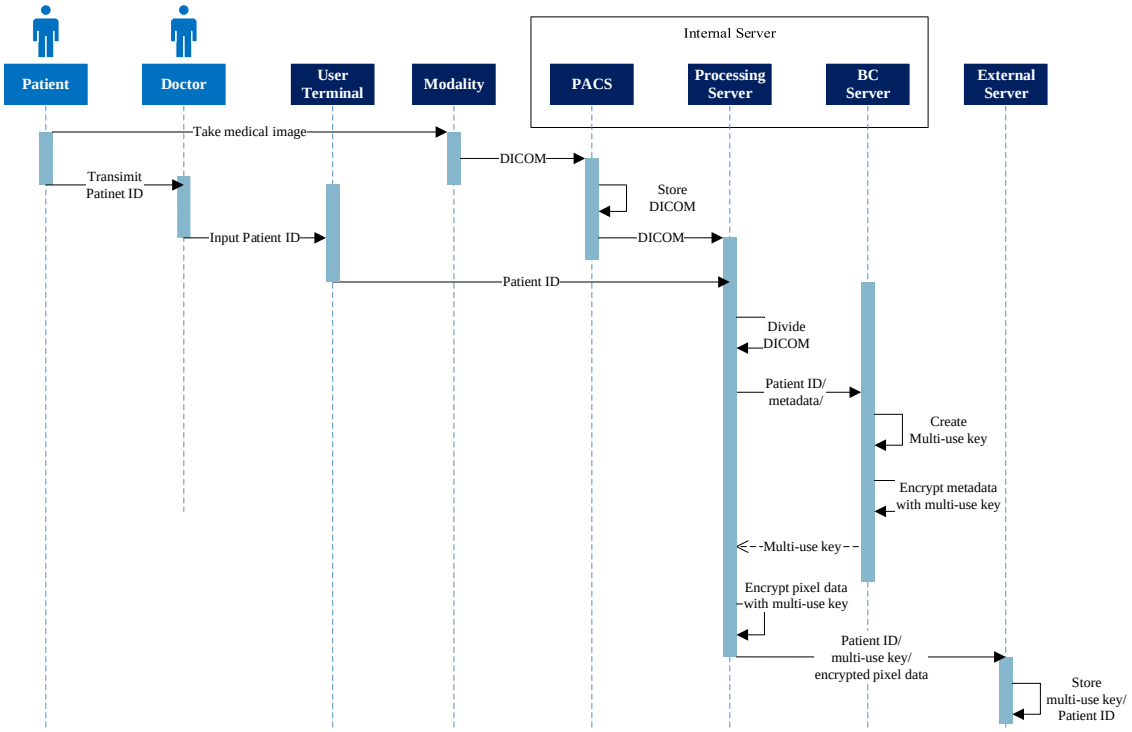

Figure 24. Sequence diagram: Create block

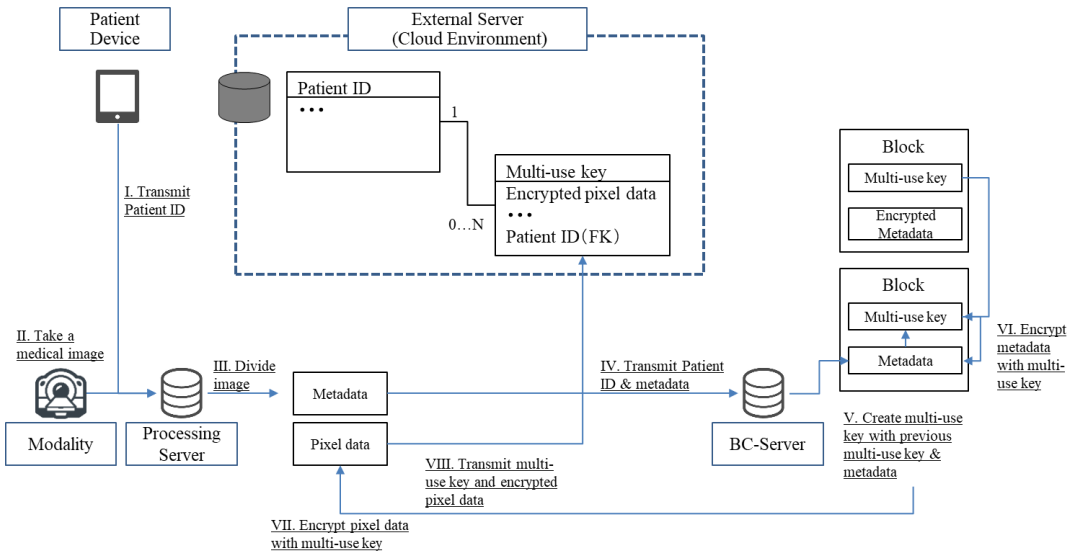

Figure 25. System configuration: Create block

I. I assume the case that a medical image is taken in a hospital. The patient transmits his or her own patient ID to the processing server in the hospital.

II. The medical image is taken with some modality.

III. This medical image is divided into metadata and pixel data.
IV. The processing server transmits the patient ID and metadata to the blockchain server.
V. A multi-use key is created with the metadata and previous multi-use key on the blockchain server. When a block is created for the first time, dummy data are assigned to the previous multi-use key information.
VI. Metadata are encrypted with this key.
VII. The key is returned to the processing server, and the pixel data are encrypted with this key.
VIII. The encrypted pixel data, multi-use key and Patient ID are transmitted to an external managing server, and stored.

The separation of the medical images into metadata and pixel data can efficiently use the hardware resource, which will increase with the introduction of blockchains. Thus, it enables medical image data to be transmitted through the cloud with efficient operation and effective security.

3.4.4 Data Synchronization

After a block is created, each hospital has to synchronize its data in the blockchain server. Encrypted communication is required to transmit block information. To synchronize the blockchain information, how to arrange the order is especially critical issue. I have to construct the rule so that each hospital will not be confused to select the block which is add new block and hash them. A possible way is to decide on which hospital prior to other establishments for blockchain processing. Fortunately, there isn't much merit in processing order unlike in the case of bitcoin literature. Fig. 26 shows how to synchronize data.

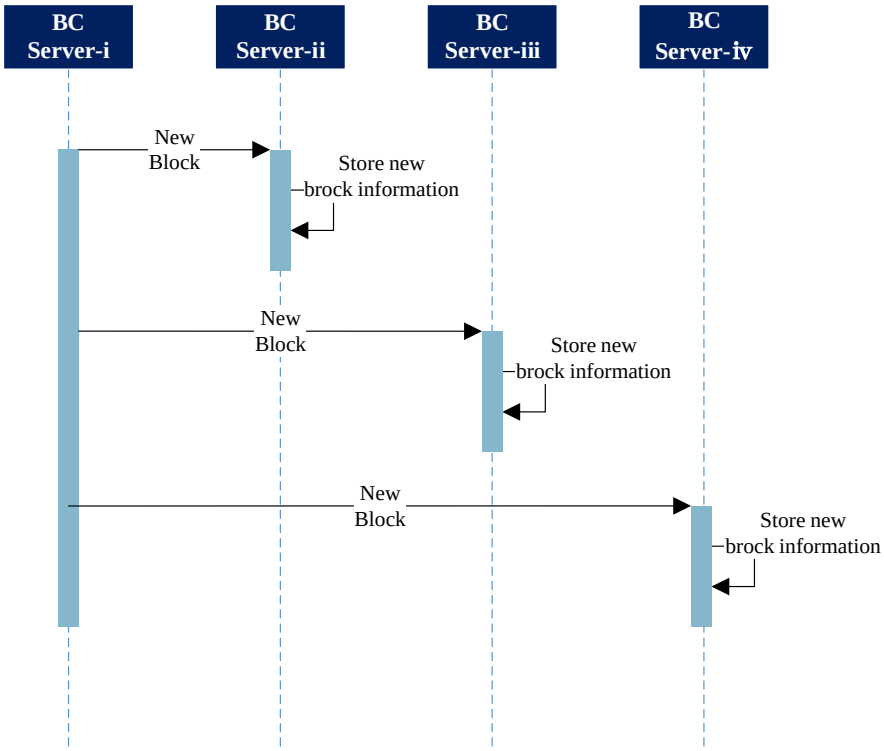

Figure 26. Sequence diagram: Data synchronization

3.4.5 Acquisition of Medical Image Data

A blockchain demands a huge amount of hardware resources; if I add blocks for each medical image, it is not feasible to apply blockchains to medical image data. It was estimated that over 1 billion diagnostic imaging procedures will be performed in a year to generate about 100 Petabytes of data in the US [338], and also estimated that about 33% of the world's storage demands could have relation to medical imaging storage [339]. Therefore, the hardware resources required for managing medical image is quite tremendous. Thus, the metadata and pixel data must be separated, as proposed above. However, diagnosis and intervention require the patient information to be recoverable. Although pseudonymisation is proposed for secondary use, using medical images including false data might lead to wrong diagnosis. In addition, the dissemination of medical data is beneficial because it enables patients to receive a second opinion on a diagnosis and researchers to conduct large-scale cohort studies. However, for such practical use and applications, anonymous data lacking demographic and other health- and medical-related data reduces the opportunity and potential to be utilized. With this system, every hospital can acquire every patient's medical image information by using the patient ID in the blockchain server as a key. For instance, a patient lets the

blockchain server know his or her patient ID by using his or her device. The blockchain server sends it to the external managing server, and this managing server identifies the multi-use key from the patient ID. This managing server transmits the multi-use key and patient pixel data to the blockchain server. The blockchain server identifies the patient metadata with the multi-use key, and both data are shown. Fig. 27 shows this flow in detail.

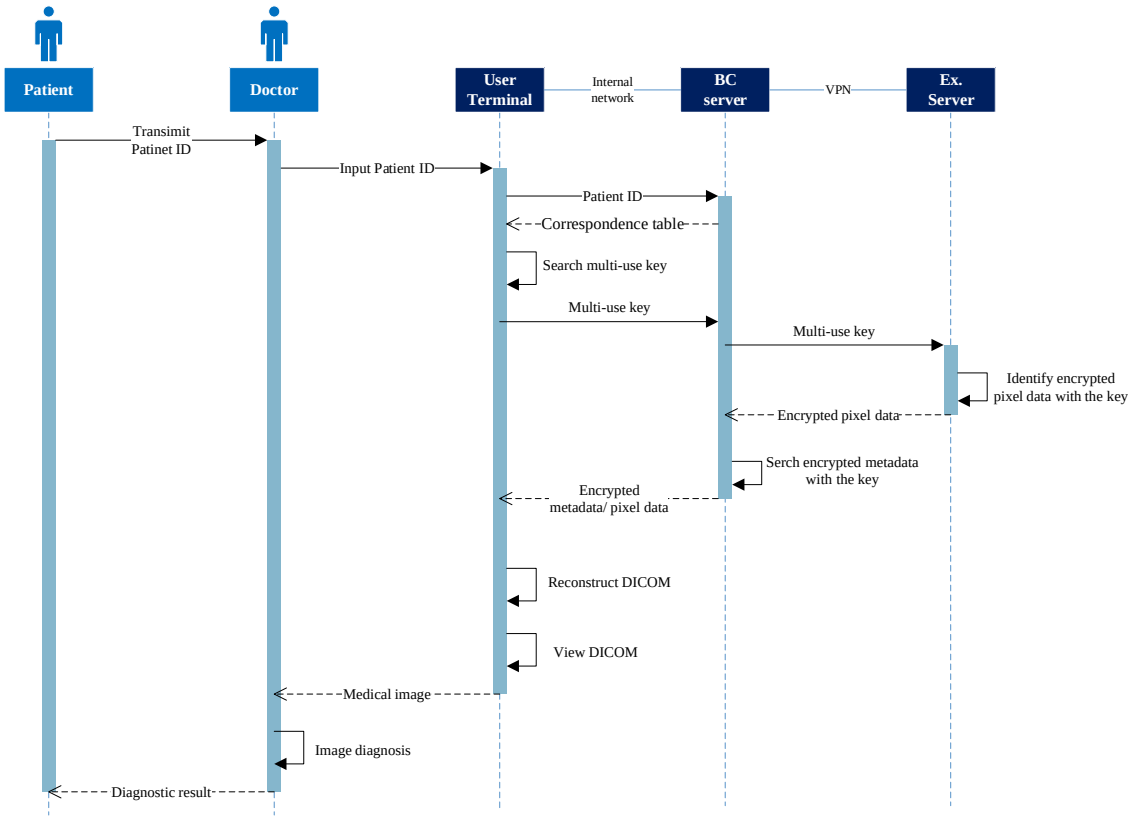

Figure 27. Sequence diagram: Acquisition of medical image data

3.4.6 Experiments

I implemented the core of our methodology for creating blocks as follows. In my test environment, the OS was Windows 10, the runtime and software development kit (SDK) was .NET Framework 4.6, the programing language was Microsoft Visual C# 2015, integrated development environment (IDE) was Visual Studio 2015 Update 3, and the compiler was MSBuild 14.0. The device had 16 GB memory. First, I generated the multi-use key. The applied hashing algorithm was SHA-256 [341] (1). SHA-256 is a member of the SHA-2 cryptographic hash functions, and SHA stands for Secure Hash Algorithm. SHA-256 is one of the most novel hash functions computed with 32-bit and fulfill the sufficient collision resistance (i.e. nobody is not able to find two different input values that result in the same hash output). In addition, I deployed a Merkle tree,

and it merged and hashed the information of each patient with DICOM (e.g., name, birthdate, sex) (Fig. 28) [342], [343]. A Merkle tree is a hash based data structure which is generalized of several hash lists. Merkle tree has a tree structure in which each leaf node is a hash of a block of data, and each non-leaf node is a hash of its children. I also added the information of each patient to ten random characters as "salt" [344]. Salt is a random string that strengthens a hash by being appended or prepended to hashed data. Second, I encrypted the metadata and pixel data with the corresponding multi-use key. The encryption algorithm was Advanced Encryption Standard; Rijndael [345], [346]. Rijndael is a block cipher and Both Rijndael's input, block length and key length, are variable. They could independently be varied between 128 and 256 bits in increments of 32 bits. I used open data as the test sample [347]. Furthermore, I estimate scalability to evaluate the feasibility of the proposed method. Previous research roughly calculated that over 1 billion diagnostic imaging procedures has been performed in a year in the U.S. [338]. In addition to the study, I make two assumptions for our evaluation. First, several medical images are taken in a diagnostic imaging procedure, therefore, I assumed that one hundred medical images are taken on the average per procedure. Second, although number of diagnosis has its ups and downs, I assumed that the number of diagnosis is same in each day, in brief about 270 million images are taken per day in U.S.

$$H^{(i)} = H^{(i-1)} + C_{M^{(i)}}\left(H^{(i-1)}\right), \quad (1)$$

Here, M^i is the message block, C is the SHA-256 compression function, and $+$ represents the word-wise mod 2^{32} addition. $H^{(N)}$ is the hash of M.

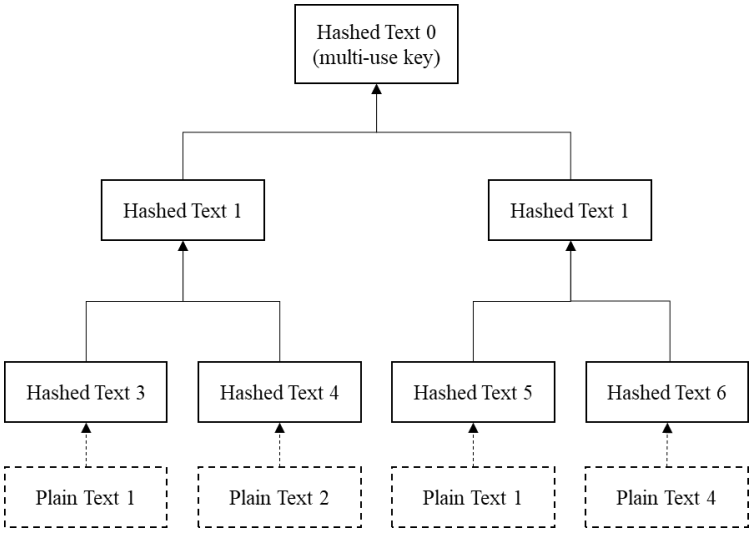

Figure 28 Merkle tree diagram

In addition to performance and scalability, I qualitatively assess the security of the proposal. Many frameworks to evaluate security has been proposed from various viewpoint [348], [349]. A framework divided security subjects into five layers; “People and identity,” “Data and information,” “Application and process,” “Network, server and end point”, and “Physical infrastructure” [350]. I focus on the “Data and information” (i.e., metadata and pixel data) layer, because contribution of our proposal is mainly related to how to handle data and other security subjects highly depend on the conventional technology or system architecture.

3.5 Result

3.5.1 Performance and Scalability

The performance of my proposal should be discussed. I tried to improve the security when managing medical images with a specific key. This key is used to encrypt the metadata and pixel data, detect falsification, and connect the metadata and pixel data to control the metadata in a secure hospital environment, as discussed above. Therefore, the core of my proposal is this key, and I can evaluate the efficiency of an IT resource by measuring the processing time to create the key and encrypt data with it. Table.11 presents the average processing time and standard deviation (σ) for 50 tests, and Figure 29 shows linear interpolation for processing time. The horizontal axis indicates the number of processing including creating multi-use key and encryption for metadata and pixel data, and the vertical axis shows processing time on the second-time scale. Furthermore, hardware resources can be considered to be equivalent to cloud computing. In my test environment, the metadata size was 2.36 kB, and the pixel data size was 0.3

MB. The former data are duplicated by the blockchain; however, the impact on the hardware resources is sufficiently small.

Table 11 Processing time results

Processing Time [sec]

	Number of iterating =1		Number of iterating =10		Number of iterating =100		Number of iterating =1000	
	Average	σ	Average	σ	Average	σ	Average	σ
Generate Multi-use key	0.004780042	1.10682E-06	0.02972608	3.00792E-06	0.27401501	1.83029E-05	2.707774932	0.001063826
Encrypt MetaData	0.00182842	3.93431E-08	0.012826358	7.12591E-07	0.118594514	1.12177E-05	1.18809799	0.000138849
Encrypt Pixel Data	0.010292386	2.29412E-06	0.010606298	1.75293E-06	0.015804878	5.51299E-07	0.031431174	1.53928E-06

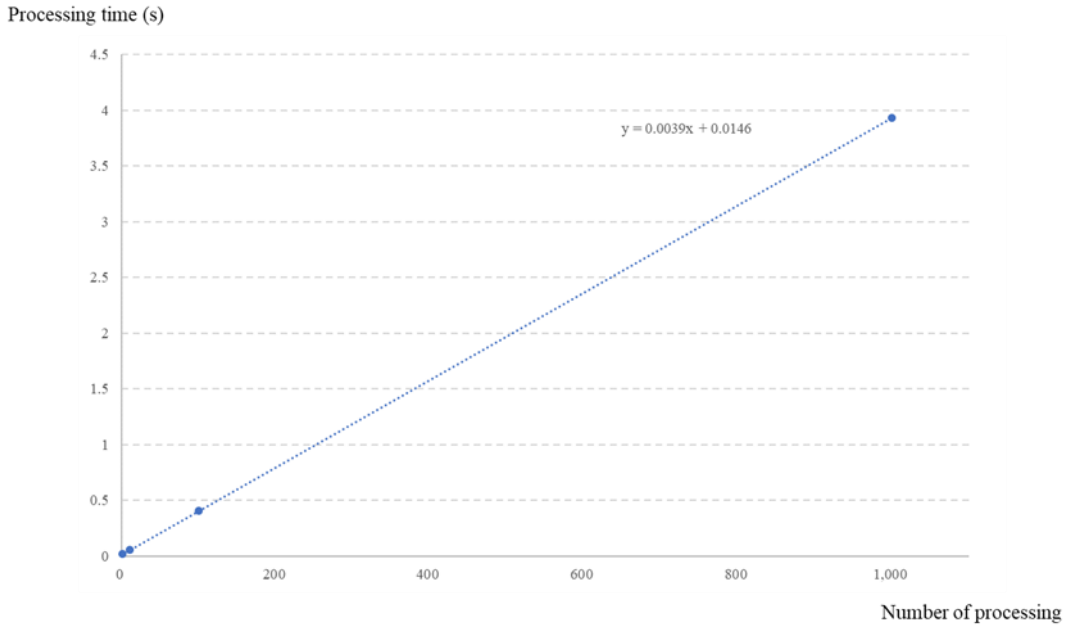

Figure 29 Linear interpolation of processing time

As can be seen from the Figure 28, processing time of our proposal could increase approximately linearly with number of processing (i.e., number of medical images managed by this proposal). Therefore, I could estimate the relationship between duration and number of server as shown in Figure 30.

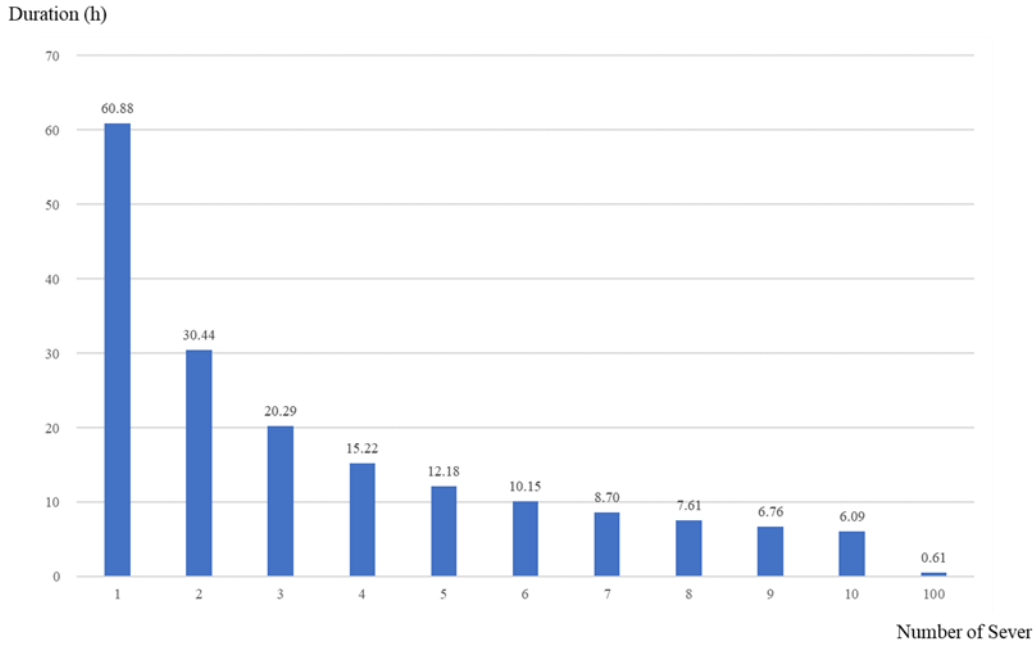

Figure 30 Estimation for relationship between duration and number of server

3.5.2 Security

Furthermore, I show an evaluation result related to security. First is about metadata security. In our proposal, the metadata are managed with the multi-use key, which is created by hashing and includes previous key information. Therefore, if an attacker falsifies metadata or hospital personnel make a mistake, all of the multi-use key values are changed, and the falsification and error can be detected. This can strengthen metadata integrity with a cloud computing. Metadata confidentiality could also be improved. Metadata, which include highly sensitive information, can be controlled by using the internal hospital server. An intranet environment is generally considered more secure than the Internet [351]. Furthermore, this method only allows entities with the right to access the metadata and even a third-party vendor usually could not access it. This could not only strengthen confidentiality, but also privacy level. The splitting DICOM and encryption metadata also could improve privacy related to metadata (Table 12). On the other hand, pixel data confidentiality and privacy level could be better due to encryption, and especially defacing problems could be resolved (Table 13). The applied algorithm is Rijndael (Table 12) [345], [346]. Rijndael has been selected by the US National Institute of Standards and Technology (NIST) as a candidate for the Advanced Encryption Standard (AES). It is considered one of the strongest algorithms against several attacks [352]. Furthermore, I can add any number of characters to raw metadata for practical application, and it is quite difficult to specify the multi-use key

because the key is created not rigidly. However, the availability and accountability depend on features of the conventional cloud service and will not be improved by our proposal. This evaluation summary is shown in Figure 31.

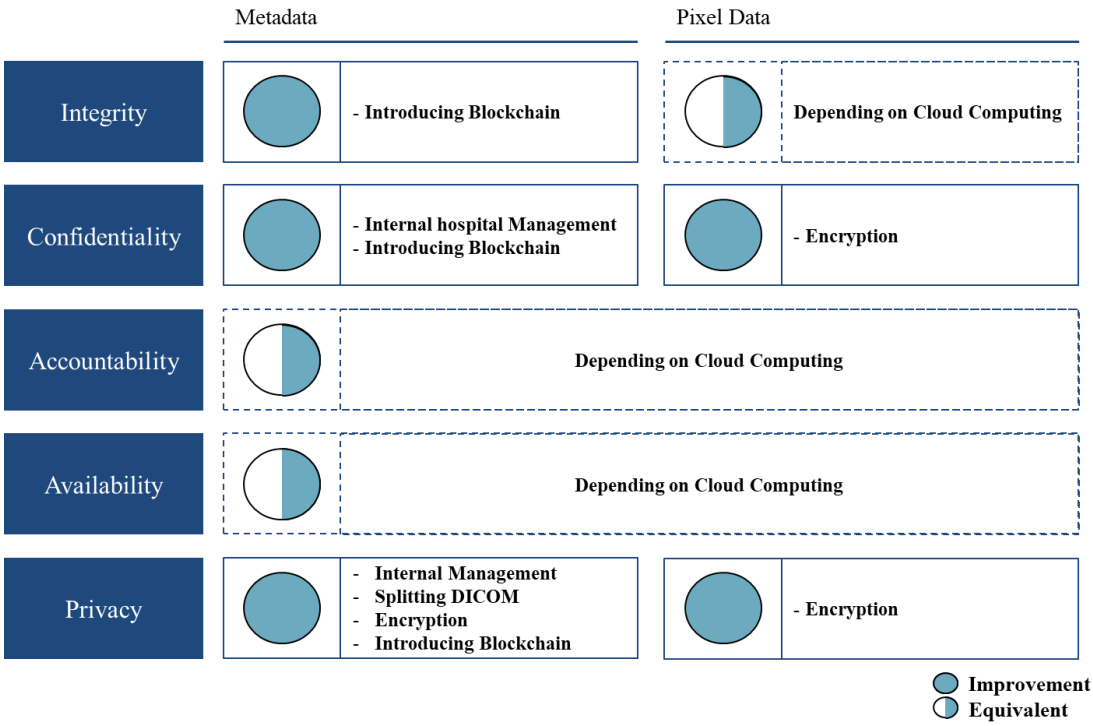

Figure 31 Security evaluation result

Table 12 Comparison of raw metadata and encrypted metadata

	Raw Metadata	Encrypted Metadata
GroupLength	174	ytk+8JhTvRz+l+ShL/T2qA==
FileMetaInformationVersion	[00 01]	j7fZ5GQfNgoSKX4ClrF7eg==
MediaStorageSOPClassUID	1.2.840.10008.5.1.4.1.1.4	yVsRkDbviAl7so5REKyqdl01NbtCzSjdnXT91sbnzm8=
MediaStorageSOPInstanceUID	1.2.392.200036.8120.100.20041012.1123100.2001002010	ii9yWv++6+0sLEh9k18/NrVuhOziO8Z1Wjp31jLo+Y7xL9L6cEpE7bca6GfAO1LSczpKJb+wvJ4nx4yWTcLOew==
TransferSyntaxUID	1.2.840.10008.1.2.4.70	7SB/2K6aAoTblIVlQ8YjJmLVqZSPf51twSHxrIYtmcQ=
ImplementationClassUID	1.2.826.0.1.3680043.2.1545.1	1j4TCVKQvVWxTYMvU4aO+8rktZneJ/MXqUScuDNtK6Q=
ImageType	ORIGINAL\PRIMARY\OTHER	LdRFbUv04dafHAalSZVH56obzjSj4Y3fTrghKC2YCmQ=
SOPClassUID	1.2.840.10008.5.1.4.1.1.4	yVsRkDbviAl7so5REKyqdl01NbtCzSjdnXT91sbnzm8=
SOPInstanceUID	1.2.392.200036.8120.100.20041012.1123100.2001002010	ii9yWv++6+0sLEh9k18/NrVuhOziO8Z1Wjp31jLo+Y7xL9L6cEpE7bca6GfAO1LSczpKJb+wvJ4nx4yWTcLOew==
StudyDate	20041012	jPd1ZSFHL4pJlux+dUsLqA==
SeriesDate	20041012	jPd1ZSFHL4pJlux+dUsLqA==
AcquisitionDate	20041012	jPd1ZSFHL4pJlux+dUsLqA==
StudyTime	123100	QknqkgYdxyEmUZDMCh3LSQ==
SeriesTime	123403	VI+GxEAEUI0qRg4eObUJIQ==
AcquisitionTime	123403	VI+GxEAEUI0qRg4eObUJIQ==
AccessionNumber	2.00E+11	PGtqs/dHY1/G4nu3EmkmCg==
Modality	MR	dDrxerxxndnGC4bSBKifXg==
Manufacturer	JIRA	x91/2OxKKDO6Q1s8kMg9gg==
InstitutionName	JIRA HOSPITAL	jJoeyHoOEs/3S8qMmPcWaA==
ReferringPhysiciansName	SHIROGANE^HIDEO	cPCezp6m8K4670lBMeoOyA==
ManufacturersModelName	MR0010	OGzSocZcuPT+ADfbX74H+A==
PatientsName	SUIDOBASHI^SABURO	nv8AddSjvkV036ul8VhGnQYOlIJr5OJej76kB20HoUw=
PatientID	999999-004	cuCN80pXlfAOpr8verspXg==
PatientsBirthDate	19820815	4BsiJoSI0nVsILRVGli8/w==
PatientsSex	M	l/+mNA8gC7SCFLPNaFEisQ==
PatientsSize	1.45	HDyrgik7kaxtDaoB4W4K0w==
PatientsWeight	50	Fppo6FGXZ+stzItneRsPWw==
BodyPartExamined	HEAD	fr5ZhzcWOzX2uyz9bV7uRQ==
ScanningSequence	SE	BZlzeIS6qC671mFrw7gvuA==
SequenceVariant	NONE	7BMcj5K8AAdhnK2ygORBFA==
ScanOptions		i8SOStLBdGccpf2gY2lpfA==
MRAcquisitionType	2D	CqmXRvk62uiFvebcRk/mFA==
SliceThickness	6	OTzqSPFY4iAtVefb3r0AzQ==
RepetitionTime	4500	OZvpr1pv4T3V8LWFRxN4rw==
EchoTime	100	tTppBPzQHaOp5yuY4XJECw==
NumberofAverages	1	qImiSD/XVpKVFBOQmkCz3g==
ImagingFrequency	63.83899097	3wphnfwqyiLh+gXUvtVvQQ==
ImagedNucleus	H	hnHBMMotYFlO1sil2xjV6w==
EchoNumbers	1	qImiSD/XVpKVFBOQmkCz3g==
SpacingBetweenSlices	7	Fqj2K3JqkwbjKf2jzTXOlg==
NumberofPhaseEncodingSteps	304	eIjfmX1i277Pk8KSsxkKYA==
EchoTrainLength	19	J+I6WoSe5gJkmjD7CvkvCg==
PercentPhaseFieldofView	100	tTppBPzQHaOp5yuY4XJECw==
AcquisitionMatrix	@	u9rlPk3vaZN4cTbV9OrYhw==
PhaseEncodingDirection	ROW	/d0Jv7eBT8xlkkbA0+2ESw==
FlipAngle	90	4yERxFzsIA+FJd86eoh2Pg==
PatientPosition	HFS	dFXzq6uiImyqasaXyy91fw==
StudyInstanceUID	1.2.392.200036.8120.100.20041012.1123100.2001	ii9yWv++6+0sLEh9k18/NrVuhOziO8Z1Wjp31jLo+Y5t6OiycnZrMRexqKqOiB3e
SeriesInstanceUID	1.2.392.200036.8120.100.20041012.1123100.2001002	ii9yWv++6+0sLEh9k18/NrVuhOziO8Z1Wjp31jLo+Y7xL9L6cEpE7bca6GfAO1LSxiVic2bH4tfTJFNGCvnO2Q==
StudyID	2322	0hunVBC27yct+rBv0norFA==
SeriesNumber	2	d4yJp1Vo/IMAZrqgynlHHQ==
InstanceNumber	10	ohEJsTU55ujnVVqKqj+XsA==
ImagePosition	-98.0000\-150.6077\34.6318	pgNHsxvRRxlGJIcYQbtD0GyccSg1ZhaI0Tv9w8VtKwM=
ImageOrientation	1.00000\0.00000\-0.00000\0.00000\0.99027312\0.13913701	ElizmH4f7IbapnhPNpDRzyoubeRzVbcljUewscbX/fPUFheA4JjtjZiXfNqP4GNINl5k49/qJq4Gw9L5++6usQ==
FrameofReferenceUID	1.2.392.200036.8120.100.20041012.1123100.2001.11	ii9yWv++6+0sLEh9k18/NrVuhOziO8Z1Wjp31jLo+Y7Zz4bwCva420HXXgHHErmQn0xy3fHNWaFExUKA3la8xw==
Laterality		i8SOStLBdGccpf2gY2lpfA==
PositionReferenceIndicator		i8SOStLBdGccpf2gY2lpfA==
SliceLocation	-7	YinoaGHVJtdfwZN4BavSmw==
SamplesperPixel	1	qImiSD/XVpKVFBOQmkCz3g==
PhotometricInterpretation	MONOCHROME2	xan38X+PtqQX9t9zfSvDDg==
Rows	320	fOlSWPfLZeacFPgHcnfsXg==
Columns	320	fOlSWPfLZeacFPgHcnfsXg==
PixelSpacing	0.6875\0.6875	CCXs2iOpWzwjENvpyIbv6A==
BitsAllocated	16	ZyjFUR8NyBlivrC8vUP1Bg==
BitsStored	16	ZyjFUR8NyBlivrC8vUP1Bg==
HighBit	15	8bqDn0TS4DXv6Y9ZY9Fe7w==
PixelRepresentation	1	qImiSD/XVpKVFBOQmkCz3g==
WindowCenter	4468.7402	38LjZc5Qs41oCgSJ/mxg8A==
WindowWidth	11062.5195	n4YQdV4gD3nCF3eGch0Y/A==

Table 13 Comparison of raw pixel data and encrypted pixel data

	Raw Pixel Data																Encrypted Pixel Data															
	1	2	3	4	5	6	7	8	9	10	11	12	13	14	15	16	1	2	3	4	5	6	7	8	9	10	11	12	13	14	15	16
1	42	4D	36	B0	04	00	00	00	00	00	36	00	00	00	28	00	75	C0	E0	44	EB	94	A8	51	25	47	78	2D	04	EA	40	FC
2	00	00	40	01	00	00	40	01	00	00	01	00	18	00	00	00	67	CF	E6	10	F9	CD	28	44	47	B0	26	EE	33	D9	0A	60
3	00	00	00	B0	04	00	C4	0E	00	00	C4	0E	00	00	00	00	A4	DC	C7	A4	82	FF	3C	83	E1	EB	9B	89	A0	C7	93	B4
4	00	00	00	00	00	00	1C	1C	1C	1E	1E	1E	1F	1F	1F	1E	3F	28	3E	AA	36	41	D6	4E	73	3A	32	92	72	A1	26	BB
5	1E	1E	1E	1E	1E	1F	1F	1F	1F	1F	1F	1E	1E	1E	1E	1E	B6	7B	36	64	4A	E2	4C	B9	78	8C	2B	8F	23	FA	03	31
6	1E	1D	1D	1D	1D	1D	1D	1E	1E	1E	1F	1F	1F	20	20	20	A3	B9	C7	0F	A6	CB	D7	63	5B	4D	6B	A5	09	B7	68	96
7	20	20	20	1F	1F	1F	21	21	21	20	20	20	1E	1E	1E	1D	92	FC	B3	19	87	36	11	C7	A6	D4	E9	F0	7F	CB	44	63
8	1D	1D	1E	1E	1E	1F	1F	1F	20	20	20	21	21	21	1F	1F	08	AE	37	7F	15	A1	29	89	94	56	22	F8	BD	0A	CB	86
9	1F	1E	1E	1E	1E	1E	1E	1E	1E	1E	1E	1E	1E	1D	1D	1D	2D	17	68	C9	69	D6	58	6C	7A	D5	90	EA	24	8E	38	3F
10	1D	1D	1D	1C	1C	1C	1E	1E	1E	1F	1F	1F	1F	1F	1F	20	41	DA	32	89	12	FE	40	7D	6A	F5	4C	5B	2B	17	FF	37
…	…	…	…	…	…	…	…	…	…	…	…	…	…	…	…	…	…	…	…	…	…	…	…	…	…	…	…	…	…	…	…	…
19194	1D	1C	1C	1C	1C	1C	1C	1C	1C	1C	1C	1C	1C	1C	1C	1C	FC	2B	0B	E7	5E	D1	B2	B9	3A	42	BF	3F	57	45	16	54
19195	1C	1C	1C	1D	1D	1D	1B	1B	1B	1C	1C	1C	1C	1C	1C	1C	45	F3	CE	53	62	5A	DF	68	85	81	03	23	C3	7F	95	6C
19196	1C	1C	1B	1B	1B	1B	1B	1B	1C	1C	1C	1C	1C	1C	1A	1A	DA	25	91	7A	CC	FD	E3	3A	67	AA	0B	4C	74	D6	9E	1D
19197	1A	1B	1B	1B	1B	1B	1B	1B	1B	1B	1C	1C	1C	1C	1C	1C	B5	9E	68	61	24	E4	E7	77	62	14	08	AA	85	90	93	20
19198	1D	1D	1D	1D	1D	1D	1D	1D	1D	1B	1B	1B	1B	1B	1B	1D	B1	66	31	35	94	C0	62	D1	C1	13	07	62	82	B4	D8	BC
19199	1D	1D	1C	1C	1C	1A	1A	1A	1A	1A	1A	1C	1C	1C	1D	1D	6C	1E	CD	E2	0A	34	CA	26	31	49	FB	75	25	1D	F5	D3
19200	1D	1D	1D	1D	1D	1D	1D	1D	1D	1D	1D	1D	1D	1D	1D	1D	FA	4F	6B	DC	7F	C5	11	2D	4C	13	E0	69	1B	47	0B	1B
19201	1D	1D	1D	1D	1D	1D	1B	1B	1B	1C	1C	1C	1D	1D	1D	1D	F3	FE	5D	53	6C	2D	0B	50	DF	B8	F7	D8	DD	70	45	31
19202	1D	1D	1E	1E	1E	1E	1E	1E	1F	1F	1F	1F	1F	1F	1F	1F	D3	CC	D1	13	C1	B7	8C	43	5A	93	9D	31	66	8F	7A	33
19203	1F	1E	1E	1E	1F	1F	1F	21	21	21	21	21	21	1F	1F	1F	A3	DC	0A	4A	0E	F0	3A	06	8C	BA	3D	5A	FA	07	CB	F3

3.6 System Architecture

3.6.1 Overview

In addition to the present proposal, matters related to the system used to realize societal implementation of image sharing are discussed herein. Engineering research should be ultimately used to create new technologies that promise to improve the lives of people. However, there is a large gap between technology and business [353], and a large number of steps are required. Because regulations, business practices, and stages of technological infrastructure development differ in various regions, this study focuses on implementation for the Japanese healthcare industry. Although a way to share medical images is proposed, this area should be more deeply discussed to consider a complete system architecture for practical use because the security level and system performance, among other factors, strongly depend on these business and system requirements. Furthermore, if each technology component becomes more prominent and the latest technologies are applied, business requirements will not necessarily be fulfilled. Regardless of whether such desires are realizable, diverse components such as hardware capability, network bandwidth, database designs, external coordination, business operations, and of course applied technologies, will be affected. Therefore, a system architecture for social implementation should be discussed. First, business and functional requirements, referring to regulations and the multi-stakeholder meetings conducted for this study, are defined herein. Second, the non-functional requirements that mainly depend on stakeholder opinions are considered. In addition, an architecture overview for development is constructed. Third, a component model, which is a more concrete figure than an architectural overview from a functional requirement

perspective, is demonstrated.

3.6.2 Business and Functional Requirements

The requirements related to businesses and system functions are first summarized. A requirement is the capability a system must possess to satisfy a need or objective; in particular, business requirements are a series of needs that must be fulfilled to achieve a high-level objective. This usually describes why an organization wants a particular system, the benefits that the organization or its customers expect to receive from undertaking a particular project, and the aim and end goal of the project [354]. When we realize a social implementation, business requirements can help the project owner, stakeholders, and development team get onto the same page. Considering the system requirements, although a vast amount of knowledge has been accumulated in the IT industry, a determination of the system requirements still remains one of the major challenges for development. System requirements have to meet the business requirements, and clarify how such requirements can be realized by the IT system.

First, the fundamental factors required by a system are determined herein. The sharing of medical images has various benefits for healthcare establishments, patients, and society. Improved access to patients' medical imaging histories, real-time collaboration by specialists, the avoidance of duplicate care to reduce costs, decreased radiation exposure for patients, remote accessibility of expertise and specialized opinions for patients, and of course, the CAD system itself, will achieve a significant social impact if CAD developers can access medical image data for research and development. As a result, the quality of care can increase, patient satisfaction can grow, and healthcare expenditures can decrease. However, medical images include some sensitive information, and healthcare establishments have a resistance to store such data in an external environment (e.g., a cloud server). Therefore, the system should be implemented with a function allowing medical images to be share without keeping sensitive data in a cloud environment. Furthermore, high scalability to deal with a large number of healthcare establishments and medical images is necessary. Additional operations for the provided healthcare are of course undesirable, and CAD developers would like to access medical image databases without access to the patients' sensitive information. The system must comply with the corresponding laws, regulations, and other rules.

Second, actors related to the business process are determined. One of the main actors is a patient using this system. The patient needs to manage their personal data, and provide their unique ID to the doctors applying the system on their behalf. Of course,

they should be able to manage and delete their own information. Healthcare establishments are also important actors in the system. They include not only medical doctors, but also administrators controlling the system, which is inside the establishment, and radiologists who communicate with the hospital PACS and blockchain server. An external server in a cloud environment has to be managed by system administrators. People who want to use a large number of medical images (e.g., CAD system developers) should also be considered key actors. A function allowing access only to external non-sensitive data is also required.

Third, the fundamental functions used to operate the system, such as login/logout, user communication, daily operation, and managing functions should be taken into account, and accident provisions should be created. To obtain all functions, each function by each actor was written out, as shown in Table 14.

Table 14 Functional requirement

No	Actor	Business Process	Function	
			Client	Server
1	Outside User			
1	Patient			
1		Register user information		
1			Input Mail address/Password	
2			Check format of input information	
3			Transmit user information	
4				Receive user information
5				Confirm recept information
6				Register user information
7				Notice complete registration
2		Manage user infromtion		
1			Login	
2			Logout	
3			Compile user information	
4			Delete user information	
5			Notece own patient ID	
2	Secondary user			
1		Access medical images	Download pixel data	
2			Decrypt image data	
2	Healthcare Establishment			
1	Administrator			
1		Agreement	Out of the scope of the system	
2		Register hospital information	Out of the scope of the system	
3		Install Blockchain system	Out of the scope of the system	
4		Receiving inspection	Out of the scope of the system	
5		Manage user accounts		
1			Issue accounts	
2			Delete accounts	
6		System operation	Out of the scope of the system	
7		System maintenance	Out of the scope of the system	
2	Radiologist			
1		Input patient information to modality	Out of the scope of the system	
2		Upload medical image to PACS	Out of the scope of the system	
3		Upload medical image to Blockchain system		
1			Read DICOM	
2			Check DICOM format	
3			Divide DICOM into metadata and pixel data	
4			Create hash value	
5			Encrypt metadata	
6			Encrypt pixel data	
7			Upload pixel data to outside server	
8			Archive encrypted metada and hash value	
9			Broadcast hash values	
10			Receive hash values	
3	Medical doctor			
1		Manage user information		
1			Lonin	
2			Logout	
3			Compile user information	
2		View patient medical image		
1			Search for patient ID	
2			Receve patient ID	
3			Search for metadata with patient ID	
4				Search for pixel data with patient ID
5			Reconstruct DICOM	
6			Store DICOM	
3		Image diagnosis	Out of the scope of the system	
3	Cloud Administrator			
1	Administrator			
1		Manage healthcare establishment		
1				Register hospital information
2				Notice complete registration
3				Delete hospital information
2		Operate cloud service		
1				Store access log
2				Output access log
3				Alive monitoring
3		Operate Blockchain system		
1				Store access log
2				Output access log
3				Alive monitoring
4		Managing batch processing		
1				Batch processing

3.6.3 Non-functional Requirements

Generally speaking, non-functional requirements describe how a system works, whereas functional requirements describe what the system should do. There are four main elements to this: availability, performance, scalability, and security [355]. A system's availability, or "uptime," is the amount of time that it is operational and available for use. This is specified because certain systems are designed with an expected downtime for activities such as database upgrades and backups. Performance is the answer for questions such as "what should the system response times be, as measured from any point, and under what circumstances?" Software that is scalable has the ability to handle a wide variety of system configuration sizes. The non-functional requirements should specify the ways in which the system may be expected to scale up (e.g., by increasing the hardware capacity, or adding machines or devices). Security is one of the most important issues in the non-functional requirement of the proposed method. Security requirements can come in many different forms, namely, privacy, physical, and access requirements, and can dictate the protection of sensitive information. Some types of privacy requirements include data encryption for database tables, and policies regarding the transmission of data to third parties (e.g., scrambling user account numbers). Considering physical security, such requirements must relate to the physical protection of the system. Physical requirements include items such as elevated floors for server cooling, and fire prevention systems. On the other hand, access requirements define the account types/groups and their access rights. An example of an access requirement could be to limit each account to one login at a time, or to restrict where an application can be deployed or used.

First, matters related to availability are discussed. The most important subject regarding availability is the operation schedule. The system deals with healthcare infrastructure, and ideally requires 24-h nonstop access. However, all systems have to be maintained, and the maintenance time is excluded. The recovery time and operational rate should be considered, and these metrics, obtained through the meetings conducted, were set equivalent to those of a conventional system, namely, recovery within 1 h from the point of failure, and a 99.99% operational rate. When a disaster occurs, a degeneration operation can be conducted.

Second, the performance objectives were determined. Before defining such objectives, the number of processes required for medical imaging per year was roughly estimated. The Japanese Ministry of Health, Labor, and Welfare showed the total number of medical imaging exams per month to be about 9.6 million [356], and it was determined through this study that the maximum throughput per day will be 3,000

images if an examination takes ten medical images and one out of a hundred people are introduced into the system. Furthermore, a CT image has 2.36 kB of metadata and 0.3 MB of pixel data. Therefore, the necessary performance of the system can be estimated, namely, about 3 TB of cloud server data per year, 30 GB of blockchain server data, and at most 3,000 blocks created per day related to throughput. On the other hand, the response time as determined through the meetings is 5 s for an image view with exigency (i.e., over the last 5 years), whereas without exigency 60 s is set as target for viewing an image.

Third, scalability of the system is discussed. Through the stakeholder meeting described in the section above, hospitals were shown to have managed patient images for the past 20 years at most. Therefore, the proposed system should control medical images over the last 20 years through a standard flow. The images taken more than 20 years earlier will be managed through a limited performance server without specific requirements.

Finally, security matters should also be defined. This is the main purpose for developing the proposal described in this paper, and is strongly related to the functional requirements. Patient privacy is the most notable subject in discussion on security. The proposed system has four noteworthy points. First, the system divides DICOM data into metadata and pixel data, and therefore data sensitivity may be lower. Second, the divided metadata are also encrypted through a multi-use key, and the Rijndael algorithm is applied, resulting in stronger security. Third, such encrypted metadata are managed internally within the hospital and not in a cloud environment. Fourth, pixel data, which are low-sensitivity data, are also encrypted in the same way. In addition to privacy matters, physical security should be considered. The location where the physical server is placed may require an entrance and exit room control system. Furthermore, network communication such as blockchain server to blockchain server, and blockchain server to cloud server, apply encrypted communication or a VPN. For an audit trail, both servers must monitor logs regarding data access and manipulation. User ID and password management, along with server identification, are measures for controlling access rights. A summary of the non-functional requirements is given in Table 15.

Table 15. Non-functional requirement summary

No	Item	System Metrics
1	Availability	
1	Operation Schedule	24-hour nonstop, except for mentenance
2	Recovery Time Objective	Recovery within an hour from the point of failure excluding disaster situation
3	Operation Rates	99.99%
4	Failure Resistance	Duplex cloud server, and cold stand-by
5	Disaster Resistance	Prepearing disaster server with degeneration operation
2	Performance	
1	Data Volume	
1	Cloud Server	3TB per year
2	Blockchain Server	30GB per year
2	Throughput	At most 3,000 block creating per day
3	Response Time	5 second for display medical image
3	Scalability	
1	Resource Scalability	
1	Cloud Server	20 years volume of medical images in standard server
2	Blockchain Server	20 years volume of medical images in standard server
4	Security	
1	Privacy	
1	Metadata	Metadata division management
2	Metadata	Metadata internal management
3	Metadata	Encrypt metadata
4	Pixel Data	Encrypt pixel data
2	Physical	
1	Blockchain Server	Secure room management with entry restriction
2	Communication	Encrypted communication to cloud server and other hospital server
3	Access	
1	Access Control	Access right management
2	Access Log Management	Store access and manupulate log in both server

3.6.4 Architecture Overview

Next, an overview of the designed architecture is described. The architecture is a high-level perspective of a system in the context of its environment, dependencies, and technology components. The architecture also describes the structure, behavior, integration, and aesthetics. An architectural overview is composed of certain diagrams that can describe substances regarding architectural elements, including the structure of the system, architectural pattern usage, primary interfaces between subsystems and external systems combined with target deployment platform information, critical data

schema, and important service, component, class, and module structures.

Before discussing the proposed system architecture, a conventional hospital system structure should be described. There have been three main systems applied in hospitals: a hospital information system (HIS), radiology information system (RIS), and PACS [357]. An HIS can be defined as a system that processes any type of hospital data, such as financial, patient-related, and strategic management data, as well as patient accounts, patient tracking, payroll, reimbursements, taxes, and statistics [358]. On the other hand, an RIS can be defined as a system for managing medical images and associated data. An RIS is applied specifically for tracking radiology imaging orders and billing information, and introduced to connect with a PACS for managing an image archive [359]. A PACS, as referred to in Section 3.2, can be defined as an infrastructure that links modalities, workstations, an image archive, and a medical record information system into an integrated system [311]. A PACS generally consists of three parts: an image server, a report server, and a viewer. The image server mainly controls and manages DICOM data, and can transmit DICOM to a personal device through WEB. The report server is related to clinical reports, and sends data to an internal device through WEB. Finally, the viewer displays DICOM and clinical report information. HIS, RIS, and PACS have been applied together in close coordination for DICOM management [357], and an example of the connectivity for these three systems is shown below.

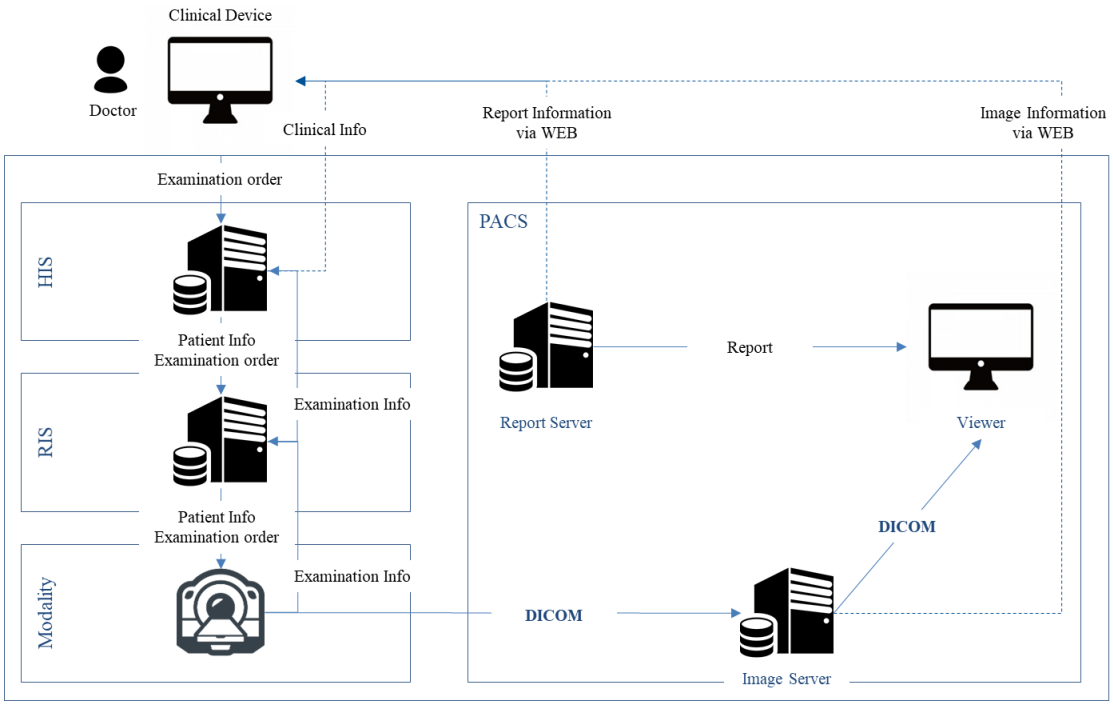

Figure 32 Standard work flow of hospital conventional systems

Next, the proposed system architecture is defined. As a non-functional requirement, image data have different priorities according to when they were taken. Images taken within the past five years tend to be referred to more frequently, and are strictly required by law to be archived. Therefore, these images are controlled internally in a hospital PACS, particularly an image server, which many hospitals want to maintain. However, other establishments may want to access such data, and the system must also be able to control these parties (i.e., a blockchain server or cloud server must be maintained). On the other hand, 20 years could be a threshold for image management. Although hospitals are not required to manage images that are older than 5 years, some images may be referred to even up to 20 years after they are taken. Therefore, the system manages such type of images in a high-performance server. Images taken beyond the last 20 years have less value for medical practice, and system development and regulation have not defined how to manage them; therefore, a server with a limited performance is sufficient to archive and manage these images. For the above reasons, the proposed system architecture includes five servers: the main server, a spare server, a limited server with a cloud environment, and another main server and sub-server for blockchain-related functions. An overview of this is shown below.

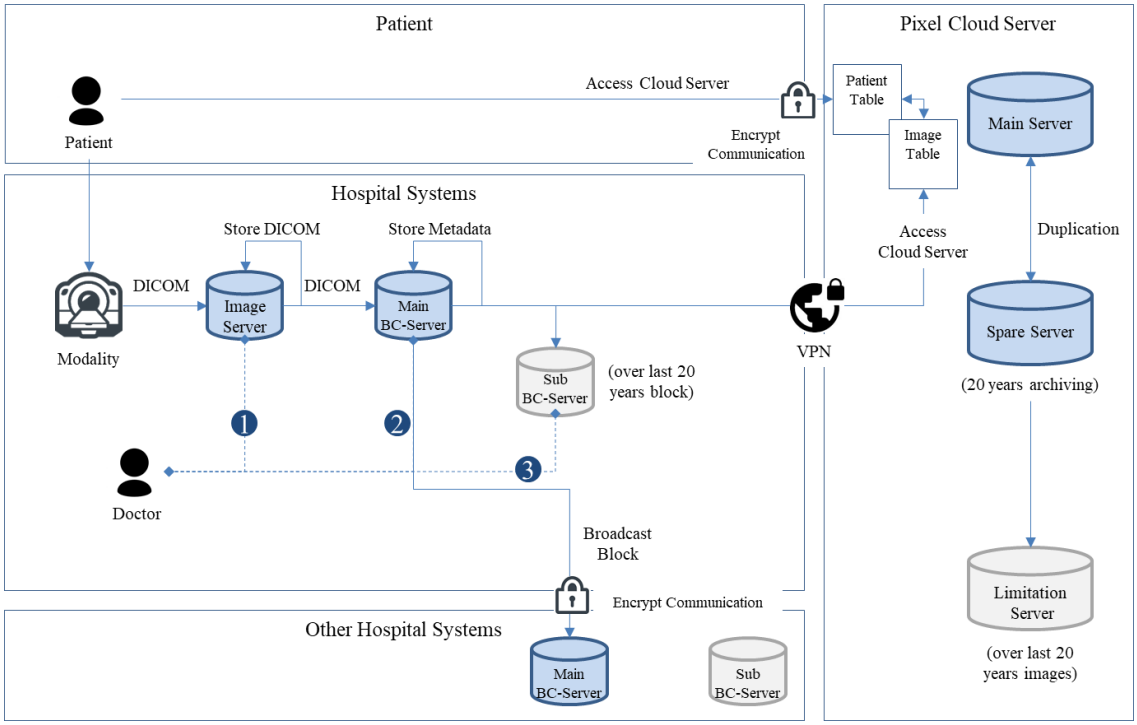

Figure 33. System architecture overview

*Supplementation:

1. For medical images taken within 5 years.

2. For medical images taken in-hospital more than five years earlier, and images taken with the past 20 years at another hospital.
3. For medical images taken more than twenty years ago.

3.7 Discussion

3.7.1 Noteworthy Points

Noteworthy points of the proposal system, along with limitations and future work, are discussed in this section. First, the performance and scalability of the proposal are detailed. The above results seem to indicate a sufficient scalability to processing vast numbers of medical images because even at 100 units, the low-spec PC applied in this study were able to handle all medical images taken in the U.S. Furthermore, our proposal does not waste much additional hardware resources because the metadata duplicated by the blockchain are significantly smaller in amount than the pixel data. Second, this method can improve the security of cloud computing, particularly with regard to integrity, confidentiality, and privacy. Third, the proposed system can achieve synergy on conventional systems such as a large-scale PACS. For example, the system can collaborate with a PACS through the creation of blocks, as shown in Figure 22. The scheme can improve the large-scale PACS scalability because it does not need permission from each individual hospital or a tremendous amount of construction costs.

Second, previous studies related to blockchain technology for healthcare use can only deal with the small data such as electronic health records or health information [335], [336], [360]. In contrast, the proposed system can handle large amounts of medical data (i.e., DICOM), and apply cloud computing for scalability.

Finally, from the perspective of contributing to innovation science, this research conducted not only an analysis but also a design and implementation depending on the analysis result. Therefore, it will contribute practically to innovative science.

3.7.2 Limitations

There are some limitations and challenges to using this methodology in practice. First, my proposal is novel in how it integrates two technologies; cloud computing and blockchain. The discrete algorithms that I applied are established approaches (e.g., SHA-256, and Randel). Therefore, I should reconsider algorithms, including “what metadata is managed by blockchain” or “what encrypt algorithm I apply considering the encryption strength and processing time,” and reevaluate the total performance required for practical use. When we use and view the DICOM data, some examination tags related to modality and filming conditions are required, except for patient information. For example, “modality code”, “Row code”, “Column code” and “Pixel spacing code”

might be necessary to make use of pixel data considering stake-holder hearing. Second, my test results indicate sufficient performance because even my low-performance PC could execute my methodology in a short amount of time. However, system performance highly depends on not only technological component, but also system architecture. Furthermore, it may be difficult to create blocks and synchronize all hospitals' databases in a timely manner from a network bandwidth perspective if many healthcare establishments participate in this platform. One possible solution is to create and synchronize almost all blocks outside business hours (e.g., mainly at night) if transactions are low in priority, because it is not a regular situation for medical examinations and medical images to be required at several hospitals per day for every patient. Third, it is debatable whether data are more secure when managed in a cloud by a big IT professional company such as Amazon or in an intranet environment by a small establishment. Therefore, my system may not work securely for small medical establishments without IT experts as I had assumed, and it cannot be introduced for worldwide use. Fourth, I encrypted the metadata and pixel data with the corresponding decryption keys in my test case. It was easy to identify the connection between the key and encrypted data. Therefore, I should take measures to ensure a more secure environment by using a different pair of keys to encrypt data according to some kind of rule. Fifth, I have to take special measures to protect medical establishments from spoofing because a conventional blockchain systems usually does not have an administrator and could not intervene the work flow. However, the proposal assumes applying private blockchain, it could be resolved by access controlling. Sixth, there are standard image management systems such as PACS that allow for efficient electronic distribution and storage of medical images and access to medical record data [310]. I must consider how to communicate with these systems efficiently for practical and user-friendliness. As I showed in architecture overview, VPN connection is eligible and contacting PACS vendor may be required for system setting. Seventh, the patient ID can be misused because it is stored in the patient's device. Therefore, a conventional solution such as fingerprint [361] or face authentication [362] may be required. For example, patient all patient has to do is to such authentication to send their patient ID with smart device application. Eighth, although I proposed limited server usage for my architecture, data migration is one of the most herculean task and I synchronize all data in each hospital. Therefore, I have to assume how to migrate all data in the detailed design phase. Ninth, my proposal divides DICOM data into metadata and pixel data, therefore, when the system reconstruct the data, it has some functions to assure data integrity. Finally, the systems and databases in a hospital are difficult to maintain.

Therefore, a large amount of highly specialized manpower may be required to keep the system working if so many hospitals make use of the systems.

3.7.3 Future Work

In future work, three subjects will be studied. The first is related to clinical report sharing. Medical image sharing can be more valuable with clinical reports because each doctor can determine a patient's condition more deeply, and reduce any misunderstandings. Therefore, a way to securely share clinical reports including diagnostic results and observations will be considered. To show a possible method for this, clinical reports are formed from a block in the same way, and broadcast by another blockchain line after diagnosis (i.e., the hospital has two lines of blockchains, and both chains are related to the multi-use key). Clinical reports should be written with flexibility in a widely accepted format, such as JavaScript Object Notation (JSON) [363]. JSON is an open, text-based data exchange format, and is human-readable and platform-independent with a wide availability of implementations. JSON is not limited to any particular applications, and can be used in virtually any situation where applications need to exchange or store structured information as text.

Second, insensitive healthcare data such as blood pressure, cholesterol levels, blood-sugar level, and medication history will be shared for wide application and unified patient management. This type of information can be applied to the design of new drugs, an analysis of the curative effect, and the discovery of side effects. The proposed system architecture can offer an environment to anonymize and diffuse patient data. For example, the system architecture can be expanded to three layers for sharing a variety of healthcare data. The bottom is a private blockchain layer used to control the data securely in a healthcare establishment. Personal information and clinical reports correspond to this type of data. The second layer is used to archive moderately sensitive or high-volume data such as DICOM pixel data. This layer requires the user to have appropriate access rights. The top layer is for the least sensitive and low-volume data, and is applied to the public blockchain. The data in this layer can be used by anyone. All information is connected using the proposed key, and patients can manage the unified data. This mechanism allows patients to decide whether to have their information diffused, and thus the system could be widely accepted by users. To control any type of health information, the system can be applied not only to a CAD system, but also to a DSS for development purposes. A chart of future work is shown in Fig. 34.

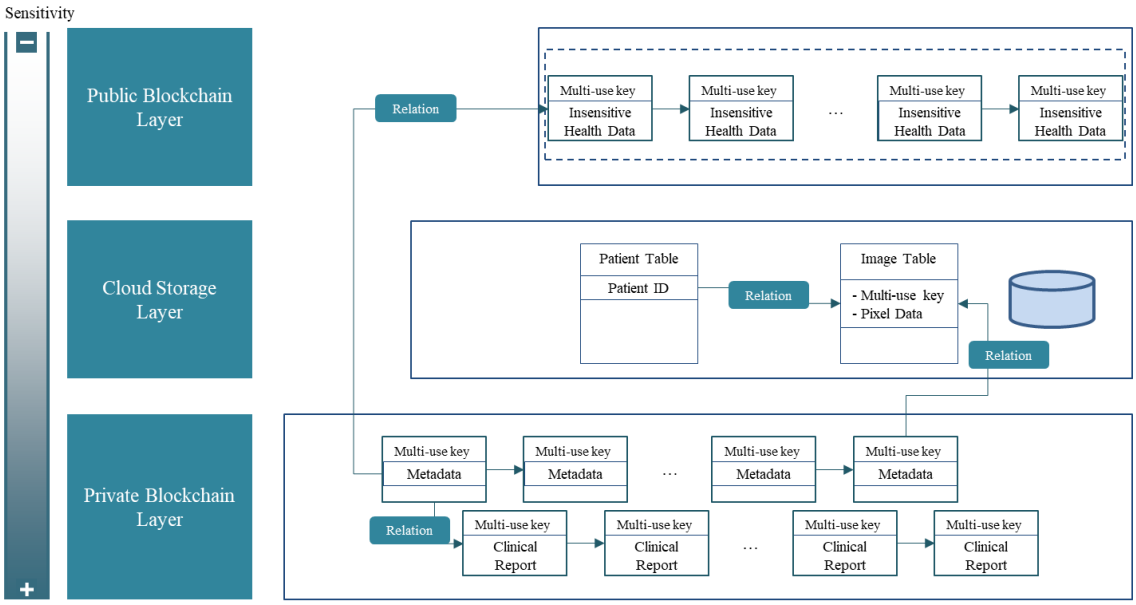

Figure 34. Future work concept

Third, shared-data usage from "diagnosis" to "surgical planning" will be expanded in future work, and describing tissue that cannot be viewed in a medical image is a very critical issue. Diagnosis can be considered a judgment process regarding a particular illness or problem. On the other hand, surgical planning is a preoperative to making decisions related to how a surgeon should treat a patient disorder in an operating room (e.g., how to remove a tumor, or where to conduct a craniotomy). Therefore, it must be different from the required information level between both processes. Diagnosis focuses on the region of interest around a lesion, whereas surgical planning requires more detailed information such as where the critical tissue is and what tissues are connected to lesions. However, some micro-tissue such as gray matter fibers in the brain may not be clearly caught through a modern modality. Hence, the accuracy of surgical planning can be improved if micro-tissue can be supplemented through the application of mass data. The example below will be proposed.

For neurosurgical planning, identifying the white matter pathways of the brain has been a challenge for a long time because white matter has an effect on brain functionality, modulating the distribution of action, and coordinating communication among different parts of the brain [364], and cannot be drawn through a modern modality owing to the current resolution [365]. As an aid to identifying safe margins of resection and treatment, a visualization of the brain's white matter pathways through diffusion magnetic resonance imaging, namely, tractography, has been receiving increasing attention with regard to neurosurgical planning [366]. This methodology is applied to utilize data from diffusion tensor imaging. A diffusion MRI is a typical

technique used to produce images of the molecular diffusion process in tissues, and water molecules tend to diffuse along, rather than across, white matter fibers in the brain. It is possible to depict the structure and integrity of the major water matter tracts in 3D using tractography, and MR tractography is non-invasive, relatively fast, and can be repeated multiple times without destroying important tissue [367]. However, tractography suffers from certain limitations, as it is indirect, inaccurate, and difficult to quantify, namely false positives and false negatives occur. The most challenging issue of tractography is likely the fact that it has not been fully validated [368]. Furthermore, the technique is often not able to be used to reconstruct correct trajectories in heterogeneous fiber arrangements, such as axonal crossings [369]. Hence, a supplementation to correct the tractography results is required.

A possible solution is to apply data from electrocorticography. Some neurosurgical operations use the electrocorticography signal power to express a cortical mapping from arrays of subdural electrodes [370]. This brain mapping can grab the white matter of the brain more accurately; however, intraoperative brain mapping takes a long time and is invasive. Hence, using only a tractography model for operation is better for patients and healthcare providers. Although brain-mapping data are not managed in a hospital, and the data format used to control this type of data seems complicated, there may be a chance to apply brain-mapping data to tractography. Furthermore, images taken in an operative room may be useful to improve the tractography if a model is created from the image and the tractography algorithm provides feedback.

3.7.4 Overall Discussion

First, the system is discussed from a societal cost perspective. In chapter 2, it was concluded that the impact of the medical image sharing effect can be large, and its cost threshold is about 40 US$ per diagnosis. For social implementation, the cost for some of the major components is broken down here. One of the largest parts could be the cost related to system development. Such cost includes the hiring of system engineers, hardware/software procurement, and patent licensing fees if needed. On the other hand, the system has to be maintained by certain vendors, and therefore, a maintenance cost is also generated. This cost is composed of alive-monitoring, system extension, and vulnerability management. Furthermore, for diffusion of the system, an introduction cost to each stakeholder may also be incurred. To introduce the system to healthcare establishments, the costs for constructing the environment internally in a hospital, a legal procedural acceptance test, and the training of personnel will be needed. From a patient perspective, with the exception of legal procedural costs, promotion costs for

diffusion might be required. CAD or image-based system developers are also important stakeholders, and incur costs such as legal procedural costs and the costs of applying training datasets to systems. In addition to these costs, regulatory compliance costs and a variety of indirect costs will be required for social implementation. With the exception of system maintenance costs, and the cost of introducing the system to patients, fixed costs could be major portion of the total costs. Therefore, the system business model is strongly related to the economy of scale.

Furthermore, this proposal can resolve four challenges for the healthcare industry. First, long-term management costs for medical images may be decreased because images are archived in a cloud environment. Second, the sharing of medical images can improve the healthcare quality because medical doctors are able to make the most of patient images taken in the past. This advantage could have a significant effect on progressive disorders, such as Alzheimer's dementia and certain types of cancers. Third, our proposed image-guided system supplies developer with sufficient training datasets that they can use to develop systems with a higher performance. This data supply scheme will be less complicated than it is now because developers can use datasets with permission. Fourth, patients can also benefit. If hospitals are allowed to refer to image data, healthcare quality may be improved. Furthermore, diagnosing without the need for additional imaging can decrease exposure to radiation and save lives. Finally, as concluded in chapter 2, the cost-effectiveness can also be improved from a social perspective. Furthermore, concrete requirements related to functional/non-functional matters were revealed that may accelerate the societal implementation of the proposed system.

Finally, a possible service model for societal implementation was described. Before modeling the service, a Japanese market analysis from a competitor perspective was conducted in the present study. Where to archive medical images has been a critical issue from a regulation perspective for a long time. Medical images have only been stored in healthcare establishments in past years. A public notification published in 2002 by the Ministry of Health, Labor, and Welfare allowed healthcare establishments to manage medical images in an external server; however, this server had to be controlled by the healthcare establishments themselves or a government agency. In 2010, this notification was revised, and private businesses could finally launch a service for medical image storing. Therefore, the history of medical image cloud services is relatively short, and a de facto standard service has yet to be fixed. The market environment is reviewed below through an analysis of some major services. The first company that broke into this market was GE Healthcare Japan in 2011 [371]. This

service could decrease the management costs for medical images, and the cloud service type applied was Storage as a Service. The second entry service was launched by Toshiba Medical Systems Corporation in 2012 [372]. This service had almost the same concept as the GE healthcare service. Fuji film corporation also took part in this market in 2012 [373]. This service could be applied to disaster recovery, and constructed on-premises. One of the latest services was launched by Canon, Inc. [374], and had some application functions such as teleradiology and a 3D volume analyzer. A summary of the history of such service development is provided in Fig. 35. Furthermore, a possible service model based on the market environment is shown. The present proposal requires economy of scale for practical use because the discussion above and because the costs of constructing a cloud environment can be diluted by the number of customers, and introducing more hospitals to the system implies that more training datasets can be accumulated. Therefore, I propose a possible service model, which should be conducted in four steps. In the first phase, the proposed system is applied solely as an external archiving service for a hospital. In this phase, a number of hospital user must be gained. During the second phase, the system will be expanded to share medical images between healthcare establishments, and sharing with image-based system developers will be implemented during the third phase. For the last phase, the system will be expanded to manage all types of health data including electronic health records and medical diaries using the blockchain system. This concept is shown in Fig. 36.

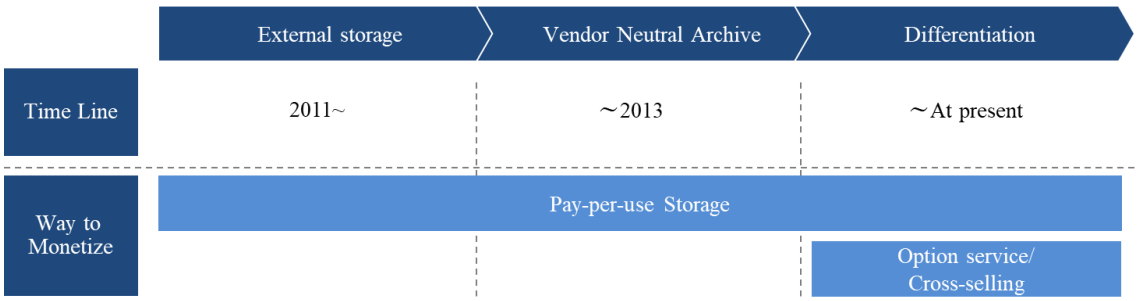

Figure 35 Medical image cloud service model

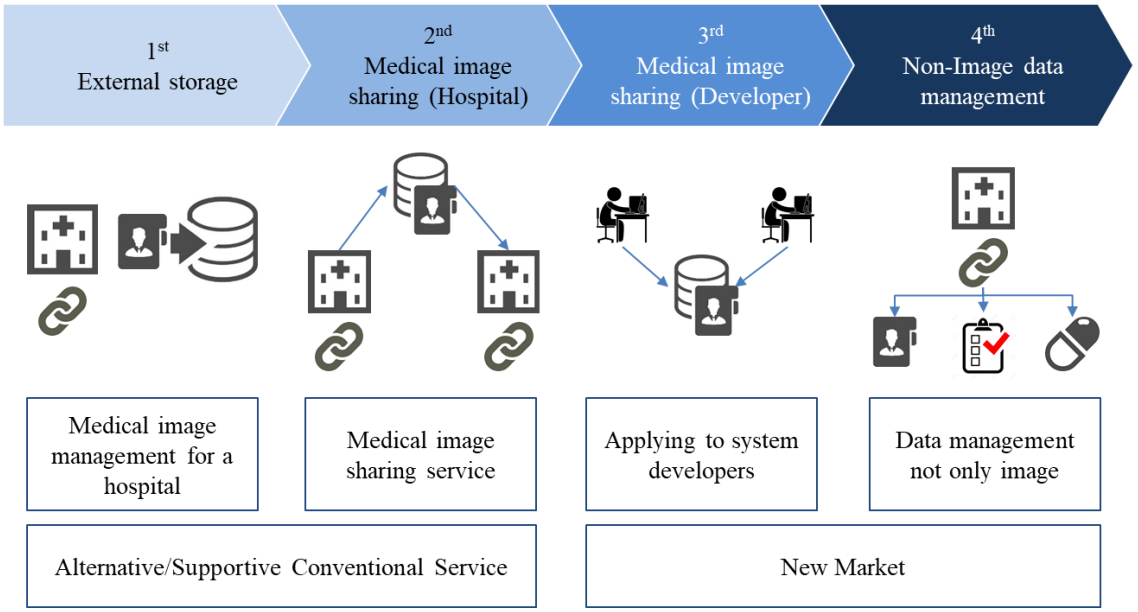

Figure 36 Service model concept

3.8 Conclusion

A method for sharing medical images was proposed. The proposed method can be more secure than a conventional cloud service, and seems to fulfill the scalability requirements for practical use when considering the test results. In addition to suggesting and developing a prototype, a multi-stakeholder meeting was conducted to determine the needs and wants of such a system in practical use, and an architecture was proposed based on the results of the meeting. This discussion revealed that medical image sharing using the proposed system can contribute not only to image-based system developers, but also to patients, doctors, and hospital management. Furthermore, the capability of realizing the proposed system was determined through a meeting with a regulation authority and an internal hospital management system vendor. In the next chapter, some concluding remarks regarding Chapters 1–3 and directions for future work are provided.

3.9 Appendix

		Hearing Items	Answers
1. Needs	1.1 Healthcare Establishments	1.1.1 Is there high demand for straging medical images in cloud enviornment? And what?	1.1.1 Yes, and the high volume of medical images is leading to scalability and maintenance issues
		1.1.2 Is there high demand for sharing medical images between healthcare establishments?	1.1.2 Yes, if access to previous patient images, doctor could add other modality images with low cost.
		- What the purpose do you require for sharing medical images in practice?	- Improving medical treatment quality and surpress cost for medical imaging.
		- Is it necessary to share medical images anytime?	- No, it isn't necessarily. Rapid development disease require retake medical image.
	1.2 System Developer	1.2.1 Is there high demand for utilizing medical images to develop healthcare systems?	1.2.1 Yes, recently it is inevitable to accumulate health data to develop systems.
		- (if any) What kinds of information do you want (e.g. sex, age)?	- From DICOM tag perspective, sex, age, modality-code are required.
		- (if any) How do you assemble the data?	- From partner healthcare establishments.
2. Business Requirements	2.1 Hospital Regulations	2.1.1 Regulation for archiving medical images in hospital.	2.1.1 Regulation for archiving medical images in hospital.
		- How long does hospital archive medical images?	- In regulations, 5 years are required, but hospitals usually tend to keep more than 10, at most 20 years.
		- Does hospital generally have dedicated server for medical image?	- Yes, especially large scale establishments.
		- Could hospital compress medical images for straging?	- Yes, and a trend is seen in that older data has been more frequently compressed.
		- What kinds of data format does hospital control except for DICOM?	- Jpeg format is also managed by hospital because many endoscope could only output jpeg data.
		2.1.2 Regulation for archiving medical images in cloud environment.	2.1.2 Regulation for archiving medical images in cloud environment.
		- Is it required for deleting personal information from medical images?	- From the regal aspect, no it isn't, but hospitals usually require to delete DICOM tag data.
		- What level of service availability is expected?	- 24 hours a day, 365 days a year support is ideal, but could accept a little halt for mentenace.
		2.1.3 Requirement for sharing medical images between healthcare establishments.	2.1.3 Requirement for sharing medical images between healthcare establishments.
		- Are contract required between healthcare establishments?	- Yes, and usually exchange a pledge.
		- Does hospital specially manage other establishment's medical images?	- Yes, usually data from other establishment is stored in different table.
		2.1.4 How to deal with diagnosis result	2.1.4 How to deal with diagnosis result
		- Can diagnosis result be shared in public if patients would not be identified?	- Yes, but original documments could not be output easily.
		2.1.5 Permission level to access internal sytem.	2.1.6 Permission level to access internal sytem.
		- What kinds of permission level to access internal systems avirable?	- Administrators only access the internal system. Even doctor can't access directly without permission.
		2.1.6 Is there private room to manage internal server?	2.1.7 Yes, and many hospitals apply physical security countermeasure.
	2.2 Normal Diagnostic Flow	2.2.1 Actor to access DICOM server.	2.2.1 Actor to access DICOM server.
		- Can medical doctor get DICOM data by him/herself?	- No, he/she can view the DICOM data in approved device.
		2.2.2 How long does it take to view DICOM data in medical doctor's screen?	2.2.2 5 seconds seems upper limit in general.
		2.2.3 Has a doctor ever re-write DICOM data? And When?	2.2.3 Yes, but it is quiet rare. If it write wrong data into DICOM, doctor asked an administrator to correct.
		2.2.4 How do you control the clinical report?	2.2.4 Clinical report is written in PACS reprot server by ragiologists not medical doctor. Doctor can only see it.
		2.2.5 Does a doctor deal with the DICOM datta after diagnosis?	2.2.5 No, doctor only view DICOM data, he/she could not complile.
	2.3 Others	2.3.1 Is there regulational issue except for personal information and privacy?	2.3.1 If the sysytem divide the meidical data, data integrity must be assured.
		2.3.2 How do we improve systems with AI technology?	2.3.2 At present, if sysmte is improved by AI technology, this system must be sold by different type of product.

4 CONCLUSION

Some concluding remarks are given in this chapter. A rapid increase in government healthcare expenditure has been seen globally, and one of the main factors for this increase is considered the significant progresses made in health technologies. In particular, radiology is now being threatened by its own success. A promising key technology to resolve this threat is a computerized analysis of medical images, known as computer-aided detection/diagnosis (CAD). Using CAD, doctors can use computer support as a "second opinion" and make a final decision more quickly and with greater confidence. Research related to an improvement in the cost-effectiveness of CAD was conducted in this study, and will eventually contribute to resolving some aspects of rising healthcare costs.

In Chapter 1, a bibliometric analysis using a citation network for a systematic review of CAD research was conducted, and the challenges related to this technology were explored. It was determined that non-standardization and an insufficiency of datasets applied to CAD development are significant challenges. Furthermore, it was concluded that medical image sharing may resolve these challenges.

In Chapter 2, based on a cost-effectiveness analysis, it was confirmed that medical image sharing can have an effect on societal efficacy, effectiveness, and cost-effectiveness. Three models related to a CAD system diagnosis were developed: breast cancer (BC), colorectal cancer (CRC), and Alzheimer's disease (AD) models. Although the cost-effectiveness of AD CAD could not be improved in a base case analysis, that of BC and CRC CAD could be drastically improved. However, if medical doctors give priority to image diagnosis results, the cost-effectiveness of AD CAD can also be improved. Overall, it can be concluded that the sharing of medical image data is valuable for our society from a CAD diagnostic perspective.

In Chapter 3, a methodology promoting the sharing of medical images was proposed. Although medical image sharing has a positive effect, with the exception of CAD performance improvements such as healthcare quality improvements and a reduction of redundancy, such sharing has not widely spread owing to security, privacy, and scalability issues. Medical images can be shared through various means, and cloud computing currently seems to be quite promising owing to its scalability. However, this technology has certain challenges regarding security, such as integrity, confidentiality, accountability, and availability, and medical images containing certain types of personal information as metadata. Therefore, the diffusion of cloud computing for the sharing of medical images is limited. A method applying blockchain technology to a cloud-based environment for the secure sharing of medical images was developed in this study. The

feasibility of this technology was confirmed through a test implementation and stake-holder meeting. Furthermore, how to implement the proposed system was discussed in detail. In general, there is a large gap between technology and business, and a number of steps are required. One necessary step is to design and construct an overall picture of the system. First, the functional and non-functional requirements depending on the stake-holder meeting were determined. Next, a system architecture overview according to both requirements was constructed. Although this method and architecture have some technical, business usage, regulation, and competitor challenges, the plot has certain ramifications for patients, doctors, system developers, and hospital management. However, future work includes expanding the system to control clinical reports, and electronic health records. Such research can make medical imaging more valuable, and improve the system development. A second area of improvement is to share insensitive health information with the public. Both types of data control can be implemented using three-layer management: a private blockchain layer, a cloud archive layer, and a public blockchain layer. Furthermore, applying medical image data to surgical planning may also be a promising future research direction. It is necessary for surgical planning to obtain more detailed image data for an image diagnosis. Therefore, certain types of data, not from medical images, but rather from electrocorticography or non-medical images, can improve the limitation of medical imaging. The present and future research can improve the cost-effectiveness and contribute to decreasing healthcare costs.

REFERENCES

[1] J. L. Dieleman *et al.*, "National spending on health by source for 184 countries between 2013 and 2040," *The Lancet*, vol. 387, no. 10037, pp. 2521–2535, Jun. 2016.

[2] OECD, "OECD Health Data 2015," *OECD Library*. [Online]. Available: http://www.oecd.org/els/health-systems/health-data.htm. [Accessed: 18-Sep-2017].

[3] "Seven Factors Driving Up Your Health Care Costs," *PBS NewsHour*. [Online]. Available: http://www.pbs.org/newshour/rundown/seven-factors-driving-your-health-care-costs/. [Accessed: 15-Jul-2017].

[4] U. Chaikledkaew, P. Pongchareonsuk, N. Chaiyakunapruk, and B. Ongphiphadhanakul, "Factors affecting health-care costs and hospitalizations among diabetic patients in Thai public hospitals," *Value Health J. Int. Soc. Pharmacoeconomics Outcomes Res.*, vol. 11 Suppl 1, pp. S69-74, Mar. 2008.

[5] K. E. Thorpe, "The Rise In Health Care Spending And What To Do About It," *Health Aff. (Millwood)*, vol. 24, no. 6, pp. 1436–1445, Nov. 2005.

[6] R. Yao *et al.*, "Three-dimensional printing: review of application in medicine and hepatic surgery," *Cancer Biol. Med.*, vol. 13, no. 4, pp. 443–451, Dec. 2016.

[7] J. J. Cuaron, S. M. MacDonald, and O. Cahlon, "Novel applications of proton therapy in breast carcinoma," *Chin. Clin. Oncol.*, vol. 5, no. 4, p. 52, Aug. 2016.

[8] D. B. Johnson, C. Peng, and J. A. Sosman, "Nivolumab in melanoma: latest evidence and clinical potential," *Ther. Adv. Med. Oncol.*, vol. 7, no. 2, pp. 97–106, Mar. 2015.

[9] Jun Okamoto, Ken Masamune, Hiroshi Iseki, and Yoshihiro Muragaki, "Development of Next-generation operating room SCOT(Smart Cyber Operating Theater)," *MEDIX*, vol. 66, pp. 4–8, 2017.

[10] K. A. Miles, "Cancer imaging: is it cost-effective?," *Cancer Imaging*, vol. 4, no. 2, pp. 97–103, May 2004.

[11] I. of M. (US) C. on T. I. in Medicine, A. C. Gelijns, and E. A. Halm, *The Diffusion of New Technology: Costs and Benefits to Health Care*. National Academies Press (US), 1991.

[12] P. M. McMahon, S. S. Araki, E. A. Sandberg, P. J. Neumann, and G. S. Gazelle, "Cost-effectiveness of PET in the diagnosis of Alzheimer disease," *Radiology*, vol. 228, no. 2, pp. 515–522, Aug. 2003.

[13] B. van Ginneken, C. M. Schaefer-Prokop, and M. Prokop, "Computer-aided

Diagnosis: How to Move from the Laboratory to the Clinic," *Radiology*, vol. 261, no. 3, pp. 719–732, Dec. 2011.

[14] T. W. Freer and M. J. Ulissey, "Screening Mammography with Computer-aided Detection: Prospective Study of 12,860 Patients in a Community Breast Center," *Radiology*, vol. 220, no. 3, pp. 781–786, Sep. 2001.

[15] S. G. Armato, M. L. Giger, C. J. Moran, J. T. Blackburn, K. Doi, and H. MacMahon, "Computerized Detection of Pulmonary Nodules on CT Scans," *RadioGraphics*, vol. 19, no. 5, pp. 1303–1311, Sep. 1999.

[16] C.-M. Chen *et al.*, "Breast Lesions on Sonograms: Computer-aided Diagnosis with Nearly Setting-Independent Features and Artificial Neural Networks," *Radiology*, vol. 226, no. 2, pp. 504–514, Feb. 2003.

[17] R. A. Castellino, "Computer aided detection (CAD): an overview," *Cancer Imaging*, vol. 5, no. 1, pp. 17–19, Aug. 2005.

[18] Global Industry Analysis Inc, "COMPUTER-AIDED DETECTION (CAD)- A US AND EUROPEAN MARKET REPORT," *A World Business Strategy & Market Intelligence Source*. [Online]. Available: http://www.strategyr.com/pressMCP-6036.asp. [Accessed: 23-Sep-2017].

[19] K. Doi, "Computer-Aided Diagnosis in Medical Imaging: Historical Review, Current Status and Future Potential," *Comput. Med. Imaging Graph. Off. J. Comput. Med. Imaging Soc.*, vol. 31, no. 4–5, pp. 198–211, 2007.

[20] U. Bagci *et al.*, "Segmentation and Image Analysis of Abnormal Lungs at CT: Current Approaches, Challenges, and Future Trends," *RadioGraphics*, vol. 35, no. 4, pp. 1056–1076, Jul. 2015.

[21] H. D. Cheng, J. Shan, W. Ju, Y. Guo, and L. Zhang, "Automated breast cancer detection and classification using ultrasound images: A survey," *Pattern Recognit.*, vol. 43, no. 1, pp. 299–317, Jan. 2010.

[22] K. Korotkov and R. Garcia, "Computerized analysis of pigmented skin lesions: A review," *Artif. Intell. Med.*, vol. 56, no. 2, pp. 69–90, Oct. 2012.

[23] E. Helbren *et al.*, "The effect of computer-aided detection markers on visual search and reader performance during concurrent reading of CT colonography," *Eur. Radiol.*, vol. 25, no. 6, pp. 1570–1578, Jun. 2015.

[24] H. P. Chan *et al.*, "Improvement in radiologists' detection of clustered microcalcifications on mammograms. The potential of computer-aided diagnosis," *Invest. Radiol.*, vol. 25, no. 10, pp. 1102–1110, Oct. 1990.

[25] Y. Jiang, R. M. Nishikawa, R. A. Schmidt, C. E. Metz, M. L. Giger, and K. Doi, "Improving breast cancer diagnosis with computer-aided diagnosis," *Acad.*

Radiol., vol. 6, no. 1, pp. 22–33, Jan. 1999.

[26] L. J. Warren Burhenne *et al.*, "Potential contribution of computer-aided detection to the sensitivity of screening mammography," *Radiology*, vol. 215, no. 2, pp. 554–562, May 2000.

[27] H. P. Chan *et al.*, "Improvement of radiologists' characterization of mammographic masses by using computer-aided diagnosis: an ROC study," *Radiology*, vol. 212, no. 3, pp. 817–827, Sep. 1999.

[28] W. P. Kegelmeyer, J. M. Pruneda, P. D. Bourland, A. Hillis, M. W. Riggs, and M. L. Nipper, "Computer-aided mammographic screening for spiculated lesions," *Radiology*, vol. 191, no. 2, pp. 331–337, May 1994.

[29] Y. Wu, M. L. Giger, K. Doi, C. J. Vyborny, R. A. Schmidt, and C. E. Metz, "Artificial neural networks in mammography: application to decision making in the diagnosis of breast cancer," *Radiology*, vol. 187, no. 1, pp. 81–87, Apr. 1993.

[30] Y. Jiang *et al.*, "Malignant and benign clustered microcalcifications: automated feature analysis and classification," *Radiology*, vol. 198, no. 3, pp. 671–678, Mar. 1996.

[31] N. Arikidis, K. Vassiou, A. Kazantzi, S. Skiadopoulos, A. Karahaliou, and L. Costaridou, "A two-stage method for microcalcification cluster segmentation in mammography by deformable models," *Med. Phys.*, vol. 42, no. 10, pp. 5848–5861, Oct. 2015.

[32] X. Liu and Z. Zeng, "A new automatic mass detection method for breast cancer with false positive reduction," *Neurocomputing*, vol. 152, pp. 388–402, Mar. 2015.

[33] J. Dheeba and N. A. Singh, "Computer Aided Intelligent Breast Cancer Detection: Second Opinion for Radiologists—A Prospective Study," *ResearchGate*, vol. 575, pp. 397–430, Jan. 2015.

[34] S. Sharma and P. Khanna, "Computer-aided diagnosis of malignant mammograms using Zernike moments and SVM," *J. Digit. Imaging*, vol. 28, no. 1, pp. 77–90, Feb. 2015.

[35] B. Liu, "Application of artificial neural networks in computer-aided diagnosis," *Methods Mol. Biol. Clifton NJ*, vol. 1260, pp. 195–204, 2015.

[36] C. D. Lehman, R. D. Wellman, D. S. M. Buist, K. Kerlikowske, A. N. A. Tosteson, and D. L. Miglioretti, "Diagnostic Accuracy of Digital Screening Mammography With and Without Computer-Aided Detection," *JAMA Intern. Med.*, vol. 175, no. 11, pp. 1828–1837, Nov. 2015.

[37] F. Pak, H. R. Kanan, and A. Alikhassi, "Breast cancer detection and classification

in digital mammography based on Non-Subsampled Contourlet Transform (NSCT) and Super Resolution," *Comput. Methods Programs Biomed.*, vol. 122, no. 2, pp. 89–107, Nov. 2015.

[38] X. Liu, M. Mei, J. Liu, and W. Hu, "Microcalcification detection in full-field digital mammograms with PFCM clustering and weighted SVM-based method," *EURASIP J. Adv. Signal Process.*, vol. 2015, no. 1, p. 73, Dec. 2015.

[39] J. Celaya-Padilla *et al.*, "Bilateral Image Subtraction and Multivariate Models for the Automated Triaging of Screening Mammograms," *BioMed Res. Int.*, vol. 2015, p. e231656, Jul. 2015.

[40] M. Elter and A. Horsch, "CADx of mammographic masses and clustered microcalcifications: A review," *Med. Phys.*, vol. 36, no. 6, pp. 2052–2068, Jun. 2009.

[41] M. L. Giger, H.-P. Chan, and J. Boone, "Anniversary Paper: History and status of CAD and quantitative image analysis: The role of Medical Physics and AAPM," *Med. Phys.*, vol. 35, no. 12, pp. 5799–5820, Dec. 2008.

[42] R. Nithya and B. Santhi, "Computer Aided Diagnosis System for Mammogram Analysis: A Survey," *J. Med. Imaging Health Inform.*, vol. 5, no. 4, pp. 653–674, Aug. 2015.

[43] W. Jorritsma, F. Cnossen, and P. M. A. van Ooijen, "Improving the radiologist–CAD interaction: designing for appropriate trust," *Clin. Radiol.*, vol. 70, no. 2, pp. 115–122, Feb. 2015.

[44] Y. Lee, T. Hara, H. Fujita, S. Itoh, and T. Ishigaki, "Automated detection of pulmonary nodules in helical CT images based on an improved template-matching technique," *IEEE Trans. Med. Imaging*, vol. 20, no. 7, pp. 595–604, Jul. 2001.

[45] M. L. Giger, K. T. Bae, and H. MacMahon, "Computerized detection of pulmonary nodules in computed tomography images," *Invest. Radiol.*, vol. 29, no. 4, pp. 459–465, Apr. 1994.

[46] K. Kanazawa *et al.*, "Computer-aided diagnosis for pulmonary nodules based on helical CT images," *Comput. Med. Imaging Graph.*, vol. 22, no. 2, pp. 157–167, Mar. 1998.

[47] M. N. Gurcan *et al.*, "Lung nodule detection on thoracic computed tomography images: preliminary evaluation of a computer-aided diagnosis system," *Med. Phys.*, vol. 29, no. 11, pp. 2552–2558, Nov. 2002.

[48] M. L. Giger, K. Doi, and H. MacMahon, "Image feature analysis and computer-aided diagnosis in digital radiography. 3. Automated detection of

nodules in peripheral lung fields," *Med. Phys.*, vol. 15, no. 2, pp. 158–166, Apr. 1988.

[49] S. G. Armato, M. L. Giger, and H. MacMahon, "Automated detection of lung nodules in CT scans: preliminary results," *Med. Phys.*, vol. 28, no. 8, pp. 1552–1561, Aug. 2001.

[50] T. Kobayashi, X. W. Xu, H. MacMahon, C. E. Metz, and K. Doi, "Effect of a computer-aided diagnosis scheme on radiologists' performance in detection of lung nodules on radiographs," *Radiology*, vol. 199, no. 3, pp. 843–848, Jun. 1996.

[51] K. Awai *et al.*, "Pulmonary nodules at chest CT: effect of computer-aided diagnosis on radiologists' detection performance," *Radiology*, vol. 230, no. 2, pp. 347–352, Feb. 2004.

[52] G. D. Rubin, "Lung nodule and cancer detection in computed tomography screening," *J. Thorac. Imaging*, vol. 30, no. 2, pp. 130–138, Mar. 2015.

[53] E. Taşcı and A. Uğur, "Shape and Texture Based Novel Features for Automated Juxtapleural Nodule Detection in Lung CTs," *J. Med. Syst.*, vol. 39, no. 5, p. 46, May 2015.

[54] B. J. Bartholmai *et al.*, "Pulmonary nodule characterization, including computer analysis and quantitative features," *J. Thorac. Imaging*, vol. 30, no. 2, pp. 139–156, Mar. 2015.

[55] N. Duggan *et al.*, "A Technique for Lung Nodule Candidate Detection in CT Using Global Minimization Methods," *ResearchGate*, pp. 478–491, Jan. 2015.

[56] B. Wang *et al.*, "Pulmonary nodule detection in CT images based on shape constraint CV model," *Med. Phys.*, vol. 42, no. 3, pp. 1241–1254, Mar. 2015.

[57] H. Han, L. Li, F. Han, B. Song, W. Moore, and Z. Liang, "Fast and Adaptive Detection of Pulmonary Nodules in Thoracic CT Images Using a Hierarchical Vector Quantization Scheme," *IEEE J. Biomed. Health Inform.*, vol. 19, no. 2, pp. 648–659, Mar. 2015.

[58] S. Shen, A. A. T. Bui, J. Cong, and W. Hsu, "An automated lung segmentation approach using bidirectional chain codes to improve nodule detection accuracy," *Comput. Biol. Med.*, vol. 57, pp. 139–149, Feb. 2015.

[59] E.-F. Kao, G.-C. Liu, L.-Y. Lee, H.-Y. Tsai, and T.-S. Jaw, "Computer-aided detection system for chest radiography: reducing report turnaround times of examinations with abnormalities," *Acta Radiol. Stockh. Swed. 1987*, vol. 56, no. 6, pp. 696–701, Jun. 2015.

[60] K. M. Prabusankarlal, P. Thirumoorthy, and R. Manavalan, "Computer Aided Breast Cancer Diagnosis Techniques in Ultrasound: A Survey," *J. Med. Imaging*

Health Inform., vol. 4, no. 3, pp. 331–349, Jun. 2014.

[61] D. R. Chen, R. F. Chang, and Y. L. Huang, "Computer-aided diagnosis applied to US of solid breast nodules by using neural networks," *Radiology*, vol. 213, no. 2, pp. 407–412, Nov. 1999.

[62] D.-R. Chen, R.-F. Chang, W.-J. Kuo, M.-C. Chen, and Y. u-Len Huang, "Diagnosis of breast tumors with sonographic texture analysis using wavelet transform and neural networks," *Ultrasound Med. Biol.*, vol. 28, no. 10, pp. 1301–1310, Oct. 2002.

[63] S. Joo, Y. S. Yang, W. K. Moon, and H. C. Kim, "Computer-aided diagnosis of solid breast nodules: use of an artificial neural network based on multiple sonographic features," *IEEE Trans. Med. Imaging*, vol. 23, no. 10, pp. 1292–1300, Oct. 2004.

[64] R.-F. Chang, W.-J. Wu, W. K. Moon, and D.-R. Chen, "Automatic ultrasound segmentation and morphology based diagnosis of solid breast tumors," *Breast Cancer Res. Treat.*, vol. 89, no. 2, pp. 179–185, Jan. 2005.

[65] K. Drukker, M. L. Giger, K. Horsch, M. A. Kupinski, C. J. Vyborny, and E. B. Mendelson, "Computerized lesion detection on breast ultrasound," *Med. Phys.*, vol. 29, no. 7, pp. 1438–1446, Jul. 2002.

[66] L. A. Meinel, A. H. Stolpen, K. S. Berbaum, L. L. Fajardo, and J. M. Reinhardt, "Breast MRI lesion classification: improved performance of human readers with a backpropagation neural network computer-aided diagnosis (CAD) system," *J. Magn. Reson. Imaging JMRI*, vol. 25, no. 1, pp. 89–95, Jan. 2007.

[67] W. Chen, M. L. Giger, L. Lan, and U. Bick, "Computerized interpretation of breast MRI: investigation of enhancement-variance dynamics," *Med. Phys.*, vol. 31, no. 5, pp. 1076–1082, May 2004.

[68] W. Gómez Flores, W. C. de A. Pereira, and A. F. C. Infantosi, "Improving classification performance of breast lesions on ultrasonography," *Pattern Recognit.*, vol. 48, no. 4, pp. 1125–1136, Apr. 2015.

[69] W. K. Moon *et al.*, "Computer-aided diagnosis for distinguishing between triple-negative breast cancer and fibroadenomas based on ultrasound texture features," *Med. Phys.*, vol. 42, no. 6, pp. 3024–3035, Jun. 2015.

[70] N. Uniyal *et al.*, "Ultrasound RF time series for classification of breast lesions," *IEEE Trans. Med. Imaging*, vol. 34, no. 2, pp. 652–661, Feb. 2015.

[71] A. Shimauchi *et al.*, "Evaluation of Kinetic Entropy of Breast Masses Initially Found on MRI using Whole-lesion Curve Distribution Data: Comparison with the Standard Kinetic Analysis," *Eur. Radiol.*, vol. 25, no. 8, pp. 2470–2478, Aug.

2015.

[72] R. Rodrigues, R. Braz, M. Pereira, J. Moutinho, and A. M. G. Pinheiro, “A Two-Step Segmentation Method for Breast Ultrasound Masses Based on Multi-resolution Analysis,” *Ultrasound Med. Biol.*, vol. 41, no. 6, pp. 1737–1748, Jun. 2015.

[73] L. Cai, X. Wang, Y. Wang, Y. Guo, J. Yu, and Y. Wang, “Robust phase-based texture descriptor for classification of breast ultrasound images,” *Biomed. Eng. OnLine*, vol. 14, p. 26, 2015.

[74] A. Gubern-Mérida *et al.*, “Automated localization of breast cancer in DCE-MRI,” *Med. Image Anal.*, vol. 20, no. 1, pp. 265–274, Feb. 2015.

[75] C.-M. Lo, W. K. Moon, C.-S. Huang, J.-H. Chen, M.-C. Yang, and R.-F. Chang, “Intensity-Invariant Texture Analysis for Classification of BI-RADS Category 3 Breast Masses,” *Ultrasound Med. Biol.*, vol. 41, no. 7, pp. 2039–2048, Jul. 2015.

[76] J. Wang *et al.*, “Identifying Triple-Negative Breast Cancer Using Background Parenchymal Enhancement Heterogeneity on Dynamic Contrast-Enhanced MRI: A Pilot Radiomics Study,” *PloS One*, vol. 10, no. 11, p. e0143308, 2015.

[77] M. Xian, Y. Zhang, and H. D. Cheng, “Fully automatic segmentation of breast ultrasound images based on breast characteristics in space and frequency domains,” *Pattern Recognit.*, vol. 48, no. 2, pp. 485–497, Feb. 2015.

[78] Y. Peng *et al.*, “Quantitative analysis of multiparametric prostate MR images: differentiation between prostate cancer and normal tissue and correlation with Gleason score--a computer-aided diagnosis development study,” *Radiology*, vol. 267, no. 3, pp. 787–796, Jun. 2013.

[79] A. Tabesh *et al.*, “Multifeature prostate cancer diagnosis and Gleason grading of histological images,” *IEEE Trans. Med. Imaging*, vol. 26, no. 10, pp. 1366–1378, Oct. 2007.

[80] C. M. A. Hoeks *et al.*, “Prostate cancer: multiparametric MR imaging for detection, localization, and staging,” *Radiology*, vol. 261, no. 1, pp. 46–66, Oct. 2011.

[81] P. C. Vos, T. Hambrock, C. A. Hulsbergen-van de Kaa, J. J. Fütterer, J. O. Barentsz, and H. J. Huisman, “Computerized analysis of prostate lesions in the peripheral zone using dynamic contrast enhanced MRI,” *Med. Phys.*, vol. 35, no. 3, pp. 888–899, Mar. 2008.

[82] P. C. Vos, T. Hambrock, J. O. Barenstz, and H. J. Huisman, “Computer-assisted analysis of peripheral zone prostate lesions using T2-weighted and dynamic contrast enhanced T1-weighted MRI,” *Phys. Med. Biol.*, vol. 55, no. 6, pp. 1719–

1734, Mar. 2010.

[83] T. Hambrock, P. C. Vos, C. A. Hulsbergen-van de Kaa, J. O. Barentsz, and H. J. Huisman, “Prostate cancer: computer-aided diagnosis with multiparametric 3-T MR imaging--effect on observer performance,” *Radiology*, vol. 266, no. 2, pp. 521–530, Feb. 2013.

[84] E. Niaf, O. Rouvière, F. Mège-Lechevallier, F. Bratan, and C. Lartizien, “Computer-aided diagnosis of prostate cancer in the peripheral zone using multiparametric MRI,” *Phys. Med. Biol.*, vol. 57, no. 12, pp. 3833–3851, Jun. 2012.

[85] U. Scheipers, H. Ermert, H.-J. Sommerfeld, M. Garcia-Schürmann, T. Senge, and S. Philippou, “Ultrasonic multifeature tissue characterization for prostate diagnostics,” *Ultrasound Med. Biol.*, vol. 29, no. 8, pp. 1137–1149, Aug. 2003.

[86] W. K. Moon, S.-C. Chang, C.-S. Huang, and R.-F. Chang, “Breast tumor classification using fuzzy clustering for breast elastography,” *Ultrasound Med. Biol.*, vol. 37, no. 5, pp. 700–708, May 2011.

[87] P.-W. Huang and C.-H. Lee, “Automatic classification for pathological prostate images based on fractal analysis,” *IEEE Trans. Med. Imaging*, vol. 28, no. 7, pp. 1037–1050, Jul. 2009.

[88] M. E. Celebi, G. Schaefer, H. Iyatomi, and W. V. Stoecker, “Lesion Border Detection in Dermoscopy Images,” *Comput. Med. Imaging Graph. Off. J. Comput. Med. Imaging Soc.*, vol. 33, no. 2, pp. 148–153, Mar. 2009.

[89] H. Iyatomi *et al.*, “An improved Internet-based melanoma screening system with dermatologist-like tumor area extraction algorithm,” *Comput. Med. Imaging Graph. Off. J. Comput. Med. Imaging Soc.*, vol. 32, no. 7, pp. 566–579, Oct. 2008.

[90] H. Müller, N. Michoux, D. Bandon, and A. Geissbuhler, “A review of content-based image retrieval systems in medical applications-clinical benefits and future directions,” *Int. J. Med. Inf.*, vol. 73, no. 1, pp. 1–23, Feb. 2004.

[91] P. Schmid-Saugeona, J. Guillodb, and J.-P. Thirana, “Towards a computer-aided diagnosis system for pigmented skin lesions,” *Comput. Med. Imaging Graph. Off. J. Comput. Med. Imaging Soc.*, vol. 27, no. 1, pp. 65–78, 2003.

[92] M. E. Celebi *et al.*, “Border detection in dermoscopy images using statistical region merging,” *Skin Res. Technol. Off. J. Int. Soc. Bioeng. Skin ISBS Int. Soc. Digit. Imaging Skin ISDIS Int. Soc. Skin Imaging ISSI*, vol. 14, no. 3, pp. 347–353, Aug. 2008.

[93] M. Burroni *et al.*, “Melanoma computer-aided diagnosis: reliability and

feasibility study," *Clin. Cancer Res. Off. J. Am. Assoc. Cancer Res.*, vol. 10, no. 6, pp. 1881–1886, Mar. 2004.

[94] M. Emre Celebi, Y. Alp Aslandogan, W. V. Stoecker, H. Iyatomi, H. Oka, and X. Chen, "Unsupervised border detection in dermoscopy images," *Skin Res. Technol. Off. J. Int. Soc. Bioeng. Skin ISBS Int. Soc. Digit. Imaging Skin ISDIS Int. Soc. Skin Imaging ISSI*, vol. 13, no. 4, pp. 454–462, Nov. 2007.

[95] M. Niemeijer, B. van Ginneken, J. Staal, M. S. A. Suttorp-Schulten, and M. D. Abràmoff, "Automatic detection of red lesions in digital color fundus photographs," *IEEE Trans. Med. Imaging*, vol. 24, no. 5, pp. 584–592, May 2005.

[96] K. Hoffmann *et al.*, "Diagnostic and neural analysis of skin cancer (DANAOS). A multicentre study for collection and computer-aided analysis of data from pigmented skin lesions using digital dermoscopy," *Br. J. Dermatol.*, vol. 149, no. 4, pp. 801–809, Oct. 2003.

[97] W.-Y. Chang *et al.*, "The feasibility of using manual segmentation in a multifeature computer-aided diagnosis system for classification of skin lesions: a retrospective comparative study," *BMJ Open*, vol. 5, no. 4, p. e007823, May 2015.

[98] K. Møllersen, H. Kirchesch, M. Zortea, T. R. Schopf, K. Hindberg, and F. Godtliebsen, "Computer-Aided Decision Support for Melanoma Detection Applied on Melanocytic and Nonmelanocytic Skin Lesions: A Comparison of Two Systems Based on Automatic Analysis of Dermoscopic Images," *BioMed Res. Int.*, vol. 2015, p. 579282, 2015.

[99] K. Shimizu, H. Iyatomi, M. E. Celebi, K.-A. Norton, and M. Tanaka, "Four-class classification of skin lesions with task decomposition strategy," *IEEE Trans. Biomed. Eng.*, vol. 62, no. 1, pp. 274–283, Jan. 2015.

[100] K. H. Ng, O. Faust, V. Sudarshan, and S. Chattopadhyay, "Data Overloading in Medical Imaging: Emerging Issues, Challenges and Opportunities in Efficient Data Management," *ResearchGate*, vol. 5, no. 4, Aug. 2015.

[101] M. R. K. Mookiah, J. H. Tan, C. K. Chua, E. Y. K. Ng, A. Laude, and L. Tong, "Automated characterization and detection of diabetic retinopathy using texture measures," *J. Mech. Med. Biol.*, vol. 15, no. 04, p. 1550045, Jan. 2015.

[102] L. Guo, J.-J. Yang, L. Peng, J. Li, and Q. Liang, "A computer-aided healthcare system for cataract classification and grading based on fundus image analysis," *Comput. Ind.*, vol. 69, pp. 72–80, May 2015.

[103] M. R. K. Mookiah *et al.*, "Application of different imaging modalities for diagnosis of Diabetic Macular Edema: A review," *Comput. Biol. Med.*, vol. 66, pp.

295–315, Nov. 2015.

[104] T. K. Lee, S. Khakabi, P. Wighton, H. Lui, D. I. McLean, and M. S. Atkins, *Tree Structure for Modeling Skin Lesion Growth*. 2014.

[105] F. Oloumi, R. M. Rangayyan, P. Casti, and A. L. Ells, "Computer-aided diagnosis of plus disease via measurement of vessel thickness in retinal fundus images of preterm infants," *Comput. Biol. Med.*, vol. 66, pp. 316–329, Nov. 2015.

[106] K. S. Vidya, E. Y. K. Ng, U. R. Acharya, S. M. Chou, R. S. Tan, and D. N. Ghista, "Computer-aided diagnosis of Myocardial Infarction using ultrasound images with DWT, GLCM and HOS methods: A comparative study," *Comput. Biol. Med.*, vol. 62, pp. 86–93, Jul. 2015.

[107] K. Korotkov and R. Garcia, "Computerized analysis of pigmented skin lesions: A review," *Artif. Intell. Med.*, vol. 56, no. 2, pp. 69–90, Oct. 2012.

[108] H. Yoshida and J. Näppi, "Three-dimensional computer-aided diagnosis scheme for detection of colonic polyps," *IEEE Trans. Med. Imaging*, vol. 20, no. 12, pp. 1261–1274, Dec. 2001.

[109] G. Kiss, J. Van Cleynenbreugel, M. Thomeer, P. Suetens, and G. Marchal, "Computer-aided diagnosis in virtual colonography via combination of surface normal and sphere fitting methods," *Eur. Radiol.*, vol. 12, no. 1, pp. 77–81, Jan. 2002.

[110] H. Yoshida, Y. Masutani, P. MacEneaney, D. T. Rubin, and A. H. Dachman, "Computerized detection of colonic polyps at CT colonography on the basis of volumetric features: pilot study," *Radiology*, vol. 222, no. 2, pp. 327–336, Feb. 2002.

[111] R. M. Summers *et al.*, "Computed tomographic virtual colonoscopy computer-aided polyp detection in a screening population," *Gastroenterology*, vol. 129, no. 6, pp. 1832–1844, Dec. 2005.

[112] S. B. Göktürk *et al.*, "A statistical 3-D pattern processing method for computer-aided detection of polyps in CT colonography," *IEEE Trans. Med. Imaging*, vol. 20, no. 12, pp. 1251–1260, Dec. 2001.

[113] H. Yoshida and A. H. Dachman, "CAD techniques, challenges, and controversies in computed tomographic colonography," *Abdom. Imaging*, vol. 30, no. 1, pp. 26–41, Feb. 2005.

[114] H. Yoshida, J. Näppi, P. MacEneaney, D. T. Rubin, and A. H. Dachman, "Computer-aided diagnosis scheme for detection of polyps at CT colonography," *Radiogr. Rev. Publ. Radiol. Soc. N. Am. Inc*, vol. 22, no. 4, pp. 963–979, Aug. 2002.

[115] R. M. Summers, A. K. Jerebko, M. Franaszek, J. D. Malley, and C. D. Johnson, “Colonic polyps: complementary role of computer-aided detection in CT colonography,” *Radiology*, vol. 225, no. 2, pp. 391–399, Nov. 2002.

[116] H. Yoshida and J. Näppi, “CAD in CT colonography without and with oral contrast agents: progress and challenges,” *Comput. Med. Imaging Graph. Off. J. Comput. Med. Imaging Soc.*, vol. 31, no. 4–5, pp. 267–284, Jul. 2007.

[117] Z. Wang *et al.*, “Reduction of false positives by internal features for polyp detection in CT-based virtual colonoscopy,” *Med. Phys.*, vol. 32, no. 12, pp. 3602–3616, Dec. 2005.

[118] Y. Motai, D. Ma, A. Docef, and H. Yoshida, “Smart Colonography for Distributed Medical Databases with Group Kernel Feature Analysis,” *ACM Trans Intell Syst Technol*, vol. 6, no. 4, p. 58:1–58:24, Jul. 2015.

[119] H. Wang *et al.*, “An adaptive paradigm for computer-aided detection of colonic polyps,” *Phys. Med. Biol.*, vol. 60, no. 18, pp. 7207–7228, Sep. 2015.

[120] C. Thilo *et al.*, “Computer-aided stenosis detection at coronary CT angiography: effect on performance of readers with different experience levels,” *Eur. Radiol.*, vol. 25, no. 3, pp. 694–702, Mar. 2015.

[121] R. A. Nasirudin *et al.*, “A comparison of material decomposition techniques for dual-energy CT colonography,” *Proc. SPIE-- Int. Soc. Opt. Eng.*, vol. 9412, Feb. 2015.

[122] J. Liu, S. Wang, M. G. Linguraru, J. Yao, and R. M. Summers, “Computer-aided detection of exophytic renal lesions on non-contrast CT images,” *Med. Image Anal.*, vol. 19, no. 1, pp. 15–29, Jan. 2015.

[123] K. Suzuki *et al.*, “Development of Computer-Aided Diagnostic (CADx) System for Distinguishing Neoplastic from Nonneoplastic Lesions in CT Colonography (CTC): Toward CTC beyond Detection,” in *2015 IEEE International Conference on Systems, Man, and Cybernetics*, 2015, pp. 2262–2266.

[124] A. A. Plumb *et al.*, “Small Polyps at Endoluminal CT Colonography Are Often Seen But Ignored by Radiologists,” *AJR Am. J. Roentgenol.*, vol. 205, no. 4, pp. W424-431, Oct. 2015.

[125] M. Koizumi *et al.*, “Evaluation of a computer-assisted diagnosis system, BONENAVI version 2, for bone scintigraphy in cancer patients in a routine clinical setting,” *Ann. Nucl. Med.*, vol. 29, no. 2, pp. 138–148, Feb. 2015.

[126] E. S. Lee *et al.*, “Effect of different reconstruction algorithms on computer-aided diagnosis (CAD) performance in ultra-low dose CT colonography,” *Eur. J. Radiol.*, vol. 84, no. 4, pp. 547–554, Apr. 2015.

[127] R. Chaves *et al.*, “SVM-based computer-aided diagnosis of the Alzheimer’s disease using t-test NMSE feature selection with feature correlation weighting,” *Neurosci. Lett.*, vol. 461, no. 3, pp. 293–297, Sep. 2009.

[128] M. M. Lopez *et al.*, “SVM-based CAD system for early detection of the Alzheimer’s disease using kernel PCA and LDA,” *Neurosci. Lett.*, vol. 464, no. 3, pp. 233–238, Oct. 2009.

[129] P. Saxena, D. G. Pavel, J. Quintana, and B. Horwitz, “An automatic threshold-based seating method for enhancing the usefulness of Tc-HMPAO SPECT in the diagnosis of Alzheimer’s disease,” *Lect. Notes Comput. Sci.*, vol. 1496, pp. 623–630, Oct. 1998.

[130] M. López *et al.*, “Principal component analysis-based techniques and supervised classification schemes for the early detection of Alzheimer’s disease,” *Neurocomputing*, vol. 74, no. 8, pp. 1260–1271, Mar. 2011.

[131] I. A. Illán *et al.*, “18F-FDG PET Imaging Analysis for Computer Aided Alzheimer’s Diagnosis,” *Inf Sci*, vol. 181, no. 4, pp. 903–916, Feb. 2011.

[132] F. J. Martínez-Murcia, J. M. Górriz, J. Ramírez, C. G. Puntonet, and D. Salas-González, “Computer Aided Diagnosis tool for Alzheimer’s Disease based on Mann–Whitney–Wilcoxon U-Test,” *Expert Syst. Appl.*, vol. 39, no. 10, pp. 9676–9685, Aug. 2012.

[133] M. Graña *et al.*, “Computer aided diagnosis system for Alzheimer disease using brain diffusion tensor imaging features selected by Pearson’s correlation,” *Neurosci. Lett.*, vol. 502, no. 3, pp. 225–229, Sep. 2011.

[134] J. Ramírez *et al.*, “Computer aided diagnosis system for the Alzheimer’s disease based on partial least squares and random forest SPECT image classification,” *Neurosci. Lett.*, vol. 472, no. 2, pp. 99–103, Mar. 2010.

[135] F. Segovia *et al.*, “A comparative study of feature extraction methods for the diagnosis of Alzheimer’s disease using the ADNI database,” *Neurocomputing*, vol. 75, no. 1, pp. 64–71, Jan. 2012.

[136] I. A. Illán *et al.*, “Computer aided diagnosis of Alzheimer’s disease using component based SVM,” *Appl. Soft Comput.*, vol. 11, no. 2, pp. 2376–2382, Mar. 2011.

[137] Y. Zhang *et al.*, “Detection of subjects and brain regions related to Alzheimer’s disease using 3D MRI scans based on eigenbrain and machine learning,” *Front. Comput. Neurosci.*, vol. 9, p. 66, 2015.

[138] Y. Zhang and S. Wang, “Detection of Alzheimer’s disease by displacement field and machine learning,” *PeerJ*, vol. 3, p. e1251, 2015.

[139] Y. Zhang, Z. Dong, S. Wang, G. Ji, and J. Yang, “Preclinical Diagnosis of Magnetic Resonance (MR) Brain Images via Discrete Wavelet Packet Transform with Tsallis Entropy and Generalized Eigenvalue Proximal Support Vector Machine (GEPSVM),” *Entropy*, vol. 17, no. 4, pp. 1795–1813, Mar. 2015.

[140] S. Wang *et al.*, “Pathological Brain Detection by a Novel Image Feature—Fractional Fourier Entropy,” *Entropy*, vol. 17, no. 12, pp. 8278–8296, Dec. 2015.

[141] L. Khedher, J. Ramírez, J. M. Górriz, A. Brahim, and F. Segovia, “Early diagnosis of Alzheimer′s disease based on partial least squares, principal component analysis and support vector machine using segmented MRI images,” *Neurocomputing*, vol. 151, Part 1, pp. 139–150, Mar. 2015.

[142] Y. Zhang, S. Wang, Z. Dong, P. Phillip, G. Ji, and J. Yang, “Pathological Brain Detection in Magnetic Resonance Imaging Scanning by Wavelet Entropy and Hybridization of Biogeography-Based Optimization and Particle Swarm Optimization,” *ResearchGate*, vol. 152, pp. 41–58, Jan. 2015.

[143] Y.-D. Zhang, S. Chen, S.-H. Wang, J.-F. Yang, and P. Phillips, “Magnetic resonance brain image classification based on weighted-type fractional Fourier transform and nonparallel support vector machine,” *ResearchGate*, vol. 25, no. 4, pp. 317–327, Dec. 2015.

[144] L. Khedher, J. Ramírez, J. M. Górriz, A. Brahim, and I. A. Illán, “Independent Component Analysis-Based Classification of Alzheimer’s Disease from Segmented MRI Data,” in *Artificial Computation in Biology and Medicine*, J. M. F. Vicente, J. R. Álvarez-Sánchez, F. de la P. López, F. J. Toledo-Moreo, and H. Adeli, Eds. Springer International Publishing, 2015, pp. 78–87.

[145] A. Brahim, J. M. Górriz, J. Ramírez, and L. Khedher, “Intensity normalization of DaTSCAN SPECT imaging using a model-based clustering approach,” *Appl. Soft Comput.*, vol. 37, pp. 234–244, Dec. 2015.

[146] I. Beheshti, H. Demirel, and Alzheimer’s Disease Neuroimaging Initiative, “Probability distribution function-based classification of structural MRI for the detection of Alzheimer’s disease,” *Comput. Biol. Med.*, vol. 64, pp. 208–216, Sep. 2015.

[147] A. Berger, “Positron emission tomography,” *BMJ*, vol. 326, no. 7404, p. 1449, Jun. 2003.

[148] P. Coupé *et al.*, “Detection of Alzheimer’s disease signature in MR images seven years before conversion to dementia: Toward an early individual prognosis,” *Hum. Brain Mapp.*, vol. 36, no. 12, pp. 4758–4770, Dec. 2015.

[149] M. L. Giger, N. Karssemeijer, and S. G. Armato, “Guest editorial computer-aided diagnosis in medical imaging,” *IEEE Trans. Med. Imaging*, vol. 20, no. 12, pp. 1205–1208, Dec. 2001.

[150] M. S. Kavitha, A. Asano, A. Taguchi, T. Kurita, and M. Sanada, “Diagnosis of osteoporosis from dental panoramic radiographs using the support vector machine method in a computer-aided system,” *BMC Med. Imaging*, vol. 12, p. 1, 2012.

[151] X. Qi, M. V. Sivak, G. Isenberg, J. E. Willis, and A. M. Rollins, “Computer-aided diagnosis of dysplasia in Barrett’s esophagus using endoscopic optical coherence tomography,” *J. Biomed. Opt.*, vol. 11, no. 4, p. 044010, Aug. 2006.

[152] D.-T. Lin, C.-C. Lei, and S.-W. Hung, “Computer-aided kidney segmentation on abdominal CT images,” *IEEE Trans. Inf. Technol. Biomed. Publ. IEEE Eng. Med. Biol. Soc.*, vol. 10, no. 1, pp. 59–65, Jan. 2006.

[153] A. Z. Arifin *et al.*, “Computer-aided system for measuring the mandibular cortical width on dental panoramic radiographs in identifying postmenopausal women with low bone mineral density,” *Osteoporos. Int.*, vol. 17, no. 5, pp. 753–759, May 2006.

[154] S.-J. Lim, Y.-Y. Jeong, and Y.-S. Ho, “Automatic liver segmentation for volume measurement in CT Images,” *ResearchGate*, vol. 17, no. 4, pp. 860–875, Aug. 2006.

[155] T. Chan, “Computer aided detection of small acute intracranial hemorrhage on computer tomography of brain,” *Comput. Med. Imaging Graph. Off. J. Comput. Med. Imaging Soc.*, vol. 31, no. 4–5, pp. 285–298, Jul. 2007.

[156] Y. Chen *et al.*, “Effects of axial resolution improvement on optical coherence tomography (OCT) imaging of gastrointestinal tissues,” *Opt. Express*, vol. 16, no. 4, pp. 2469–2485, Feb. 2008.

[157] S.-J. Lim, Y.-Y. Jeong, C.-W. Lee, and Y.-S. Ho, “Automatic segmentation of the liver in CT images using the watershed algorithm based on morphological filtering,” *ResearchGate*, May 2004.

[158] S. S. Kumar, R. S. Moni, and J. Rajeesh, “Automatic liver and lesion segmentation: a primary step in diagnosis of liver diseases,” *Signal Image Video Process.*, vol. 7, no. 1, pp. 163–172, Jan. 2013.

[159] K. Horiba *et al.*, “Automated classification of mandibular cortical bone on dental panoramic radiographs for early detection of osteoporosis,” 2015, vol. 9414, p. 94142J–94142J–6.

[160] G. Sethi and B. S. Saini, “Abdomen disease diagnosis in CT images using

flexiscale curvelet transform and improved genetic algorithm," *Australas. Phys. Eng. Sci. Med.*, vol. 38, no. 4, pp. 671–688, Dec. 2015.

[161] J. K. Wrosch *et al.*, "Feasibility and Diagnostic Accuracy of Ischemic Stroke Territory Recognition Based on Two-Dimensional Projections of Three-Dimensional Diffusion MRI Data," *Front. Neurol.*, vol. 6, 2015.

[162] M. S. Kavitha *et al.*, "Texture analysis of mandibular cortical bone on digital dental panoramic radiographs for the diagnosis of osteoporosis in Korean women," *Oral Surg. Oral Med. Oral Pathol. Oral Radiol.*, vol. 119, no. 3, pp. 346–356, Mar. 2015.

[163] U. R. Acharya, O. Faust, F. Molinari, S. V. Sree, S. P. Junnarkar, and V. Sudarshan, "Ultrasound-based tissue characterization and classification of fatty liver disease: A screening and diagnostic paradigm," *Knowl.-Based Syst.*, vol. 75, pp. 66–77, Feb. 2015.

[164] J. Sun, L. Huang, H. Shuai, Y. Huang, H. Lu, and F. Gao, "Automatic Computer-Aided Diagnosis of Liver Disease Based on Multi-Cascade and Multi-Featured Classifier," *J. Med. Imaging Health Inform.*, vol. 5, no. 2, pp. 322–325, Apr. 2015.

[165] L. Bonanno, S. Marino, P. Bramanti, and F. Sottile, "Validation of a Computer-Aided Diagnosis System for the Automatic Identification of Carotid Atherosclerosis," *Ultrasound Med. Biol.*, vol. 41, no. 2, pp. 509–516, Feb. 2015.

[166] M. Hori *et al.*, "Quantitative Imaging: Quantification of Liver Shape on CT Using the Statistical Shape Model to Evaluate Hepatic Fibrosis," *Acad. Radiol.*, vol. 22, no. 3, pp. 303–309, Mar. 2015.

[167] "The top 10 leading causes of death in the US," *Medical News Today*. [Online]. Available: http://www.medicalnewstoday.com/articles/282929.php. [Accessed: 16-Jun-2016].

[168] S. Yamada, K. Komatsu, and T. Ema, "Computer-aided diagnosis system for medical use," US5235510 A, 10-Aug-1993.

[169] T. Ema and E. Nishihara, "Medical information processing system for supporting diagnosis," US5779634 A, 14-Jul-1998.

[170] K. Taguchi, S. Yamada, and T. Ema, "Medical information processing system for supporting diagnosis," US5807256 A, 15-Sep-1998.

[171] S. Levanon, R. Goldenberg, and M. Levy, "Method and system for automatic quality control used in computerized analysis of CT angiography," US7940970 B2, 10-May-2011.

[172] S. Levanon, R. Goldenberg, and M. Levy, "Method and system for automatic

quality control used in computerized analysis of ct angiography," US20080219530 A1, 11-Sep-2008.

[173] B. Zheng, X. Wang, D. Lederman, J. Tan, and D. Gur, "Computer-Aided Detection: The Effect of Training Databases on Detection of Subtle Breast Masses," *Acad. Radiol.*, vol. 17, no. 11, pp. 1401–1408, Nov. 2010.

[174] M.-M. Zhang, H. Yang, Z.-D. Jin, J.-G. Yu, Z.-Y. Cai, and Z.-S. Li, "Differential diagnosis of pancreatic cancer from normal tissue with digital imaging processing and pattern recognition based on a support vector machine of EUS images," *Gastrointest. Endosc.*, vol. 72, no. 5, pp. 978–985, Nov. 2010.

[175] M. Zhu *et al.*, "Differentiation of Pancreatic Cancer and Chronic Pancreatitis Using Computer-Aided Diagnosis of Endoscopic Ultrasound (EUS) Images: A Diagnostic Test," *PLOS ONE*, vol. 8, no. 5, p. e63820, May 2013.

[176] A. Das, C. C. Nguyen, F. Li, and B. Li, "Digital image analysis of EUS images accurately differentiates pancreatic cancer from chronic pancreatitis and normal tissue," *Gastrointest. Endosc.*, vol. 67, no. 6, pp. 861–867, May 2008.

[177] M. Ozkan *et al.*, "Age-based computer-aided diagnosis approach for pancreatic cancer on endoscopic ultrasound images," *Endosc. Ultrasound*, vol. 5, no. 2, pp. 101–107, 2016.

[178] C. Wu, M. H. Lin, and J. L. Su, "Computer-Aided Diagnosis System for Pancreatic Tumor Detection in Ultrasound Images," in *5th Kuala Lumpur International Conference on Biomedical Engineering 2011*, N. A. A. Osman, W. A. B. W. Abas, A. K. A. Wahab, and H.-N. Ting, Eds. Springer Berlin Heidelberg, 2011, pp. 627–630.

[179] T. Nakazawa *et al.*, "Difficulty in diagnosing autoimmune pancreatitis by imaging findings," *Gastrointest. Endosc.*, vol. 65, no. 1, pp. 99–108, Jan. 2007.

[180] T. Doel *et al.*, "GIFT-Cloud: A data sharing and collaboration platform for medical imaging research," *Comput. Methods Programs Biomed.*, vol. 139, pp. 181–190, Feb. 2017.

[181] C. S. White, T. Flukinger, J. Jeudy, and J. J. Chen, "Use of a computer-aided detection system to detect missed lung cancer at chest radiography," *Radiology*, vol. 252, no. 1, pp. 273–281, Jul. 2009.

[182] R. Llobet, J. C. Pérez-Cortés, A. H. Toselli, and A. Juan, "Computer-aided detection of prostate cancer," *Int. J. Med. Inf.*, vol. 76, no. 7, pp. 547–556, Jul. 2007.

[183] M. Li and Z. H. Zhou, "Improve Computer-Aided Diagnosis With Machine Learning Techniques Using Undiagnosed Samples," *IEEE Trans. Syst. Man*

Cybern. - Part Syst. Hum., vol. 37, no. 6, pp. 1088–1098, Nov. 2007.

[184] D. L. Hunt, R. B. Haynes, S. E. Hanna, and K. Smith, "Effects of computer-based clinical decision support systems on physician performance and patient outcomes: a systematic review," *JAMA*, vol. 280, no. 15, pp. 1339–1346, Oct. 1998.

[185] R. A. Miller, "Medical diagnostic decision support systems--past, present, and future: a threaded bibliography and brief commentary," *J. Am. Med. Inform. Assoc. JAMIA*, vol. 1, no. 1, pp. 8–27, Feb. 1994.

[186] B. Kaplan, "Evaluating informatics applications--clinical decision support systems literature review," *Int. J. Med. Inf.*, vol. 64, no. 1, pp. 15–37, Nov. 2001.

[187] J. Wyatt and D. Spiegelhalter, "Field trials of medical decision-aids: potential problems and solutions.," *Proc. Annu. Symp. Comput. Appl. Med. Care*, pp. 3–7, 1991.

[188] F. Velickovski *et al.*, "Clinical Decision Support Systems (CDSS) for preventive management of COPD patients," *J. Transl. Med.*, vol. 12, no. Suppl 2, p. S9, Nov. 2014.

[189] Y. Kajikawa, J. Yoshikawa, Y. Takeda, and K. Matsushima, "Tracking emerging technologies in energy research: Toward a roadmap for sustainable energy," *Technol. Forecast. Soc. Change*, vol. 75, no. 6, pp. 771–782, Jul. 2008.

[190] Naoki Shibata, Yuya Kajikawa, and Ichiro Sakata, "Detecting potential technological fronts by comparing scientific papers and patents," *Foresight*, vol. 13, no. 5, pp. 51–60, Aug. 2011.

[191] N. Shibata, Y. Kajikawa, and I. Sakata, "Measuring relatedness between communities in a citation network," *J. Am. Soc. Inf. Sci. Technol.*, vol. 62, no. 7, pp. 1360–1369, Jul. 2011.

[192] Y. Kajikawa and Y. Takeda, "Structure of research on biomass and bio-fuels: A citation-based approach," *Technol. Forecast. Soc. Change*, vol. 75, no. 9, pp. 1349–1359, Nov. 2008.

[193] N. Shibata, Y. Kajikawa, Y. Takeda, and K. Matsushima, "Comparative study on methods of detecting research fronts using different types of citation," *J. Am. Soc. Inf. Sci. Technol.*, vol. 60, no. 3, pp. 571–580, Mar. 2009.

[194]M. E. J. Newman, "Fast algorithm for detecting community structure in networks," *Phys. Rev. E*, vol. 69, no. 6, p. 066133, Jun. 2004.

[195] V. Ittipanuvat, K. Fujita, I. Sakata, and Y. Kajikawa, "Finding linkage between technology and social issue: A Literature Based Discovery approach," *J. Eng. Technol. Manag.*, vol. 32, pp. 160–184, Apr. 2014.

[196] A. T. Adai, S. V. Date, S. Wieland, and E. M. Marcotte, “LGL: creating a map of protein function with an algorithm for visualizing very large biological networks,” *J. Mol. Biol.*, vol. 340, no. 1, pp. 179–190, Jun. 2004.

[197] M. D. Gordon and S. Dumais, “Using latent semantic indexing for literature based discovery,” *J. Am. Soc. Inf. Sci.*, vol. 49, no. 8, pp. 674–685, Jan. 1998.

[198] B. Zheng, X. Wang, D. Lederman, J. Tan, and D. Gur, “Computer-Aided Detection: The Effect of Training Databases on Detection of Subtle Breast Masses,” *Acad. Radiol.*, vol. 17, no. 11, pp. 1401–1408, Nov. 2010.

[199] D. P. Kernick, “Introduction to health economics for the medical practitioner,” *Postgrad. Med. J.*, vol. 79, no. 929, pp. 147–150, Mar. 2003.

[200] J. S. Mandelblatt, D. G. Fryback, M. C. Weinstein, L. B. Russell, and M. R. Gold, “Assessing the effectiveness of health interventions for cost-effectiveness analysis,” *J. Gen. Intern. Med.*, vol. 12, no. 9, pp. 551–558, Sep. 1997.

[201] J. Beck and S. Pauker, “The Markov Process in Medical Prognosis,” *Med. Decis. Making*, vol. 3, no. 4, pp. 419–458, 1983.

[202] K. K. Lindfors, M. C. McGahan, C. J. Rosenquist, and G. S. Hurlock, “Computer-aided detection of breast cancer: A cost-effectiveness study (vol 239, pg 710, 2006),” *Radiology*, vol. 242, no. 1, pp. 320–320, Jan. 2007.

[203] C. Guerriero, M. G. Gillan, J. Cairns, M. G. Wallis, and F. J. Gilbert, “Is computer aided detection (CAD) cost effective in screening mammography? A model based on the CADET II study,” *BMC Health Serv. Res.*, vol. 11, p. 11, 2011.

[204] M. Sato, M. Kawai, Y. Nishino, D. Shibuya, N. Ohuchi, and T. Ishibashi, “Cost-effectiveness analysis for breast cancer screening: double reading versus single plus CAD reading,” *Breast Cancer*, vol. 21, no. 5, pp. 532–541, Sep. 2014.

[205] D. Regge *et al.*, “Impact of Computer-aided Detection on the Cost-effectiveness of CT Colonography,” *Radiology*, vol. 250, no. 2, pp. 488–497, Feb. 2009.

[206] D. Regge *et al.*, “Impact of Computer-aided Detection on the Cost-effectiveness of CT Colonography,” *Radiology*, vol. 250, no. 2, pp. 488–497, Feb. 2009.

[207] S. Shapiro, “Screening - Assessment of Current Studies,” *Cancer*, vol. 74, no. 1, pp. 231–238, Jul. 1994.

[208] S. A. Feig, “Increased benefit from shorter screening mammography intervals for women ages 40-49 years,” *Cancer*, vol. 80, no. 11, pp. 2035–2039, Dec. 1997.

[209] A. Suzuki *et al.*, “Age-specific interval breast cancers in Japan: estimation of the proper sensitivity of screening using a population-based cancer registry,” *Cancer Sci.*, vol. 99, no. 11, pp. 2264–2267, Nov. 2008.

[210] L. H. Eadie, P. Taylor, and A. P. Gibson, “A systematic review of computer-assisted diagnosis in diagnostic cancer imaging,” *Eur. J. Radiol.*, vol. 81, no. 1, pp. E70–E76, Jan. 2012.

[211] “TeamNET.GanChiryo-hi.com.2008.” [Online]. Available: http://www.ganchiryohi.com/. [Accessed: 16-Apr-2017].

[212] J. Ferlay, P. Autier, M. Boniol, M. Heanue, M. Colombet, and P. Boyle, “Estimates of the cancer incidence and mortality in Europe in 2006,” *Ann. Oncol.*, vol. 18, no. 3, pp. 581–592, Mar. 2007.

[213] J. Mandel *et al.*, “Reducing Mortality from Colorectal-Cancer by Screening for Fecal Occult Blood,” *N. Engl. J. Med.*, vol. 328, no. 19, pp. 1365–1371, May 1993.

[214] O. Kronborg, C. Fenger, J. Olsen, O. D. Jorgensen, and O. Sondergaard, “Randomised study of screening for colorectal cancer with faecal-occult-blood test,” *Lancet*, vol. 348, no. 9040, pp. 1467–1471, Nov. 1996.

[215] A. Sonnenberg, F. Delco, and P. Bauerfeind, “Ts virtual colonoscopy a cost-effective option to screen for colorectal cancer?,” *Am. J. Gastroenterol.*, vol. 94, no. 8, pp. 2268–2274, Aug. 1999.

[216] S. Vijan *et al.*, “The cost-effectiveness of CT colonography in screening for colorectal neoplasia,” *Am. J. Gastroenterol.*, vol. 102, no. 2, pp. 380–390, Feb. 2007.

[217] N. Petrick *et al.*, “CT colonography with computer-aided detection as a second reader: Observer performance study,” *Radiology*, vol. 246, no. 1, pp. 148–156, Jan. 2008.

[218] J. Disario, P. Foutch, H. Mai, K. Pardy, and K. Rao, “Prevalence and Malignant Potential of Colorectal Polyps in Asymptomatic, Average-Risk Men,” *Am. J. Gastroenterol.*, vol. 86, no. 8, pp. 941–945, Aug. 1991.

[219] M. Vatn and H. Stalsberg, “The Prevalence of Polyps of the Large-Intestine in Oslo - an Autopsy Study,” *Cancer*, vol. 49, no. 4, pp. 819–825, 1982.

[220] R. R. Rickert, O. Auerbach, L. Garfinkel, E. C. Hammond, and J. M. Frasca, “Adenomatous lesions of the large bowel: an autopsy survey,” *Cancer*, vol. 43, no. 5, pp. 1847–1857, May 1979.

[221] T. C. Arminski and D. W. McLean, “Incidence and distribution of adenomatous polyps of the colon and rectum based on 1,000 autopsy examinations,” *Dis. Colon Rectum*, vol. 7, no. 4, p. 249, Oct. 2016.

[222] G. N. Stemmermann, L. K. Heilbrun, A. Nomura, K. Yano, and T. Hayashi, “Adenomatous polyps and atherosclerosis: an autopsy study of Japanese men in

Hawaii," *Int. J. Cancer*, vol. 38, no. 6, pp. 789–794, Dec. 1986.

[223] T. J. Eide, "The age-, sex-, and site-specific occurrence of adenomas and carcinomas of the large intestine within a defined population," *Scand. J. Gastroenterol.*, vol. 21, no. 9, pp. 1083–1088, Nov. 1986.

[224] D. A. Johnson *et al.*, "A prospective study of the prevalence of colonic neoplasms in asymptomatic patients with an age-related risk," *Am. J. Gastroenterol.*, vol. 85, no. 8, pp. 969–974, Aug. 1990.

[225] J. Yee, G. A. Akerkar, R. K. Hung, A. M. Steinauer-Gebauer, S. D. Wall, and K. R. McQuaid, "Colorectal neoplasia: performance characteristics of CT colonography for detection in 300 patients," *Radiology*, vol. 219, no. 3, pp. 685–692, Jun. 2001.

[226] A. R. Williams, B. A. Balasooriya, and D. W. Day, "Polyps and cancer of the large bowel: a necropsy study in Liverpool.," *Gut*, vol. 23, no. 10, pp. 835–842, Oct. 1982.

[227] J. Clark *et al.*, "Prevalence of Polyps in an Autopsy Series from Areas with Varying Incidence of Large-Bowel Cancer," *Int. J. Cancer*, vol. 36, no. 2, pp. 179–186, 1985.

[228] R. Koretz, "Malignant Polyps - Are They Sheep in Wolves Clothing," *Ann. Intern. Med.*, vol. 118, no. 1, pp. 63–68, Jan. 1993.

[229] F. Loeve *et al.*, "National Polyp Study Data: Evidence for regression of adenomas," *Int. J. Cancer*, vol. 111, no. 4, pp. 633–639, Sep. 2004.

[230] B. Hofstad *et al.*, "Growth of colorectal polyps: redetection and evaluation of unresected polyps for a period of three years.," *Gut*, vol. 39, no. 3, pp. 449–456, Sep. 1996.

[231] G. Hoff, A. Foerster, M. H. Vatn, J. Sauar, and S. Larsen, "Epidemiology of polyps in the rectum and colon. Recovery and evaluation of unresected polyps 2 years after detection," *Scand. J. Gastroenterol.*, vol. 21, no. 7, pp. 853–862, Sep. 1986.

[232] S. J. Stryker, B. G. Wolff, C. E. Culp, S. D. Libbe, D. M. Ilstrup, and R. L. MacCarty, "Natural history of untreated colonic polyps," *Gastroenterology*, vol. 93, no. 5, pp. 1009–1013, Nov. 1987.

[233] S. Welin, J. Youker, and J. S. Spratt, "THE RATES AND PATTERNS OF GROWTH OF 375 TUMORS OF THE LARGE INTESTINE AND RECTUM OBSERVED SERIALLY BY DOUBLE CONTRAST ENEMA STUDY (MALMOE TECHNIQUE)," *Am. J. Roentgenol. Radium Ther. Nucl. Med.*, vol. 90, pp. 673–687, Oct. 1963.

[234] U. Ladabaum, C. L. Chopra, G. Huang, J. M. Scheiman, M. E. Chernew, and A.

M. Fendrick, “Aspirin as an adjunct to screening for prevention of sporadic colorectal cancer. A cost-effectiveness analysis,” *Ann. Intern. Med.*, vol. 135, no. 9, pp. 769–781, Nov. 2001.

[235] “SEER Cancer Statistics Review 1973-1994 - Previous Version - SEER Cancer Statistics,” 25-Oct-2016. [Online]. Available: http://seer.cancer.gov/archive/csr/1973_1994/. [Accessed: 25-Oct-2016].

[236] “Fast Stats,” 25-Oct-2016. [Online]. Available: http://seer.cancer.gov/faststats/. [Accessed: 25-Oct-2016].

[237] B. Levin *et al.*, “Screening and surveillance for the early detection of colorectal cancer and adenomatous polyps, 2008: a joint guideline from the American Cancer Society, the US Multi-Society Task Force on Colorectal Cancer, and the American College of Radiology,” *CA. Cancer J. Clin.*, vol. 58, no. 3, pp. 130–160, Jun. 2008.

[238] S. Halligan *et al.*, “Computed Tomographic Colonography: Assessment of Radiologist Performance With and Without Computer-Aided Detection,” *Gastroenterology*, vol. 131, no. 6, pp. 1690–1699, Dec. 2006.

[239] A. H. Dachman *et al.*, “Effect of Computer-aided Detection for CT Colonography in a Multireader, Multicase Trial1,” *Radiology*, vol. 256, no. 3, pp. 827–835, Sep. 2010.

[240] C. Hassan *et al.*, “Computed tomographic colonography to screen for colorectal cancer, extracolonic cancer, and aortic aneurysm: model simulation with cost-effectiveness analysis,” *Arch. Intern. Med.*, vol. 168, no. 7, pp. 696–705, Apr. 2008.

[241] F. K. L. Tangka *et al.*, “Cost of starting colorectal cancer screening programs: results from five federally funded demonstration programs,” *Prev. Chronic. Dis.*, vol. 5, no. 2, p. A47, Apr. 2008.

[242] T. R. Levin *et al.*, “Complications of colonoscopy in an integrated health care delivery system,” *Ann. Intern. Med.*, vol. 145, no. 12, pp. 880–886, Dec. 2006.

[243] S. H. Taplin *et al.*, “Stage, Age, Comorbidity, and Direct Costs of Colon, Prostate, and Breast Cancer Care,” *J. Natl. Cancer Inst.*, vol. 87, no. 6, pp. 417–426, Mar. 1995.

[244] B. H. Fireman *et al.*, “Cost of care for cancer in a health maintenance organization,” *Health Care Financ. Rev.*, vol. 18, no. 4, pp. 51–76, 1997.

[245] M. L. Brown, G. F. Riley, A. L. Potosky, and R. D. Etzioni, “Obtaining long-term disease specific costs of care: application to Medicare enrollees diagnosed with colorectal cancer,” *Med. Care*, vol. 37, no. 12, pp. 1249–1259, Dec. 1999.

[246] K. Hahn *et al.*, “Selectively and progressively disrupted structural connectivity of functional brain networks in Alzheimer’s disease - revealed by a novel framework to analyze edge distributions of networks detecting disruptions with strong statistical evidence,” *NeuroImage*, vol. 81, pp. 96–109, Nov. 2013.

[247] “World Alzheimer Report 2015: The Global Impact of Dementia | Alzheimer’s Disease International.” [Online]. Available: https://www.alz.co.uk/research/world-report-2015. [Accessed: 11-Dec-2016].

[248] R. Brookmeyer, E. Johnson, K. Ziegler-Graham, and H. M. Arrighi, “Forecasting the global burden of Alzheimer’s disease,” *Alzheimers Dement. J. Alzheimers Assoc.*, vol. 3, no. 3, pp. 186–191, Jul. 2007.

[249] “Dementia cases set to triple by 2050 but still largely ignored,” *WHO*. [Online]. Available: http://www.who.int/mediacentre/news/releases/2012/dementia_20120411/en/. [Accessed: 29-Mar-2017].

[250] J. W. Han *et al.*, “Predictive validity and diagnostic stability of mild cognitive impairment subtypes,” *Alzheimers Dement. J. Alzheimers Assoc.*, vol. 8, no. 6, pp. 553–559, Nov. 2012.

[251] G. aël Chetelat and J.-C. Baron, “Early diagnosis of alzheimer’s disease: contribution of structural neuroimaging,” *NeuroImage*, vol. 18, no. 2, pp. 525–541, Feb. 2003.

[252] Y. Zhang and S. Wang, “Detection of Alzheimer’s disease by displacement field and machine learning,” *PeerJ*, vol. 3, p. e1251, Sep. 2015.

[253] L. Khedher, J. Ramírez, J. M. Górriz, A. Brahim, and I. A. Illán, “Independent Component Analysis-Based Classification of Alzheimer’s Disease from Segmented MRI Data,” in *Artificial Computation in Biology and Medicine*, J. M. F. Vicente, J. R. Álvarez-Sánchez, F. de la P. López, F. J. Toledo-Moreo, and H. Adeli, Eds. Springer International Publishing, 2015, pp. 78–87.

[254] J. Beck and S. Pauker, “The Markov Process in Medical Prognosis,” *Med. Decis. Making*, vol. 3, no. 4, pp. 419–458, 1983.

[255] C. C. Bennett and K. Hauser, “Artificial intelligence framework for simulating clinical decision-making: A Markov decision process approach,” *Artif. Intell. Med.*, vol. 57, no. 1, pp. 9–19, Jan. 2013.

[256] D. S. Knopman *et al.*, “Practice parameter: diagnosis of dementia (an evidence-based review). Report of the Quality Standards Subcommittee of the American Academy of Neurology,” *Neurology*, vol. 56, no. 9, pp. 1143–1153, May 2001.

[257] C. P. Hughes, L. Berg, W. L. Danziger, L. A. Coben, and R. L. Martin, “A new clinical scale for the staging of dementia,” *Br. J. Psychiatry J. Ment. Sci.*, vol. 140, pp. 566–572, Jun. 1982.

[258] K. Mirsaeedi-Farahani, C. H. Halpern, G. H. Baltuch, D. A. Wolk, and S. C. Stein, “Deep brain stimulation for Alzheimer disease: a decision and cost-effectiveness analysis,” *J. Neurol.*, vol. 262, no. 5, pp. 1191–1197, May 2015.

[259] S. L. Rogers, M. R. Farlow, R. S. Doody, R. Mohs, and L. T. Friedhoff, “A 24-week, double-blind, placebo-controlled trial of donepezil in patients with Alzheimer’s disease. Donepezil Study Group,” *Neurology*, vol. 50, no. 1, pp. 136–145, Jan. 1998.

[260] P. M. McMahon, S. S. Araki, E. A. Sandberg, P. J. Neumann, and G. S. Gazelle, “Cost-effectiveness of PET in the diagnosis of Alzheimer disease,” *Radiology*, vol. 228, no. 2, pp. 515–522, Aug. 2003.

[261] P. M. McMahon, S. S. Araki, P. J. Neumann, G. J. Harris, and G. S. Gazelle, “Cost-effectiveness of functional imaging tests in the diagnosis of Alzheimer disease,” *Radiology*, vol. 217, no. 1, pp. 58–68, Oct. 2000.

[262] J. López-Bastida, W. Hart, L. Garcí-Pérez, and R. Linertová, “Cost-Effectiveness of Donepezil in the Treatment of Mild or Moderate Alzheimer’s Disease,” *J. Alzheimers Dis.*, vol. 16, no. 2, pp. 399–407, Feb. 2009.

[263] J. C. Morris *et al.*, “Very mild Alzheimer’s disease Informant-based clinical, psychometric, and pathologic distinction from normal aging,” *Neurology*, vol. 41, no. 4, pp. 469–469, Apr. 1991.

[264] J. P. Wade, T. R. Mirsen, V. C. Hachinski, M. Fisman, C. Lau, and H. Merskey, “The clinical diagnosis of Alzheimer’s disease,” *Arch. Neurol.*, vol. 44, no. 1, pp. 24–29, Jan. 1987.

[265] G. J. Harris *et al.*, “Dynamic susceptibility contrast MR imaging of regional cerebral blood volume in Alzheimer disease: a promising alternative to nuclear medicine,” *AJNR Am. J. Neuroradiol.*, vol. 19, no. 9, pp. 1727–1732, Oct. 1998.

[266] D. G. Fryback *et al.*, “The Beaver Dam Health Outcomes Study: initial catalog of health-state quality factors,” *Med. Decis. Mak. Int. J. Soc. Med. Decis. Mak.*, vol. 13, no. 2, pp. 89–102, Jun. 1993.

[267] M. A. Kupinski and M. L. Giger, “Feature selection with limited datasets,” *Med. Phys.*, vol. 26, no. 10, pp. 2176–2182, Oct. 1999.

[268] H. P. Chan, B. Sahiner, R. F. Wagner, and N. Petrick, “Classifier design for computer-aided diagnosis: effects of finite sample size on the mean performance of classical and neural network classifiers,” *Med. Phys.*, vol. 26, no. 12, pp.

2654–2668, Dec. 1999.

[269] R. M. Nishikawa *et al.*, “Effect of case selection on the performance of computer-aided detection schemes,” *Med. Phys.*, vol. 21, no. 2, pp. 265–269, Feb. 1994.

[270] B. Zheng, Y. H. Chang, W. F. Good, and D. Gur, “Adequacy testing of training set sample sizes in the development of a computer-assisted diagnosis scheme,” *Acad. Radiol.*, vol. 4, no. 7, pp. 497–502, Jul. 1997.

[271] S. C. Park, R. Sukthankar, L. Mummert, M. Satyanarayanan, and B. Zheng, “Optimization of reference library used in content-based medical image retrieval scheme,” *Med. Phys.*, vol. 34, no. 11, pp. 4331–4339, Nov. 2007.

[272] J. Liu, S. Kabadi, R. Van Uitert, N. Petrick, R. Deriche, and R. M. Summers, “Improved computer-aided detection of small polyps in CT colonography using interpolation for curvature estimation,” *Med. Phys.*, vol. 38, no. 7, pp. 4276–4284, Jul. 2011.

[273] P. Carrera and M. J. IJzerman, “Are current ICER thresholds outdated? Valuing medicines in the era of personalized healthcare,” *Expert Rev. Pharmacoecon. Outcomes Res.*, vol. 16, no. 4, pp. 435–437, Jul. 2016.

[274] W. A. Yousef and S. Kundu, “Learning algorithms may perform worse with increasing training set size: Algorithm–data incompatibility,” *Comput. Stat. Data Anal.*, vol. 74, pp. 181–197, Jun. 2014.

[275] J. G. Einspahr, D. S. Alberts, S. M. Gapstur, R. M. Bostick, S. S. Emerson, and E. W. Gerner, “Surrogate end-point biomarkers as measures of colon cancer risk and their use in cancer chemoprevention trials,” *Cancer Epidemiol. Biomark. Prev. Publ. Am. Assoc. Cancer Res. Cosponsored Am. Soc. Prev. Oncol.*, vol. 6, no. 1, pp. 37–48, Jan. 1997.

[276] R. M. Summers, “Polyp Size Measurement at CT Colonography: What Do We Know and What Do We Need to Know?,” *Radiology*, vol. 255, no. 3, pp. 707–720, Jun. 2010.

[277] J. G. Ravenel, E. M. Scalzetti, W. Huda, and W. Garrisi, “Radiation Exposure and Image Quality in Chest CT Examinations,” *Am. J. Roentgenol.*, vol. 177, no. 2, pp. 279–284, Aug. 2001.

[278] L. W. Goldman, “Principles of CT: Radiation Dose and Image Quality,” *J. Nucl. Med. Technol.*, vol. 35, no. 4, pp. 213–225, Dec. 2007.

[279] J. G. . Jones, C. N. Mills, M. A. Mogensen, and C. I. Lee, “Radiation Dose from Medical Imaging: A Primer for Emergency Physicians,” *West. J. Emerg. Med.*, vol. 13, no. 2, pp. 202–210, May 2012.

[280] D. J. Brenner and H. Hricak, “Radiation exposure from medical imaging: time to regulate?,” *JAMA*, vol. 304, no. 2, pp. 208–209, Jul. 2010.

[281] K. Leuraud *et al.*, “Ionising radiation and risk of death from leukaemia and lymphoma in radiation-monitored workers (INWORKS): an international cohort study,” *Lancet Haematol.*, vol. 2, no. 7, pp. e276–e281, Jul. 2015.

[282] L. T. Dauer, R. H. Thornton, J. L. Hay, R. Balter, M. J. Williamson, and J. St. Germain, “Fears, Feelings, and Facts: Interactively Communicating Benefits and Risks of Medical Radiation With Patients,” *AJR Am. J. Roentgenol.*, vol. 196, no. 4, Apr. 2011.

[283] H. Braak and E. Braak, “Morphological criteria for the recognition of Alzheimer’s disease and the distribution pattern of cortical changes related to this disorder,” *Neurobiol. Aging*, vol. 15, no. 3, pp. 355-356; discussion 379-380, Jun. 1994.

[284] E. Goceri, E. Dura, and M. Gunay, “Review on Machine Learning Based Lesion Segmentation Methods from Brain MR Images,” in *2016 15th IEEE International Conference on Machine Learning and Applications (ICMLA)*, 2016, pp. 582–587.

[285] T. Nakamoto, A. Taguchi, A. Asano, and K. Tanimoto, “Osteoporosis Screening CAD using Dental Panoramic Radiographs,” *Inst. Electron. Inf. Commun. Eng.*, vol. 102, no. 575, pp. 13–17, Jan. 2003.

[286] J. R. Vest, R. Kaushal, M. D. Silver, K. Hentel, and L. M. Kern, “Health information exchange and the frequency of repeat medical imaging,” *Am. J. Manag. Care*, vol. 20, no. 11 Spec No. 17, pp. eSP16-24, Nov. 2014.

[287] D. M. Emick, T. S. Carey, A. G. Charles, and M. L. Shapiro, “Repeat imaging in trauma transfers: a retrospective analysis of computed tomography scans repeated upon arrival to a Level I trauma center,” *J. Trauma Acute Care Surg.*, vol. 72, no. 5, pp. 1255–1262, May 2012.

[288] M. N. O. Sadiku, S. M. Musa, and O. D. Momoh, “Cloud Computing: Opportunities and Challenges,” *IEEE Potentials*, vol. 33, no. 1, pp. 34–36, Jan. 2014.

[289] S. G. Shini, T. Thomas, and K. Chithraranjan, “Cloud Based Medical Image Exchange-Security Challenges,” *Procedia Eng.*, vol. 38, pp. 3454–3461, Jan. 2012.

[290] F. Rezaeibagha and Y. Mu, “Distributed clinical data sharing via dynamic access-control policy transformation,” *Int. J. Med. Inf.*, vol. 89, pp. 25–31, May 2016.

[291] R. Noumeir and A. Chafik, “Access control and confidentiality in radiology,”

2005, vol. 5748, pp. 340–347.

[292] D. T. Fetzer and O. C. West, “The HIPAA Privacy Rule and Protected Health Information: Implications in Research Involving DICOM Image Databases,” *Acad. Radiol.*, vol. 15, no. 3, pp. 390–395, Mar. 2008.

[293] J. D. Robinson, “Beyond the DICOM Header: Additional Issues in Deidentification,” *Am. J. Roentgenol.*, vol. 203, no. 6, pp. W658–W664, Nov. 2014.

[294] A. Roehrs, C. A. da Costa, R. da R. Righi, and K. S. F. de Oliveira, “Personal Health Records: A Systematic Literature Review,” *J. Med. Internet Res.*, vol. 19, no. 1, p. e13, 2017.

[295] S. Subashini and V. Kavitha, “A survey on security issues in service delivery models of cloud computing,” *J. Netw. Comput. Appl.*, vol. 34, no. 1, pp. 1–11, Jan. 2011.

[296] K. Häyrinen, K. Saranto, and P. Nykänen, “Definition, structure, content, use and impacts of electronic health records: A review of the research literature,” *Int. J. Med. Inf.*, vol. 77, no. 5, pp. 291–304, May 2008.

[297] “Digital Health in Canada - Canada Health Infoway.” [Online]. Available: https://www.infoway-inforoute.ca/en/. [Accessed: 21-Jul-2017].

[298] “[ARCHIVED CONTENT] UK Government Web Archive - The National Archives.” [Online]. Available: http://webarchive.nationalarchives.gov.uk/20130502102046/http://www.connectingforhealth.nhs.uk/. [Accessed: 21-Jul-2017].

[299] W. A. Yasnoff *et al.*, “A Consensus Action Agenda for Achieving the National Health Information Infrastructure,” *J. Am. Med. Inform. Assoc. JAMIA*, vol. 11, no. 4, pp. 332–338, 2004.

[300] H. Yoshihara, “Development of the electronic health record in Japan,” *Int. J. Med. Inf.*, vol. 49, no. 1, pp. 53–58, Mar. 1998.

[301] R. Inokuchi *et al.*, “Motivations and barriers to implementing electronic health records and ED information systems in Japan,” *Am. J. Emerg. Med.*, vol. 32, no. 7, pp. 725–730, Jul. 2014.

[302] D. E. Gobuty, “Organizing security and privacy enforcement in medical imaging technology,” *Int. Congr. Ser.*, vol. 1256, pp. 319–329, Jun. 2003.

[303] N. Mohammed, B. C. M. Fung, P. C. K. Hung, and C. Lee, “Anonymizing Healthcare Data: A Case Study on the Blood Transfusion Service,” in *Proceedings of the 15th ACM SIGKDD International Conference on Knowledge Discovery and Data Mining*, New York, NY, USA, 2009, pp. 1285–1294.

[304] P. Ruotsalainen, “A cross-platform model for secure Electronic Health Record communication,” *Int. J. Med. Inf.*, vol. 73, no. 3, pp. 291–295, Mar. 2004.

[305] P. Mildenberger, M. Eichelberg, and E. Martin, “Introduction to the DICOM standard,” *Eur. Radiol.*, vol. 12, no. 4, pp. 920–927, Apr. 2002.

[306] W. D. Bidgood, S. C. Horii, F. W. Prior, and D. E. Van Syckle, “Understanding and Using DICOM, the Data Interchange Standard for Biomedical Imaging,” *J. Am. Med. Inform. Assoc.*, vol. 4, no. 3, pp. 199–212, 1997.

[307] L. Li and J. Z. Wang, “DDIT - A Tool for DICOM Brain Images De-Identification,” in *2011 5th International Conference on Bioinformatics and Biomedical Engineering*, 2011, pp. 1–4.

[308] “Biometrics | Homeland Security.” [Online]. Available: https://www.dhs.gov/biometrics. [Accessed: 09-May-2017].

[309] *Digital Imaging and Communications in Medicine (DICOM) - A | Oleg S. Pianykh | Springer*. .

[310] I. D. Robertson and T. Saveraid, “Hospital, radiology, and picture archiving and communication systems,” *Vet. Radiol. Ultrasound Off. J. Am. Coll. Vet. Radiol. Int. Vet. Radiol. Assoc.*, vol. 49, no. 1 Suppl 1, pp. S19-28, Feb. 2008.

[311] T. K. Agarwal and Sanjeev, “Vendor neutral archive in PACS,” *Indian J. Radiol. Imaging*, vol. 22, no. 4, pp. 242–245, 2012.

[312] D. A. Clunie, D. K. Dennison, D. Cram, K. R. Persons, M. D. Bronkalla, and H. “Rik” Primo, “Technical Challenges of Enterprise Imaging: HIMSS-SIIM Collaborative White Paper,” *J. Digit. Imaging*, vol. 29, no. 5, pp. 583–614, Oct. 2016.

[313] H. U. Lemke, W. Niederlag, and H. Heuser, “Specification and evaluation of a regional PACS in the SaxTeleMed project,” presented at the Medical Imaging 2002: PACS and Integrated Medical Information Systems: Design and Evaluation, 2002, vol. 4685, pp. 1–6.

[314] H.-J. Kim, “PACS industry in Korea,” presented at the Medical Imaging 2002: PACS and Integrated Medical Information Systems: Design and Evaluation, 2002, vol. 4685, pp. 50–58.

[315] H. K. Huang, “Enterprise PACS and image distribution,” *Comput. Med. Imaging Graph.*, vol. 27, no. 2, pp. 241–253, Mar. 2003.

[316] H. Takabi, J. B. D. Joshi, and G. J. Ahn, “Security and Privacy Challenges in Cloud Computing Environments,” *IEEE Secur. Priv.*, vol. 8, no. 6, pp. 24–31, Nov. 2010.

[317] “Security Guidance : Cloud Security Alliance.” [Online]. Available:

https://cloudsecurityalliance.org/group/security-guidance/. [Accessed: 22-Mar-2017].

[318] "Top Threats : Cloud Security Alliance." [Online]. Available: https://cloudsecurityalliance.org/group/top-threats/. [Accessed: 28-Dec-2016].

[319] R. G David, *Security Engineering for Cloud Computing: Approaches and Tools: Approaches and Tools*. IGI Global, 2012.

[320] J. W. Rittinghouse and J. F. Ransome, *Cloud Computing: Implementation, Management, and Security*. Boca Raton: CRC Press, 2009.

[321] T. Garfinkel and M. Rosenblum, "When Virtual is Harder Than Real: Security Challenges in Virtual Machine Based Computing Environments," in *Proceedings of the 10th Conference on Hot Topics in Operating Systems - Volume 10*, Berkeley, CA, USA, 2005, pp. 20–20.

[322] D. Zissis and D. Lekkas, "Addressing cloud computing security issues," *Future Gener. Comput. Syst.*, vol. 28, no. 3, pp. 583–592, Mar. 2012.

[323] Z. Yan, R. H. Deng, and V. Varadharajan, "Cryptography and Data Security in Cloud Computing," *Inf. Sci.*, vol. 387, pp. 53–55, May 2017.

[324] M. Felici, T. Koulouris, and S. Pearson, "Accountability for Data Governance in Cloud Ecosystems," in *2013 IEEE 5th International Conference on Cloud Computing Technology and Science*, 2013, vol. 2, pp. 327–332.

[325] R. Jain, S. Madan, and B. Garg, "Homomorphic framework to ensure data security in cloud environment," 2016, pp. 177–181.

[326] R. Latif, H. Abbas, S. Assar, and Q. Ali, "Cloud Computing Risk Assessment: A Systematic Literature Review," in *Future Information Technology*, J. J. (Jong H. Park, I. Stojmenovic, M. Choi, and F. Xhafa, Eds. Springer Berlin Heidelberg, 2014, pp. 285–295.

[327] N.-H. Yu, Z. Hao, J.-J. Xu, W.-M. Zhang, and C. Zhang, "Review of cloud computing security," *ResearchGate*, vol. 41, no. 2, pp. 371–381, Feb. 2013.

[328] K. Hashizume, D. G. Rosado, E. Fernández-Medina, and E. B. Fernandez, "An analysis of security issues for cloud computing," *J. Internet Serv. Appl.*, vol. 4, no. 1, p. 5, Feb. 2013.

[329] M. S. Kiraz, "A comprehensive meta-analysis of cryptographic security mechanisms for cloud computing," *J. Ambient Intell. Humaniz. Comput.*, vol. 7, no. 5, pp. 731–760, Oct. 2016.

[330] M. Usman, M. Ahmad Jan, and X. He, "Cryptography-based secure data storage and sharing using HEVC and public clouds," *Inf. Sci.*, vol. 387, pp. 90–102, May 2017.

[331] J. Yli-Huumo, D. Ko, S. Choi, S. Park, and K. Smolander, “Where Is Current Research on Blockchain Technology?—A Systematic Review,” *PLOS ONE*, vol. 11, no. 10, p. e0163477, Oct. 2016.

[332] M. Swan, *Blockchain: Blueprint for a New Economy*. O’Reilly Media, Inc., 2015.

[333] “Crypto-Currency Market Capitalizations.” [Online]. Available: https://coinmarketcap.com/. [Accessed: 27-Dec-2016].

[334] D. Kondor, M. Pósfai, I. Csabai, and G. Vattay, “Do the Rich Get Richer? An Empirical Analysis of the Bitcoin Transaction Network,” *PLOS ONE*, vol. 9, no. 2, p. e86197, Feb. 2014.

[335] X. Yue, H. Wang, D. Jin, M. Li, and W. Jiang, “Healthcare Data Gateways: Found Healthcare Intelligence on Blockchain with Novel Privacy Risk Control,” *J. Med. Syst.*, vol. 40, no. 10, p. 218, Oct. 2016.

[336] “Blockchain Healthcare 2016 Report,” *Tierion*, 05-Oct-2016. .

[337] Laure A. Linn and Martha B. Koo, “Blockchain for Health Data and Its Potential Use in Health IT and Health Care.”

[338] C. C. Teng *et al.*, “A medical image archive solution in the cloud,” in *2010 IEEE International Conference on Software Engineering and Service Sciences*, 2010, pp. 431–434.

[339] “Medical Imaging Archives.” [Online]. Available: http://online.adu.edu/blog/bsrs/infographics/medical-imaging-archives/. [Accessed: 07-Sep-2017].

[340] “The conference promoting to utilize AI technology for Health and Medical Services,” *Japanese Ministry of Health, Labor and Welfare*. [Online]. Available: http://www.mhlw.go.jp/stf/shingi/other-kousei.html?tid=408914. [Accessed: 16-Sep-2017].

[341] R. Guesmi, M. A. B. Farah, A. Kachouri, and M. Samet, “Hash key-based image encryption using crossover operator and chaos,” *Multimed. Tools Appl.*, vol. 75, no. 8, pp. 4753–4769, Apr. 2016.

[342] M. Szydlo, “Merkle tree traversal in log space and time,” in *Advances in Cryptology - Eurocrypt 2004, Proceedings*, vol. 3027, C. Cachin and J. camenisch, Eds. Berlin: Springer-Verlag Berlin, 2004, pp. 541–554.

[343] P. Berman, M. Karpinski, and Y. Nekrich, “Optimal trade-off for Merkle tree traversal,” in *E-Business and Telecommunication Networks*, vol. 3, J. Filipe, H. Coelhas, and M. Saramago, Eds. Berlin: Springer-Verlag Berlin, 2007, p. 150–+.

[344] P. Gauravaram, “Security Analysis of salt||password Hashes,” in *2012 International Conference on Advanced Computer Science Applications and*

Technologies (ACSAT), 2012, pp. 25–30.

[345] I. Verbauwhede, P. Schaumont, and H. Kuo, “Design and performance testing of a 2.29-GB/s Rijndael processor,” *Ieee J. Solid-State Circuits*, vol. 38, no. 3, pp. 569–572, Mar. 2003.

[346] N. S. S. Srinivas and M. Akramuddin, “FPGA Based Hardware Implementation of AES Rijndael Algorithm for Encryption and Decryption,” *2016 Int. Conf. Electr. Electron. Optim. Tech. Iceeot*, pp. 1769–1776, 2016.

[347] “Japan Medical Imaging and Radiological Systems Industries Association: Open Data.” [Online]. Available: http://www.jira-net.or.jp/dicom/dicom_data_01_02.html. [Accessed: 21-Mar-2017].

[348] R. von Solms, H. van der Haar, S. H. von Solms, and W. J. Caelli, “A framework for information security evaluation,” *Inf. Manage.*, vol. 26, no. 3, pp. 143–153, Mar. 1994.

[349] D. M. Nicol, W. H. Sanders, and K. S. Trivedi, “Model-based evaluation: from dependability to security,” *IEEE Trans. Dependable Secure Comput.*, vol. 1, no. 1, pp. 48–65, Jan. 2004.

[350] I. B. M. Redbooks, *Cloud Security Guidelines for IBM Power Systems*. Vervante, 2015.

[351] J. Lech, *Internet and Intranet Security Management: Risks and Solutions: Risks and Solutions*. Idea Group Inc (IGI), 1999.

[352] M. Ebrahim, S. Khan, and U. B. Khalid, “Symmetric Algorithm Survey: A Comparative Analysis,” *ArXiv14050398 Cs*, May 2014.

[353] Lee Zhuang, “Bridging the gap between technology and business strategy: a pilot study on the innovation process,” *Manag. Decis.*, vol. 33, no. 8, pp. 13–21, Oct. 1995.

[354] L. Aldin and S. de Cesare, “A literature review on business process modelling: new frontiers of reusability,” *Enterp. Inf. Syst.*, vol. 5, no. 3, pp. 359–383, Aug. 2011.

[355] L. Chung, B. A. Nixon, E. Yu, and J. Mylopoulos, *Non-Functional Requirements in Software Engineering*. Springer Science & Business Media, 2012.

[356] Ministry of Health, Labor and Welfare, “statistical chart,” *statistical chart, GL08020103*. [Online]. Available: http://www.e-stat.go.jp/SG1/estat/List.do?lid=000001186905. [Accessed: 18-Sep-2017].

[357] A. R. Bakker, “HIS, RIS, and PACS,” *Comput. Med. Imaging Graph.*, vol. 15, no.

3, pp. 157–160, May 1991.

[358] M. F. Collen, “A brief historical overview of hospital information system (HIS) evolution in the United States,” *Int. J. Biomed. Comput.*, vol. 29, no. 3, pp. 169–189, Dec. 1991.

[359] J. W. Nance Jr, C. Meenan, and P. G. Nagy, “The Future of the Radiology Information System,” *Am. J. Roentgenol.*, vol. 200, no. 5, pp. 1064–1070, Apr. 2013.

[360] “Blockchain: Opportunities for health care | Deloitte US,” *Deloitte United States*. [Online]. Available: https://www2.deloitte.com/us/en/pages/public-sector/articles/blockchain-opportunities-for-health-care.html. [Accessed: 27-Dec-2016].

[361] D. Maltoni, D. Maio, A. Jain, and S. Prabhakar, *Handbook of Fingerprint Recognition*. Springer Science & Business Media, 2009.

[362] S. Marcel, Y. Rodriguez, and G. Heusch, “On the Recent Use of Local Binary Patterns for Face Authentication,” *Int. J. Image Video Process. Spec. Issue Facial Image Process.*, 2007.

[363] C. Severance, “Discovering JavaScript Object Notation,” *Computer*, vol. 45, no. 4, pp. 6–8, Apr. 2012.

[364] M. A. Koch, D. G. Norris, and M. Hund-Georgiadis, “An Investigation of Functional and Anatomical Connectivity Using Magnetic Resonance Imaging,” *NeuroImage*, vol. 16, no. 1, pp. 241–250, May 2002.

[365] S. Jbabdi and H. Johansen-Berg, “Tractography: Where Do We Go from Here?,” *Brain Connect.*, vol. 1, no. 3, pp. 169–183, Sep. 2011.

[366] W. I. Essayed, F. Zhang, P. Unadkat, G. R. Cosgrove, A. J. Golby, and L. J. O’Donnell, “White matter tractography for neurosurgical planning: A topography-based review of the current state of the art,” *NeuroImage Clin.*, vol. 15, pp. 659–672, Jun. 2017.

[367] R. Bammer, B. Acar, and M. E. Moseley, “In vivo MR tractography using diffusion imaging,” *Eur. J. Radiol.*, vol. 45, no. 3, pp. 223–234, Mar. 2003.

[368] K. Yamada, K. Sakai, K. Akazawa, S. Yuen, and T. Nishimura, “MR Tractography: A Review of Its Clinical Applications,” *Magn. Reson. Med. Sci.*, vol. 8, no. 4, pp. 165–174, 2009.

[369] P. Staempfli, T. Jaermann, G. R. Crelier, S. Kollias, A. Valavanis, and P. Boesiger, “Resolving fiber crossing using advanced fast marching tractography based on diffusion tensor imaging,” *NeuroImage*, vol. 30, no. 1, pp. 110–120, Mar. 2006.

[370] K. J. Miller, M. denNijs, P. Shenoy, J. W. Miller, R. P. N. Rao, and J. G. Ojemann,

"Real-time functional brain mapping using electrocorticography," *NeuroImage*, vol. 37, no. 2, pp. 504–507, Aug. 2007.

[371] "'Ichi no Kura'- Medical Image cloud archiving servise - GE Healthcare Japan - inNavi Suite." [Online]. Available: http://www.innervision.co.jp/suite/ge/technote/111158/index.html. [Accessed: 29-Oct-2017].

[372] "Healthcare@Cloud: Toshiba Medical Systems Corporation." [Online]. Available: http://www.healthcare-at-cloud.com/. [Accessed: 29-Oct-2017].

[373] "ASSISTA Portal-Fujifilm Corporation." [Online]. Available: http://www.innervision.co.jp/healthcareit/products/fms_it27_assistaportal. [Accessed: 29-Oct-2017].

[374] "Canon: Medical image place." [Online]. Available: http://cweb.canon.jp/mipl/index.html. [Accessed: 29-Oct-2017].

ACKNOWLEDGMENTS

I would like to thank a lot of members who have cooperated to the development of my dissertation and in whatever achievements I have made during my stay at Tokyo Institute of Technology. One of the most respected and thanked benefactor is Professor Yuya Kajikawa, my supervisor in this PhD course. I sincerely appreciate him for his enthusiastic teaching, unwavering support, encouragement and a little bit of patience.

I would also like to give special thanks to my deputy supervisor, associate professor Shintaro Sengoku. His enthusiasm support and expertise on healthcare industry corrected my research direction. Furthermore, I am grateful to professor Kazuyoshi Hidaka, professor Masahiro Hashimoto, and professor Mika Goto for my thesis examination.

I would also like to my gratitude to the entire faculty and staff and my colleagues at Tokyo Tech for supporting and assisting me while I was researching, particularly Hitomi Yamada, Hiroaki Tanaka, Ichiro Okabe, Hiroshi Someda, Rie Osawa and all Kajikawa lab members.

I also wish to extend my appreciation to Tokyo Institute of Technology for the tuition support and all the assistance during my stay in Tokyo Tech.

I am very thankful to my own company Kompath Inc. co-worker, Takehito Doke, Genken Takahashi, research & development collaborator Kin Taichi, Toki Saito, Kenji Akimoto and Toshiki Manaka, and former colleague Satoshi Ikehira and Fumiko Suzuki for untiring support and constant encouragement throughout this entire process. Especially Kenji Akimoto’s corporation for developing our system to apply blockchain strongly reinforced my thesis.

Finally, I would like to express my special gratitude to Sachiko Ishida for her warm encouragement.